Spring 1974

SOME ASPECTS OF NMR SHIFT REAGENT CHEMISTRY

CARMEN P. PACHECO

SOME ASPECTS OF NMR SHIFT REAGENT CHEMISTRY

by

CARMEN P. PACHECO

Lic., Central University of Venezuela, 1965

A THESIS

Submitted to the University of New Hampshire

In Partial Fulfillment of

The Requirements for the Degree of

Doctor of Philosophy

Graduate School

Department of Chemistry

June, 1974

This thesis has been examined and approved.

J. John Uebel

Thesis director, J. John Uebel, Asso. Prof. of Chemistry

Gloria G. Lyle

Gloria G. Lyle, Asso. Prof. of Chemistry

Kenneth K Andersen

Kenneth K. Andersen, Prof. of Chemistry

Paul R. Jones

Paul R. Jones, Prof. of Chemistry

Shan S. Kuo

Shan S. Kuo, Prof. of Mathematics

June 5, 1974

Date

ACKNOWLEDGEMENTS

I would like to express my gratitude to the Instituto Venezolano de Investigaciones Cientificas (IVIC), Republic of Venezuela, which supported me financially during my graduate studies at the University of New Hampshire. These studies have been encouraged mainly by the guidance of Dr. Gabriel Chuchani, member of IVIC.

My appreciation goes to Dr. J. John Uebel, a patient adviser, whose suggestions and discussions made this study possible. I will always be indebted to Dr. Gloria G. Lyle, for her direction in the first stage of this thesis, her moral support and understanding.

For their personal and academic involvement, I would like to acknowledge several faculty and staff members and students of the Chemistry Department of the University of New Hampshire. I am particularly grateful to Dr. Alexander R. Amell, Chairman of the Chemistry Department, for his concern and advice.

Mrs. Luz Martinez has been exceptional in the typing of this thesis, not only for the job itself, but also for her personal interest.

DEDICATION

To my husband and daughter.

TABLE OF CONTENTS

LIST OF TABLES

LIST OF FIGURES

ABSTRACT

SOME ASPECTS OF NMR SHIFT

REAGENT CHEMISTRY

by

CARMEN P. PACHECO

Shift reagents are the main subject of the present work; four aspects are investigated. They are:

1) Synthesis of new optically active shift reagents. Efforts to synthesize the β-diketone that would serve as the ligand were, however, unsuccessful.

2) Determination of complex formation shifts (CFS), using $La(dpm)_3$ as the diamagnetic complex. Pyridine and a series of aliphatic substrates are studied and in all cases, the CFS are found to be of a small magnitude. The change in coupling constants supports the interpretations in previous investigations which attributed such changes to substituent or conformational effects.

3) Correlation between geometry and lanthanide-induced shifts. A series of coordinates are derived from X-ray analysis of compounds similar to borneol, for which induced shifts are measured. Several models are tested to determine the importance of simplifications generally considered when similar analyses are performed.

4) Determination of equilibrium constants and stoichiometry between shift reagents and several substrates. A new method for the determination of these factors is developed. Besides the simplification over previous known methods, the present procedure unequivocally differentiates the stoichiometry of the adducts being formed and the interference from other equilibria that were previously ignored.

HISTORICAL BACKGROUND

Nuclear magnetic resonance (nmr) is a powerful tool for the organic chemist, because of the help it provides in elucidating the structure of compounds. In many cases, however, complicated spectral patterns result (especially for protons, pmr) from which only limited information is available. This situation arises because of a superimposition of signals corresponding to several nuclei. It has been found that the addition of a shift reagent (that is a lanthanide complex) to the sample under investigation often shifts the signals of quasi-magnetically equivalent nuclei in different proportions such that the resulting spectra can be directly analyzed (first order).

Hinckley[1], a pioneer in this field, described in 1969 how the spectrum of cholesterol was affected by the addition of small amounts of $Eu(dpm)_3 \cdot (pyridine)_2$ (dpm = dipivaloylmethanato 1, where R = R" = tert-butyl and R' = H). Since that time, several shift reagents have been synthesized, hundreds of observations have been reported and several reviews have been written on the subject[2-5].

The several shift reagents known up to date present the following common characteristics:

1) They are complexes between a lanthanide ion and three molecules of a β-diketone:

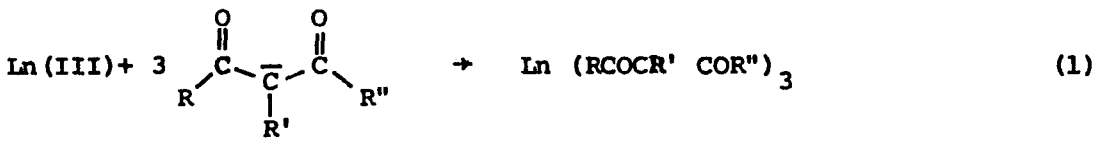

(1)

1 2

2) They are relatively stable and soluble in a number of organic solvents[6];

3) They are capable of expanding their coordination number, and so, association with one or more Lewis bases (substrate) is possible;

4) When such association occurs, the signals of nuclei in the bonding molecule are shifted by a magnitude which is related to the geometrical structure of the molecule itself.

$Eu(dpm)_3$ and $Eu(fod)_3$ (fod = 1,1,1,2,2,3,3-heptafluoro-7,7-dimethyl-4,6-octanedionato 1, where R = tert-butyl, R' = H, and R" = $CF_2CF_2CF_3$), which induce downfield shifts, and the respective complexes with praseodymium, which induce upfield shifts, are among the most common shift reagents. The optically active complexes formed between Eu (and Pr) with derivatives of camphor, have also found important applications in determining optical purity[7].

For a qualitative analysis, there is no question about the effectiveness of the shift reagents, but several problems arise with their quantitative aspects, e.g. correlation between observed shifts and structural geometry of the adduct. A few of such problems are discussed below.

1) Since only one resonance signal is observed for each nucleus, the recorded shifts for the adduct will be a weighted average of all present species (free and shift reagent bound substrate). A knowledge of the stoichiometry of the adducts (n in equation 2, where R = shift reagent and L = substrate) is necessary then, along with the corresponding values for the equilibrium constants in order to obtain chemical shifts that correspond to only one species. Determination of such quantities is still controversial.

$$\begin{aligned} R + L &\rightleftharpoons L{\cdot}R && K_1 \\ L{\cdot}R + L &\rightleftharpoons L_2{\cdot}R && K_2 \\ &\cdots\cdots\cdots\cdots && \\ L_{n-1}{\cdot}R + L &\rightleftharpoons L_n{\cdot}R && K_n \end{aligned} \qquad (2)$$

2) As described more extensively in the 'Paramagnetic Ions' section, several mechanisms can be postulated for the observed shifts. Only the so-called dipolar mechanism is transmitted through space and so directly related to the geometrical structure of the substrate. Even if the dipolar mechanism is predominant among the lanthanide ions, no effective procedure to separate the several contributions has been found.

3) Simplified models are assumed in many cases in order to correlate the observed shifts with the geometrical parameters. Several justifications have been offered, but their validity still remains to be demonstrated.

4) The geometrical parameters in the substrate are obtained either by a framework molecular model or by X-ray results from (generally a derivative of) the substrate itself. Since they represent only an approximation to the real structure in the adduct, this could give rise to erroneous conclusions when such data are used for geometrical correlations with the observed shifts. However, even when stable crystalline adducts have been isolated and their geometry established by X-ray analysis, the correlation with the observed shifts has sometimes been poor. Improvements are limited by the number of observations since they impose a limit on the number of parameters relative to the lanthanide coordinates to be adjusted. Efforts are made to determine the relative importance of each of such parameters.

These problems will be discussed in the next section of the thesis.

INTRODUCTION

General Considerations on Magnetic Properties

Charged particles determine the magnetic properties of matter. Electrons can be considered as small spheres of negative charge spinning on their axes; from classical considerations, the spinning of a charge produces a magnetic moment and since they are traveling on a closed path (orbital) this will also produce a magnetic moment. The magnetic properties of an atom or ion will be determined by a combination of these two properties; that is, the spin moments of the electron and the orbital moment resulting from the motion around the nucleus.

Based on such properties, the magnetic moment (μ) of a material (atom, ion, or group) is given by[8]:

$$\mu = \frac{eh}{4\pi mc} g\sqrt{J(J+1)} = \beta_M g\sqrt{J(J+1)} \qquad (3)$$

where J is the total angular quantum number for the material (vector sum of the spin angular quantum number, S, and the orbital angular quantum number, L), β_M is the Bohr Magneton, e is the electronic charge, h is the Planck's constant, m is the electron mass, c is the speed of light, and g is the Lande g-factor defined by

$$g = 1 + \frac{J(J+1) + S(S+1) - L(L+1)}{2J(J+1)} \qquad (4)$$

The experimental value of the magnetic moment is obtained by measuring the magnetic susceptibility of the material (χ) which is a property related to the flux of electrons induced when the material is placed in a magnetic field. Magnetic susceptibilities and magnetic moments are related by:

$$\chi = \frac{N\mu^2}{3kT} \tag{5}$$

where N is Avogadro's number, T the absolute temperature and k Boltzmann's constant.

Based on the magnitude of the magnetic susceptibility and taking vacuum as the reference ($\chi = 0$ for vacuum), two classes of materials are differentiated:

1) diamagnetic, with values of $\chi \simeq 0$
2) paramagnetic with values of $\chi > 0$, generally associated with the presence of unpaired electrons.

By a combination of equations 3 and 5, the magnetic susceptibility is related to the g-factor (and as a consequence, to the electronic configuration of the material) by:

$$\chi = \frac{Ng^2\beta_M^2\, J(J+1)}{3kT} \tag{6}$$

In an analogous way, the magnetic moment of a nucleus, μ_n, is expressed in terms of nuclear magnetons η_m[9]:

$$\mu_n = gI\eta_m = gI\,\frac{eh}{4\pi M_p c} \tag{7}$$

where M_p is the proton mass and I is the spin quantum number for the nucleus. The other terms were defined previously.

From quantum mechanics, when such a nucleus is placed in a magnetic field of magnitude H_o, 2I+1 equally spaced magnetic energy levels will arise. The energy separation between levels is given by equation 8:

$$\Delta E = h\nu_0 = \frac{\mu H_o}{I} \tag{8}$$

When a radio-frequency is applied and equation 8 is satisfied by either varying the magnetic field strength or the frequency, resonance occurs

which is detected as an absorption of energy from the radio-frequency field.

From equation 8 it is apparent that an isolated nucleus, susceptible to nmr spectroscopy, has a characteristic resonance frequency; in molecules, deviations from this frequency arise as a result of chemical and stereochemical environmental factors. Proton chemical shifts, however, show a relatively low sensitivity to such factors, and as a consequence resolution of such spectra is frequently limited.

An effective method to achieve better resolution is to alter the magnetic environment of the molecule. Two general techniques have been found useful for these purposes, aromatic solvents and paramagnetic metal complexes. The latter has been already introduced in the Historical Background section as the special case of lanthanide ion complexes (shift reagents). Let us analyze some general properties.

Diamagnetic and Paramagnetic Anisotropy

In the previous section, there was no consideration of the possible orientations that a material can take with respect to the external magnetic field. The magnetic moment was an average among all such possible orientations, since by tensor analysis:

$$g_{av}^2 = \frac{1}{3}\,(g_x^2 + g_y^2 + g_z^2) \qquad (9)$$

where g_x, g_y, and g_z are the three components (in mutually perpendicular directions) for the g factor, that now becomes the g tensor.

When $g_x = g_y = g_z$ (that is, the material possesses cubic symmetry), the magnetic moment will have identical components in the three directions with respect to the external field and the material is said to be isotropic.

When such an equality is not met, the magnetic moment will have different components in each direction and the material is said to be anisotropic[9].

Again, the term diamagnetic or paramagnetic anisotropy is assigned in relation to the magnitude of the magnetic susceptibility.

Figure 1 represents a material with symmetry $C_{\infty n}$ located in a magnetic field of magnitude H_o, with the principal magnetic axis A aligned with the external field. Along this axis, the g tensor component is $g_{||}$, or g_z if, by convention, the external field is colinear with the z axis. If the electron(s) is free to move in a closed path (orbital), this will produce a secondary magnetic field that will affect a nucleus B, located in such a field, by increasing or decreasing the separation of its magnetic energy levels according to equation 8.

For symmetry lower than O_h (cubic) and higher than C_{2v}, only one more component of $g(g_\perp)$, perpendicular to A, is necessary since $g_x = g_y = g_\perp$. McConnell[10] showed that, as a result of all random orientations, the expression for the fractional change in the nuclear resonance frequency (shielding) for nucleus B is:

$$\frac{\Delta H_B}{H_o} = C \frac{3 \cos^2 \Theta_B - 1}{r_B^3} \tag{10}$$

where r_B and Θ_B are the spherical coordinates for nucleus B (see Fig. 1). The constant C is:

$$C = - \frac{\beta_M^2 (g_{||} + 2g_\perp)(g_{||} - g_\perp) H_o S(S+1)}{27kT} \tag{11}$$

where all terms were defined previously.

The importance of anisotropy to the organic chemist is evident. If the group that displays such behavior is part of the molecule itself, conclusions about structure can easily be drawn. Otherwise, aromatic

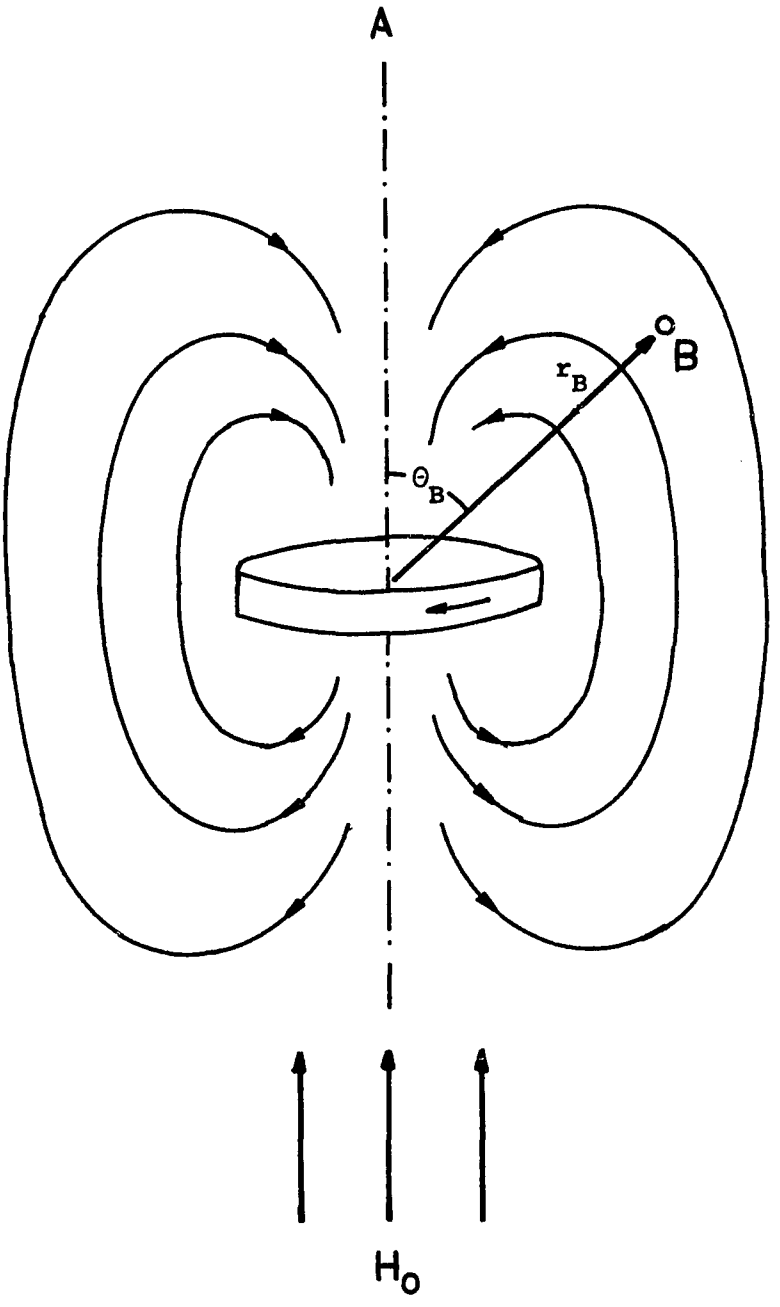

Figure 1 - Secondary Magnetic Field Induced by H_o in a Group of Symmetry $C_{\infty v}$

solvents and paramagnetic ions serve as a source for anisotropy if association with the organic molecule is possible.

Aromatic Solvent Induced Shifts (ASIS)

ASIS[11] arise from the diamagnetic anisotropy of the benzene ring, due to the circulation of π electrons in the plane of the ring. No true complex, however, is formed between the solvent molecules and the substrate, and the shielding effect is due to very short-lived collision complexes. The application of equation 10 has serious limitations in this case, since no fixed geometry is present, and even when this is achieved by a covalent bond between the aromatic moiety and the chain, the following restrictions must be considered:

1) The benzene ring is not a point dipole, for which equation 10 has been derived. Approximation to a point dipole is only valid if the affected nucleus is far from the aromatic moiety;

2) Shielding due to anisotropy decreases with the cubic power of the distance, so, when restriction 1 is fulfilled, only a small shielding will be observed;

3) Only a guess can be taken for the nmr frequency of the affected nucleus in the absence of the benzene ring, since it is not possible to eliminate such effect without altering the structure of the entire molecule.

Paramagnetic Ions

The effect of paramagnetic ions has been recognized since the discovery of the nmr phenomenon[12]. Paramagnetic anisotropy arises because of the circulation of unpaired electrons in the orbitals of the ion itself, which, contrary to the case of aromatic moiety, can be

considered as a point dipole.

Formation of a "true" complex between the paramagnetic ion and the substrate is usually achieved if such substrate has Lewis base characteristics.

The observed shifts of the frequency signals, however, arise from two major contributions[13]:

1) Transfer of electron density and/or spin polarization, via covalent bonds, from the metal ion to the binding nucleus (Fermi-contact interaction);

2) Paramagnetic anisotropy of the metal ion (pseudo-contact or dipolar interaction).

Each one deserves a special discussion.

Fermi-Contact Interaction

The Fermi-contact interaction involves direct delocalization and/or spin polarization of the unpaired electron(s) via the molecular orbitals of the substrate ligands[14-17]. It will depend then, on two factors:

1) The ability of the metal ion to transfer electron density and/or to polarize adjacent bonds;

2) The ability of the binding nucleus to accept such a transfer and/or to be polarized. Propagation through the rest of the molecule occurs through bonds and generally declines rapidly when only σ bonds are involved.

In the transition ions, the unpaired electrons occupy 3d orbitals that correspond to the external shell. The contact contribution is therefore expected to be high, and in fact, predominates when the second factor

above is also favorable[18].

On the other hand, unpaired electrons of the lanthanide (III) ions occupy 4f orbitals (see Table 1), and because of the presence of 5s and 5p electrons, do not correspond to the external shell. The contact contribution can be expected to be much lower compared to the transition ions, and the observed shifts will be primarily due to the paramagnetic anisotropy of the ions as far as the ability of the ion to induce a Fermi-contact interaction is concerned.

However, contact contributions cannot be totally ignored for the lanthanides; even if they form complexes mainly by electrostatic interactions, as little as 1% covalency could give rise to observable contact shifts[20], especially for nuclei near to the lone-pair bearing atom[21]. Furthermore, it has been suggested that contact shift is significant for aromatic amines where the second factor mentioned at the beginning of this section (that is, the susceptibility of the binding nucleus toward contact interaction) is believed favorable. This view has been contradicted by theoretical studies[22] and experimental observations with La(III)[23] (see Extrapolation of the Dipolar Contribution to the Observed Shifts).

Pseudo-contact or Dipolar Interactions

Bleaney[24] developed a theory for the anisotropy of the shift reagents which includes the effect of the ligand field of the three β-diketone molecules. For complexes of C_{3v} symmetry ($g_x = g_y = g_\perp$), Bleaney derived an equation in which the geometrical factor was the same as found by McConnell (equation 10), but the C constant was defined by:

$$C = - \frac{g_{av}^2 \beta_M^2 J(J+1) (2J-1) (2J-3)}{45(kT)^2} \langle r^2 \rangle \langle J \| \alpha \| J \rangle A_2^0 \qquad (12)$$

TABLE 1

Some Properties of Lanthanide Atoms and Ions[19].

Atomic Number	Name	Symbol	Electronic Configuration[a] Atom	M(III)	Ground State for Ions[b]	Radius of M(III) in Å
57	Lanthanum	La	$5d6s^2$	[Xe][c]	^1S_o	1.061
58	Cerium	Ce	$4f^15d^16s^2$	4f	$^2F_{5/2}$	1.034
59	Praseodymium	Pr	$4f^36s^2$	$4f^2$	$^3H_4$	1.013
60	Neodynium	Nd	$4f^46s^2$	$4f^3$	$^4I_{9/2}$	0.995
61	Promethium	Pm	$4f^56s^2$	$4f^4$	$^5I_4$	0.979
62	Samarium	Sm	$4f^66s^2$	$4f^5$	$^6H_{5/2}$	0.964
63	Europium	Eu	$4f^76s^2$	$4f^6$	^7F_o	0.950
64	Gadolinium	Gd	$4f^75d6s^2$	$4f^7$	$^8S_{7/2}$	0.938
65	Terbium	Tb	$4f^96s^2$	$4f^8$	$^7F_6$	0.923
66	Dysprosium	Dy	$4f^{10}6s^2$	$4f^9$	$^6H_{15/2}$	0.908
67	Holmium	Ho	$4f^{11}6s^2$	$4f^{10}$	$^5I_8$	0.894
68	Erbium	Er	$4f^{12}6s^2$	$4f^{11}$	$^4I_{15/2}$	0.881
69	Thulium	Tm	$4f^{13}6s^2$	$4f^{12}$	$^3H_6$	0.869
70	Ytterbium	Yb	$4f^{14}6s^2$	$4f^{13}$	$^2F_{7/2}$	0.858
71	Lutetium	Lu	$4f^{14}5d6s^2$	$4f^{14}$	^1S_o	0.848

a) The base electronic configuration corresponds to Xe.

b) The configuration corresponds to the Russell-Saunders or LS scheme, which is summarized as follows: the left superscript is the spin multiplicity (=2S+1, where S is the total electron spin quantum number); the capital letter is analogous to the hydrogen orbitals and represents the total orbital quantum number, L; the right subscript stands for the total angular momentum (vector sum of L and S).

c) [Xe] = $1s^22s^22p^63s^23p^63d^{10}4s^24p^64d^{10}5s^25p^6$.

where A_2^0 is an energy coefficient, $\langle r^2 \rangle$ is the mean second power of the electronic radius of the 4f electrons, and $\langle J \| \alpha \| J \rangle$ is a numerical coefficient.

The main difference between equations 11 and 12 is the prediction of a T^{-1} dependence of the magnetic susceptibilities (and of the observed shifts) from McConnell's derivation and a T^{-2} dependence from Bleaney's treatment. Some controversy appeared also in the experimental results[25-27] which led Horrocks et al.[28] to a third interpretation of the temperature dependence of the induced shifts. The effect of temperature on both the energy population distribution (Boltzmann law) and the magnetic susceptibility for each individual state (Curie's law) is included, so the resulting magnetic susceptibilities should follow:

$$\chi = AT^{-1} + BT^{-2} \tag{13}$$

where A and B are functions of the electronic configurations. Predominance of one term can occur, even if it is not the general case.

The present work does not deal principally with the temperature dependence, but partially with the validity of using the geometrical factor of equation 10. Lanthanide complexes (hepta- or octa-coordinated) do not belong to the C_{3v} point group[9,10] and sometimes even do not have any symmetry at all[31] as determined by single crystal X-ray. A better correlation then might possibly be expected if lower symmetry is considered.

LaMar et al.[32] derived an expression for C_{2v} symmetry, based on the same principles used by McConnell. The fractional change in the chemical shifts is given by:

$$\frac{\Delta H_i}{H_o} = C_1 \frac{3\cos^2 \Theta_i - 1}{r_i^3} - \frac{3}{2} C_2 \frac{\sin^2 \Theta_i \cos 2\Omega_i}{r_i^3} \tag{14}$$

where

$$C_1 = -\beta_M^2 S(S+1) \frac{g_z - \frac{1}{2} g_x - \frac{1}{2} g_y}{27kT} (g_x + g_y + g_z)$$

$$C_2 = -\beta_M^2 S(S+1) \frac{g_z + g_x + g_y}{27kT} (g_x - g_y) \qquad (15)$$

Here the position of the nucleus is expressed in spherical coordinates with respect to the symmetry axis of the lanthanide ion (see Figure 25 in Appendix 1).

The same consideration by Bleaney[24] (where the ligand field is included) led to the determination of C_1 and C_2 as:

$$C_1 = 2 \langle r^2 \rangle \langle J \| \alpha \| J \rangle A_o^2$$

$$C_2 = \frac{4}{3} \langle r^2 \rangle \langle J \| \alpha \| J \rangle A_2^2 \qquad (16)$$

where A_2^2 is an energy coefficient.

The difference between the two derivations is again the temperature dependence. But in any event, all theories predict the same geometrical function for a group of a given symmetry; that is, at constant temperature, equations 10 and 14 include identical geometrical factors times a constant term.

For lanthanide ions, equation 10 has found wide application when relating the shifts observed for a given nucleus in the molecule with its geometrical structure, and although, as mentioned above, there is reason to suspect that expressions based on complexes of lower symmetry (equation 14) would give more satisfactory results, this does not generally seem to be the case. Two explanations have been given to justify the reasonably good correlations obtained with equation 10, without the need of resorting to equation 14.

1) Independently Huber[33] and Briggs et al.[34] showed that if a substrate molecule (the seventh coordination site) is rotating freely about an axis which passes through the lanthanide ion, then, even if $g_x \neq g_y \neq g_z$, dipolar shifts will be given by equation 10 with

$$C = \frac{1}{2} [C_1' (\cos^2\alpha - 1) + C_2' \sin^2\alpha \cos 2\beta] \qquad (17)$$

where α is the angle between the principal magnetic axis (z) and the rotation axis, β is the angle analogous to Ω in Figure 25 (Appendix 1) for the binding atom, C_1' and C_2' are terms related to the temperature and electronic configurations. For such cases, Θ in equation 10 will be referred to the rotational axis. Argument against this possibility is that steric interactions render free rotation of the ligand impossible[28].

2) The structure of these complexes determined by X-ray cannot necessarily be extrapolated to the situation present in solution. A rapid equilibrium (or equilibria) and molecular reorganization are occurring in the liquid phase, involving exchange of the ligands (both the adduct and the diketone) which Dyer et al.[35] uses as argument to state that in the time average, the non-axial portion of the dipolar field is eliminated.

Extrapolation of the Dipolar Contribution from the Observed Shifts

As mentioned before, the lanthanide ions are used in nmr spectroscopy as the octahedral complex with three β-diketone anions as the ligands. Besides contact shifts, several factors must be analyzed in order to extract from the observed shifts the contribution due to the paramagnetic field of the lanthanide ion itself:

1) The ligands may also show some diamagnetic properties because of a small induced magnetic moment. Consequently, a small contribution

to the observed shift of the organic substrate will be observed, which cannot be considered to be produced by the same point dipole identified as the paramagnetic ion.

2) The formation of an adduct between the lanthanide complex and the organic substrate will displace some of the solvent molecules in the solvation cage of the substrate itself. This can alter the chemical shift of a given nucleus by a factor not dependent on the paramagnetism of the lanthanide ion.

3) The electronic distribution may be altered (by inductive or resonance effects) and the diamagnetic anisotropy of the substrate itself may vary in intensity and symmetry.

The following steps have been suggested by Bleaney[36] in order to assure the dipolar origin in the chemical shifts:

1) Lanthanide chelates which shift to both high and low magnetic field must be used;

2) The observed shifts must be corrected by observing shifts due to complex formation with the diamagnetic lanthanides, La(III) and Lu(III);

3) Ratios of shifts at different nuclear sites should then be compared for the different lanthanides used in step 1. If these ratios are independent of the lanthanide cation, then the shifts have their origin in dipolar coupling, and, to a good approximation, the anisotropy of the susceptibility has axial symmetry.

4) Besides the chemical shifts, line broadening data should also be included in any calculations due to their dependence[37] on $1/r^6$. To obtain such data, the use of Gd(III) chelates is suggested because of the low relaxation time for this ion.

Reexamining Table 1, a few points will be made:

1) The S state of La(III), Gd(III) and Lu(III), analogous to the s orbital in hydrogen atoms, represents a spherical model, so its g tensor will have identical components and no magnetic anisotropy will be observed. However, of the three ions, only Gd(III) has unpaired electrons which can interact with a substrate by a Fermi-contact mechanism; shifts induced by La(III) and Lu(III) (diamagnetic shifts) may be accounted for in terms of the three factors mentioned at the beginning of this section. This justifies Bleaney's second suggestion.

2) There is a significant change in the ionic radius among the lanthanides (Table 1), which may be reflected in the structure of the seven or eight coordination adducts. An example of this is the difference found between the X-ray analysis or $Eu(dpm)_3 \cdot (pyridine)_2$[19] and $Ho(dpm)_3 \cdot (4\text{-picoline})_2$[30]. They show isomorphic crystal structures with a C_2 symmetry axis, but different interatomic distances (Table 2). Since the anisotropy is not a linear function of the distance, Bleaney's third suggestion may give erroneous conclusions.

TABLE 2

Comparison Between X-Ray Bond Distances for $Eu(dpm)_3 \cdot (pyridine)_2$ and $Ho(dpm)_3 \cdot (4\text{-picoline})_2$.

Bond[a]	Bond distance in Å	
	$Eu(dpm)_3 \cdot (pyridine)_2$	$Ho(dpm)_3 \cdot (4\text{-picoline})_2$
Ln-O	2.35	2.27
Ln-N	2.651 ± 0.004	2.53 ± 0.03

a) Ln stands for lanthanide ion

Few authors dedicated their attention to the diamagnetic shift. Its importance is manifested in the study by Tori et al.[23] of the systems $La(fod)_3$ and several aromatic amines, δ-picoline-N-oxide and p-cresol. Shifts were observed that, at least on one occasion, would account for a change even in sign of the originally observed shifts with $Eu(fod)_3$ and $Pr(fod)_3$. In an aliphatic moiety, however, the diamagnetic shifts will probably be of minor importance, based on the observation of Schwarberg et al.[38] who reported that the dimethylformamide proton resonances in $La(dpm)_3$·DMF were shifted downfield by 10 Hz for the formyl proton and 1.5 and 4.5 Hz for the cis and trans methyls respectively.

Since shifts induced by Gd(III) complexes should be originated by a contact mechanism and/or a diamagnetic effect, the system $Gd(dpm)_3$/4-picoline has been analyzed by Horrocks et al.[28]. Severe signal broadening makes observations possible only for the 4-methyl group (which is found to be unshifted) without any information on the effect on the rest of the molecule, especially on the sites closer to the binding nitrogen.

A final remark about the broadening of the signals is appropriate. Table 3 summarizes some values for the line bandwidth for tert-butyl in various $Ln(dpm)_3$, (Ln = lanthanide) and methyl in 2-picoline in the presence of $Ln(dpm)_3$. In the same table, values for the contribution of dipolar to contact shifts are reported[5], which have been estimated from the magnetic susceptibilities as a first approximation by:

$$\frac{\text{dipolar}}{\text{contact}} = \frac{\chi_z - 1/2\ \chi_x - 1/2\ \chi_y}{g(g-1)J(J+1)} \qquad (18)$$

According to such data, it is apparent that while Eu(III) generally causes less severe line broadening, it also shows the higher tendency toward a contact interaction.

TABLE 3

Bandwidth and Estimated Ratios of Dipolar to Contact Contributions for Lanthanides.

Lanthanide	Bandwidth in Hz[a]	Bandwidth[b] / δ	Bandwidth in Hz[c]	Dipolar / Contact
Pr	40	0.005	5.6	1000
Nd	16	-	4.0	277
Sm	7	0.02	4.4	-
Eu	10	0.003	5.0	160
Gd	1500	-	-	-
Tb	250	0.1	96.0	503
Dy	180	-	200.0	870
Ho	180	0.02	50.0	447
Er	250	-	50.0	238
Tm	400	-	65.0	-
Yb	60	0.02	12.0	1340

a) tert-butyl in $Ln(dpm)_3$ in CCl_4 [39]

b) tert-butyl in $Ln(dpm)_3$ [40]

c) methyl in 2-picoline in the presence of $Ln(dpm)_3$ [41]

Correlation with Geometrical Factors

It would be impossible to review the hundreds of correlations between the observed chemical shifts and the structural geometry. In most of the cases, the following assumptions are made[27]:

1) The observed shifts used in the analysis are purely dipolar in origin;

2) Only a single stoichiometric complex species exists in solution in equilibrium with the uncomplexed substrate;

3) Only a single geometric isomer of this complex species is present;

4) This isomer is magnetically, axially symmetric so the shifts follow equation 10;

5) The principal magnetic axis has a particular, known orientation with respect to the substrate ligand or ligands;

6) The substrate ligand exists in a single conformation, or an appropriate averaging over internal motion is carried out.

It is amazing, however, that despite all the assumptions, reasonable values for bond angles and distances and reasonable agreement with calculated shifts are generally found. Among other applications, shift reagents have been used for structural determination of *cis* and *trans* isomers[42], conformational analysis[43], natural products[44] and peptides[45].

Shifts observed with other nuclei, especially ^{13}C, are also used, but with relatively less success, which has been attributed to a higher contribution of the contact shift mechanism[5,46].

Stoichiometry and Equilibrium Constants

Since the equilibrium (or equilibria) to form adducts between the shift reagents and the Lewis base is fast relative to the nmr time scale, only one resonance line is the result at room temperature, as an average of the free and the complexed species. In order to obtain stoichiometry and equilibrium constants for such adducts, the information has to be obtained either by other methods or by analysis of the induced chemical shifts as a function of the concentration of the several species involved.

Formation of only a 1:1 type of adduct is, of course, the most simple case, and in many cases this is assumed *a priori*.

Armitage *et al.*[47] analyzed the following two cases:

$$R + L \rightleftharpoons L \cdot R \tag{19}$$

$$R + 2L \rightleftharpoons L_2 \cdot R \tag{20}$$

where R stands for the shift reagent and L for the Lewis base or substrate. Their conclusion is that the two cases can be differentiated by a plot of $[L]_o$ *vs.* $1/\delta$ where $\delta = \delta_{obs} - \delta_{free\ substrate}$. The first case should result in a linear relation, the second one should show curvature more or less pronounced depending on the value of the equilibrium constant. As they pointed out, however, the analysis is based on the assumption that only one equilibrium is present in each case, and a multi-step binding phenomenon (Case 19 together with Case 20) to result in the formation of a 2:1 binding model, was not treated.

Assuming the formation of a 1:1 adduct (equation 19), Armitage *et al.*[47] derived the following expression based on the equilibrium constant representation:

$$[L]_o = [R]_o \Delta \left(\frac{1}{\delta}\right) - \left(\frac{1}{K} + [R]_o\right) \quad (21)$$

where Δ is the chemical shift of the 1:1 adduct relative to the free position, and K is the equilibrium constant for equation 19:

$$K = \frac{[R \cdot L]}{[R][L]} \quad (22)$$

Equation 21, however, is not exact; from equation 22 the term $[R \cdot L]^2$ has been neglected, which is valid only if the equilibrium constant has a low value.

They also used an alternative procedure through a computer program to solve equation 22 exactly. The difference in the two results was in the order of 20%.

Table 4 summarizes values of K and Δ for a few representative substrates and shift reagents obtained by the above method.

A very clever procedure, also based on the formation of only a 1:1 type of adducts was presented by Sanders et al.[48] in 1972. The pmr spectra of 2-Me-adamantan-2-ol were recorded at several constant concentrations of the substrate, varying the relative amount of $Eu(dpm)_3$. The shift reagent is assumed to be coordinated partially with water; the equilibrium constant for such hydrated species is assumed high, and as a result, their concentration constant. The total concentration of the shift reagent would then be:

$$[R]_t = [R]_{eff} + [R]_w \quad (23)$$

where $[R]_{eff}$ and $[R]_w$ represent the effective and water bound shift reagent concentrations respectively. From the equation of the equilibrium constant (equation 22), the following expression results:

TABLE 4

Values of Equilibrium Constants and Δ Determined by Plots of L_o vs. $1/\delta$, Assuming 1:1 Adducts.

Substrate	Shift Reagent	K(in M^{-1})	Δ(in ppm)	Ref
n-propylamine[a]	Eu(dpm)$_3$	43	$H_1 = 12$, $H_2 = 7$, $H_3 = 4$	47
" [a]	"	12	$H_1 = 38.7$, $H_2 = 24$, $H_3 = 13.2$	49
neopentanol[a]	"	10	$H_1 = 19$, $H_3 = 7$	47
" [a]	"	6.3	$H_1 = 23.7$, $H_3 = 9.5$	49
n-propylamine[a]	Eu(fod)$_3$	>100	$H_1 = 19$, $H_2 = 12.7$, $H_3 = 6.6$	47
neopentanol[a]	"	>100	$H_1 = 20.8$, $H_2 = 8.3$	47
isopropyl alcohol[b,c]	"	97		50a
tetrahydrofuran[b]	"	57	$H_1 = 19.48$, $H_2 = 7.93$	50a
2-butanone[b,c]	"	32		50a
propicphenone[a]	Eu(dpm)$_3$	15	$CH_2 = 6.60$, $CH_3 = 5.46$ ortho = 5.71	50b

a) in $CDCl_3$

b) in CCl_4

c) values of Δ not reported.

$$[R]_t = [R]_w + [R]_{eff} = \frac{[L]_o\ \delta}{\Delta} + \frac{\delta}{K(\Delta-\delta)} + [R]_w \qquad (24)$$

where, again, δ is the observed chemical shift relative to the free substrate, $[L]_o$ is the initial concentration of the substrate and Δ is the limiting shift for the 1:1 adduct. From equation 24 it becomes apparent that the following steps would lead to the value of the equilibrium constant:

1) Plot $[R]_t$ *vs.* $[L]_o$ at constant chemical shift and extrapolate to $[L]_o = 0$ to obtain values of $\delta/(\Delta-\delta)K + [R]_w$;

2) The slopes of such lines are δ/Δ and hence Δ is determined;

3) Plot the y intercept from step 1 *vs.* $\delta/(\Delta-\delta)$. The new extrapolation to $\delta/(\Delta-\delta) = 0$ will give $1/K$.

The method presents the disadvantage of high uncertainties, the estimated errors being in the order of 20%.

Few authors have considered the possibility of several equilibria being involved. Shapiro *et al.*[51] analyzed the system:

$$\begin{aligned} R + L &\rightleftharpoons R{\cdot}L \\ R{\cdot}L + L &\rightleftharpoons R{\cdot}L_2 \end{aligned} \qquad (25)$$

where R = $Eu(fod)_3$ and L = 3,5,5-trimethyl-3-(p-chlorophenyl)-cyclohexanone (3); analysis of the observed shifts is performed by an iterative method. The conclusion that both complexes are present, is reached by the fact that there exists a better correlation between the observed shifts and the calculated ones, when comparing the results from fits obtained using equation 25 with equation 19. If this is the case, and if the concentration of substrate is kept high with respect to the concentration of the shift reagent, then

$$\frac{1}{\delta} \approx \frac{[L]_o}{2[R]_o\Delta_2} \qquad (26)$$

and the straight line obtained by plots of $[L]_o$ *vs.* $1/\delta$ could give erroneous conclusions if equation 21 is applied.

A better approach has been introduced by Reuben[52], who also analyzed the system described by equation 25. He used dissociation constants in his calculation:

$$K_{D1} = \frac{[R] \cdot [L]}{[R \cdot L]}$$

$$K_{D2} = \frac{[R \cdot L]\,[L]}{[R \cdot L_2]} \qquad (27)$$

Complex formation equilibria involving n equivalent and independent coordination sites, are described by the Scatchard equation of the form:

$$\frac{\bar{\nu}}{L_f} = \frac{n}{K_D} - \frac{\bar{\nu}}{K_D} \qquad (28)$$

where $L_f = [L]$, $\nu = L_b/R_t$, $L_b = [R \cdot L] + 2[R \cdot L_2]$, $R_t = [R] + [R \cdot L] + [R \cdot L_2]$ and K_D results from considering $K_{D2} = 4K_{D1}$ so the system can be described with a single dissociation constant. Three cases are apparent for plots of $\bar{\nu}/L_f$ vs. $\bar{\nu}$:

1) A straight line results, indicating that a 1:1 adduct is the only complexed species present or the approximation $K_{D2} = 4K_{D1}$ is the real case. The two (or more) possibilities are differentiated by the value of the slope ($= -1/K_D$) and the intercept ($= n/K_D$).

2) A concave line results, indicating the presence of 2:1 adducts with $K_{D2} > 4K_{D1}$.

3) A convex line results, also indicating the presence of 2:1 adducts with $K_{D2} < 4K_{D1}$.

The method has the disadvantage that the values for the limiting shifts (Δ) must be known for each type of adduct. Therefore, the adopted

approach has been the following:

1) with the experimental data and the approximation $K_{D2} = 4K_{D1}$ and $\Delta_1 = \Delta_2 = \Delta_M$, K_D and Δ_M are obtained which fit the data best;

2) using Δ_M from step 1 and the experimental shifts, a Scatchard plot can be constructed with

$$\bar{\nu} = \frac{\Delta}{\rho\Delta_M}$$

$$\frac{\bar{\nu}}{L_f} = \frac{\Delta}{(\Delta_M - \Delta)R_t} \qquad (29)$$

where $\rho = R_t/L_t$, $L_t = [L] + [R{\cdot}L] + 2[R{\cdot}L_2]$. Their shape indicates which of the three above cases is present and this information is used as guide for step 3:

3) a final refinement is performed to determine values of K's and Δ's that minimize the differences between the experimental and calculated chemical shifts.

Table 5 summarizes values of equilibrium constants and limiting shifts obtained by one of the above methods.

Low temperature nmr has been used to slow down sufficiently the formation (and dissociation) rate of the adducts, so that separate signals have been detected for the free and the complex species. Table 6 summarizes such results from several authors. It is apparent that high order adducts cannot be neglected for monofunctional substrates, but a 1:1 adduct is the most thermodynamically stable species in the case of bifunctional substrates.

Osmometry was applied by Porter *et al.*[56] to the $Eu(fod)_3$-cholesterol system; a very poor determination of K is reported (K_2 in equation 25 ranges from 36.2 to 102.5 M^{-1}). A closer range is obtained

TABLE 5

Values of Equilibrium Constants and Δ Assuming Formation of 1:1 and 2:1 Adducts[a]

Substrate	K_1 (in M^{-1})	K_2 (in M^{-1})	Group	Δ_1 (in ppm)	Δ_2 (in ppm)	Ref
			3-CH_3	4.40	1.84	
3[b]	222	63.4	H_2eq	17.52	7.00	51
			H_2ax	14.56	5.87	
acetone	122	14.8	CH_3	6.36	6.36	53[c]
DMSO	625	63.7	CH_3	3.95	3.95	53[c]
2-propanol[d]	84	38.3	CH_3	5.02	8.97	53[c]
2-picoline[d]	25.3	835	CH_3	1.15	2.29	53[c]

a) Shift reagent $Eu(fod)_3$ in CCl_4

b) Only few groups in the substrate are reported in the present table.

c) Originally K_1 and K_2 were reported as dissociation constants; in the present table $K_i = 1000/K_{Di}$

d) Only the methyl groups signals were analyzed.

TABLE 6

Stoichiometry by Low-Temperature NMR.

Substrate	Shift Reagent	Solvent	n[a]	Ref
DMSO	$Eu(fod)_3$	CD_2Cl_2	1.8 - 2.0	53
3-picoline	$Eu(dpm)_3$	CS_2	2	54
DME[b]	$Eu(fod)_3$	$CDCl_3$	1	55
DME[b]	$Pr(fod)_3$	$CDCl_3$	1	55
DME[b]	$Eu(dpm)_3$	$CDCl_3$	1	55
DME[b]	$Pr(dpm)_3$	$CDCl_3$	1	55

a) n represents the stoichiometry of the adduct $L_n \cdot R$.

b) DME = dimethoxyethane

with a carbonyl iron complex, $(C_5H_5)Fe(CO)_2CN$, with $Ln(fod)_3$ (where Ln = Pr, Eu, Ho, and Yb), from which the most important feature is the observation of 3:1 adducts in the case of Pr.

Only one case has been studied spectrophotometrically: the system chloroquine-$Pr(dpm)_3$[57]. The assumption that only a 1:1 type of complex is present is based on the measurements of the absorbance at 332 nm at different concentrations of the shift reagent. A clear break is shown at $\rho = 1$ suggesting that equation 19 is the most important process involved. The evaluation of the equilibrium constant is based on the absorbance at the given wavelength, which is proportional to the concentration of the free chloroquine. Table 7 compares the results from pmr and the spectrophotometric analysis:

TABLE 7

Comparison of Equilibrium Constants from PMR and Spectrophotometric Methods[a].

Temperature	K (in M^{-1})	
°C	pmr	spectrophotometric
20	64.1	63.17
48	13.93	13.46

a) Substrate: chloroquine; shift reagent: $Pr(dpm)_3$; solvent: $(CD_3)_2CO$

Feibush et al.[58] measured the retention time of several substrates in gas-chromatographic experiments using as columns 0.131 m solutions of different shift reagents in squalene on Gas-Chrom Z (15% coating). Since the retention times can be expected to be proportional to the stability

of complexes between the substrates and the shift reagents, it is possible to establish the relative magnitudes of the corresponding equilibrium constants. From a quantitative point of view, however, such methods may not reflect their results in the nmr applications, mainly because of the different conditions the two experiments require.

RESULTS AND DISCUSSION

Optically Active Shift Reagents

In the preliminary stage of this thesis, emphasis has been placed on the synthesis of optically active β-dicarbonyl compounds which would serve as ligands in the formation of optically active complexes 2, where Ln = a lanthanide ion (III) with R" = an asymmetric center.

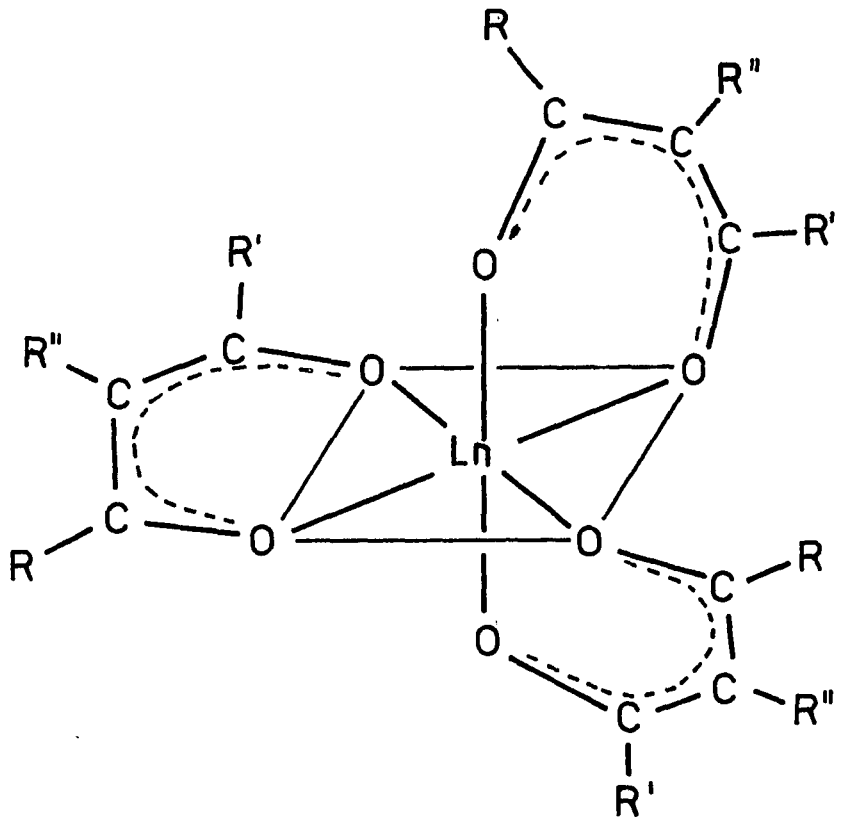

2

For complexes between acetylacetone and hexadentate ligand, the atoms in each chelate ring are coplanar[59], but the chelate itself has three C_2 and one C_3 symmetry axes (point group D_3), and it must therefore be chiral.

Figure 2 shows the possible enantiomers for trischelate octahedral complexes along with the definition of the two absolute configurations Λ and Δ, according to the nomenclature proposed by the Commission on the Nomenclature of Inorganic Chemistry of the International Union of Pure and Applied Chemistry[60].

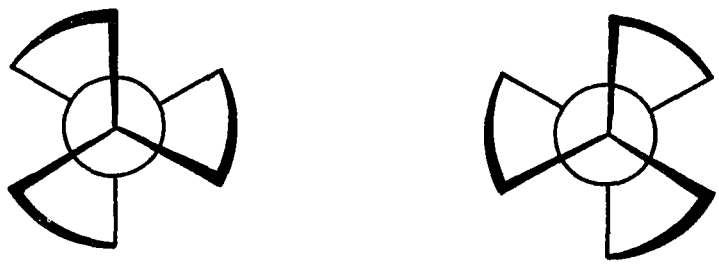

Λ Δ

Figure 2 - Nomenclature for Trischelate Octahedral Complexes.

Interaction of 2 with an enantiomeric mixture should yield four possible isomers, namely Λ(R), Λ(S), Δ(R), and Δ(S), which are not differentiated on the nmr time scale because of one of three possible reasons (or a combination of them):

1) The geometrical changes involved with extra-coordination destroy the original geometry asymmetry, resulting in a mixture of enantiomers;

2) The extra-coordination favors some exchange between the Λ and the Δ configuration;

3) The equilibrium between the lanthanide complex and the incoming molecule, to form higher coordination complexes, is fast, and only the average of all possible combinations is observed in the nmr spectrum.

Whatever the case is, the introduction of an asymmetric group in 2 would eventually produce a diastereomeric mixture: $\Lambda(R^*)$ and $\Delta(R^*)$ ($R^* = R^*$ in 2), which should induce magnetic disymmetry between the enantiomers of an optically active mixture, when this is used as the incoming new ligand.

We chose to form complex 2, using 3-substituted acetylacetone (AcAc) as the ligand ($R = R' = CH_3$ in 2), mainly because of the following reasons:

1) AcAc is readily available;

2) The complexes formed between the metal ion and AcAc are reported to be highly hygroscopic, inducing a low chemical shift in the proton signals of a substrate[61]. On the other hand, the corresponding complexes with dpmH are relatively stable and much less hygroscopic. If steric and/or inductive effects are responsible for such a difference in behavior, alkyl groups at the 3-position in AcAc may induce similar desirable properties;

3) In order to synthesize 3-substituted diketones, AcAc provides less steric effects toward the incoming alkyl group.

In choosing the optically active substituents, the following criteria must have priority:

1) It must be obtainable in high optical purity;

2) If the asymmetry is produced by a chiral center, the substituents at such center must be different enough to induce an observable non-equivalence between the possible complexes of 2 and the enantiomers of the optically active organic substrate.

With these ideas, two R* groups for 2 were chosen:

1) $R^* = \phi\text{-}C(C_2H_5)H\text{-}CH_2\text{-}$, available through the optically active

2-phenylbutyric acid. By reduction of the acid with $LiAlH_4$, the corresponding alcohol is obtained, which can be converted to the halide or tosylate.

2) R* = 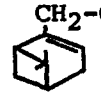 , available commercially as the optically active (-)-alcohol (nopol); due to the high tendency of this system to aromatize, only the corresponding tosylate has been used.

Several attempts, described below, were made to carry out equation 30. Unfortunately, in no case was the 3-alkylated

$$(CH_3CO)_2CH_2 + RX \longrightarrow (CH_3\text{-}CO)_2CHR \qquad (30)$$

AcAc successfully isolated.

Basic Conditions with Potassium Carbonate

Potassium carbonate was used as the base for anion formation from the acetylacetone; this ion would displace the leaving group:

$$\begin{aligned} (CH_3CO)_2CH_2 \quad &+ \quad K_2CO_3 \longrightarrow (CH_3CO)_2CH^- \; K^+ \\ (CH_3CO)_2CH^- \quad &+ \quad R\text{-}X \longrightarrow (CH_3CO)_2CHR \end{aligned} \qquad (31)$$

The method was successful with methyl iodide[62] with a yield of 75 - 77%. (Ethyl and isopropyl iodide were also used, but no yield was reported for these cases.)

However, alkali ions form salts with acetylacetone of high ionic character[63] and with very low solubility in organic media. Dimethyl sulphoxide is known for its properties as a good solvent for charged species, but in neither of these media (acetone or DMSO) the desired product was obtained. Starting materials or elimination products were isolated in high yield (see Experimental).

Besides the solubility problem, cleavage of the acetylacetone, or the alkylated product (if formed) could occur:

$$(CH_3CO)CHR + B^- \longrightarrow CH_3\text{-}\underset{\underset{O^-}{|}}{C}\text{=}CHR + \overset{O}{\overset{\|}{C}}\text{-}CH_3 \quad (B) \qquad (32)$$

Regarding the alkylating agent, the basic conditions favor elimination, which was observed in the case of 2-phenylbutyl iodide:

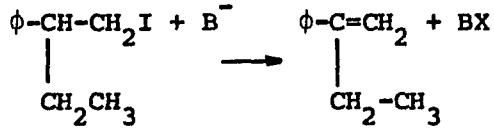

(33)

Acid Conditions with Boron Trifluoride

BF_3 is known to form complexes with acetylacetone of the type[64]:

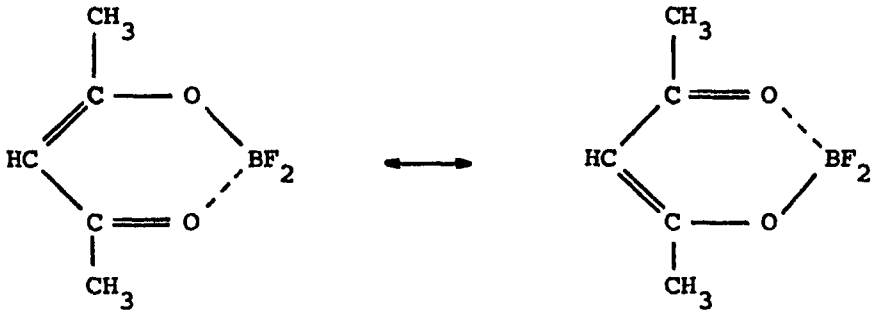

4

providing a potential nucleophile in displacement reactions:

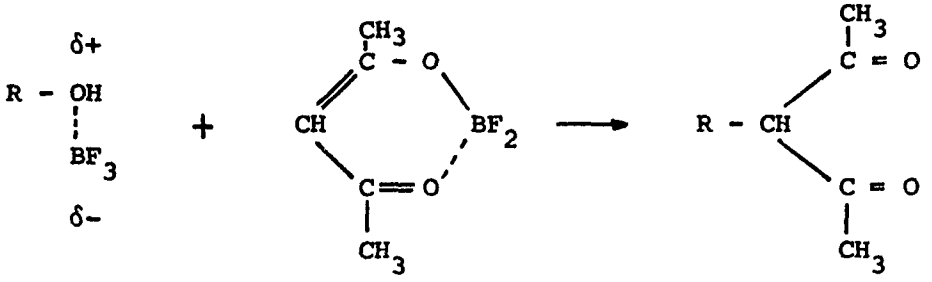

(34)

One advantage of these conditions is that the alcohol can be used directly since BF_3 also forms complexes with alcohols providing a good leaving group.

The technique has been used for ethyl acetoacetate and a series of alkylating agents with yields ranging from 60 - 67% for isopropyl alcohol to 10 - 14% for tert-butyl alcohol[65]. With acetylacetone, the 3-isopropyl derivative has been obtained in a 58% yield[66].

In our case, with acetylacetone:

1) The four member ring in the nopol was apparently unstable under the conditions of the reaction, since the pmr spectra showed a complete change in the ring system (disappearance of the methyl groups of the bridge);

2) For the 2-phenylbutyric alcohol, starting materials were reisolated in high yield.

Considering the classical procedure that leads to the formation of acetylacetone itself (equation 35), the fact that

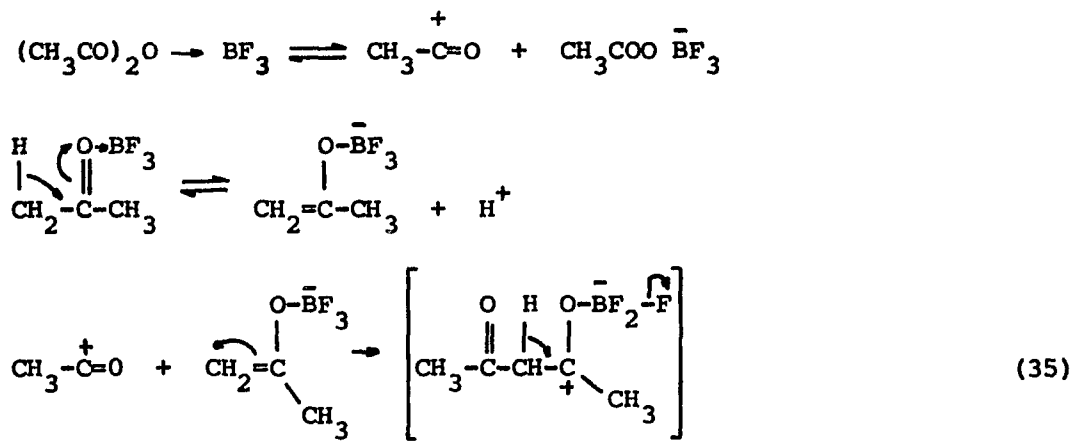

(35)

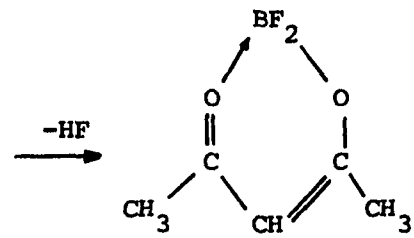

4

no product was obtained with a substituent at the 3-position is partly indicative of the high stability of the complex 4, to which an aromatic character has been attributed[67] (this property has been, however, disputed[68]).

Extractive Alkylation

This relatively new technique was introduced by Brändström et al.

in 1969[69]. It is based on the observation of Schill[70], who used ion pair extraction as an analytical method to extract anions from an aqueous layer into chloroform or methylene chloride. Analytical data clearly indicate that most anions can be extracted as ion pairs with tetrabutylammonium as the cationic part.

On a preparative scale, ion pair extraction is a surprisingly simple procedure: when a weak acid, HA, is shaken with a concentrated aqueous solution of tetrabutylammonium hydroxide, QOH, the ion pair Q^+A^- appears in the chloroform layer. In this way, compounds containing an active methylene group such as methyl acetoacetate[71], methyl cyanoacetate[72], acetylacetone[73] and dimethyl benzoylmalonate[74] have been alkylated by adding an alkyl halide to the chloroform extract. Even weaker acids, such as benzyl cyanide[75], give similar results, but for this case no separation of the two layers is performed due to the lower concentration of the ion pair. However, its reactivity is high enough to permit a rapid alkylation in the presence of an alkyl halide. With acetylacetone itself, excellent results have been obtained[73]; alkylation products have been isolated in quantitative yield.

We applied the technique to our case: 2-phenylbutyl iodide gave only elimination products (equation 33) and the corresponding tosylate gave no indication of alkylation based on pmr analysis of the resulting mixture (see Experimental).

We feel that this method could be successful if the conditions of the reactions were optimized; however, due to the increased use and effectiveness of other optically active shift reagents (from derivatives of camphor as the ligands), preparation of these new compounds is interesting only from the synthetic point of view. Since our original interest was the

interaction between the shift reagents and substrates, we directed our attention to the study of different aspects of the properties of such a useful tool in nmr analysis.

$La(dpm)_3$ as a Diamagnetic Shift Reagent

As described in the Introduction, the origin of the chemical shifts induced by paramagnetic lanthanide complexes is mainly dipolar. For geometrical correlations, however, it is necessary to assure such dipolar nature, or at least to correct the observed shifts for those produced by possible additional mechanisms; that is, for the contact induced shifts (CIS) and the complex formation shifts (CFS).

For saturated systems, the elimination of the data corresponding to the nuclei next to the coordination center has been suggested[3], since the CIS and the CFS are transmitted through bonds and decline rapidly if only σ bonds are present.

In an unsaturated system, however, π bonds may facilitate the transmission of contact mechanism and complex formation effects through the chain. The case of pyridine and derivatives is particularly recalled, since it has been the subject of several studies[46,76], with a common observation among them: The ratio between the observed shifts for a given nucleus in the presence of two different shift reagents is not a constant for all the nuclei in the molecule, which would be expected if the observed shifts were purely dipolar and the structures of the two adducts (with each shift reagent) were the same. Such non-constant ratios have been attributed to a contact mechanism, but may also be due in part to a CFS mechanism.

Corrections for the CIS could be obtained using Gd^{+3} complexes,

but unfortunately severe broadening in the signals makes such measurements useful only for line width data. Corrections for the CFS are easier to determine with the corresponding complexes of La^{+3} or Lu^{+3}.

La(III) was arbitrarily chosen in this study as the diamagnetic lanthanide ion; the dpm ligand, however, was also our choice in later studies, so it was selected by analogy. Unfortunately, the solubility of $La(dpm)_3$ in CCl_4 and $CDCl_3$ is very low, and in some cases, it was not possible to analyze the diamagnetic effects over a wide concentration range.

$La(dpm)_3$ and Pyridine

The CFS induced by $La(dpm)_3$ on the pyridine protons using CCl_4 as solvent are given in Table 8 and Figure 3 as a function of ρ(=[$La(dpm_3$]/[Pyridine]) and the concentration of the substrate.

With $CDCl_3$ as the solvent, the CFS were recorded at [Pyridine] = 0.695 M only, which are reported in Table 9 and Figure 4. In both solvents, downfield shifts are recorded as positive.

Several observations deserve comment.

It is a generalization that the chemical shifts induced by a shift reagent in CCl_4 solutions are larger than in $CDCl_3$[53]; this has been attributed to a larger equilibrium constant for adduct formation in the first solvent. This generalization cannot be applied in this case because, while the ortho protons do display this type of behavior, the meta and para protons do not. It is clear that such an explanation is not sufficient since the shifts show a completely different pattern not only in the magnitude but also in the direction of the displacement.

Especially for the CCl_4 solutions (Figure 3), a non-linear correlation between the observed chemical shifts and ρ is evident.

TABLE 8

Chemical Shifts Induced by $La(dpm)_3$ for Protons in Pyridine Using CCl_4 as Solvent.

		Chemical Shifts (in Hz)[a]		
[Pyridine]	ρ	H_2	H_3	H_4
0.548	0.87	24.39	2.53	5.14
0.548	0.63	21.50	1.14	3.86
0.548	0.60	20.06	0.91	3.26
0.548	0.31	9.24	-2.24	-0.39
0.548	0.24	6.96	-2.34	-0.99
0.274	1.26	24.26	5.96	8.61
0.274	0.74	21.86	3.16	5.96
0.274	0.69	19.86	1.71	5.09
0.274	0.35	11.46	-1.06	1.01
0.137	1.28	22.24	5.29	8.09
0.137	0.72	18.74	2.59	5.69
0.137	0.43	12.89	0.14	2.54
0.683[b]	0.	878.95	742.48	782.13

a) Relative to the position at ρ = 0 unless otherwise stated.

b) Chemical shifts in Hz relative to TMS.

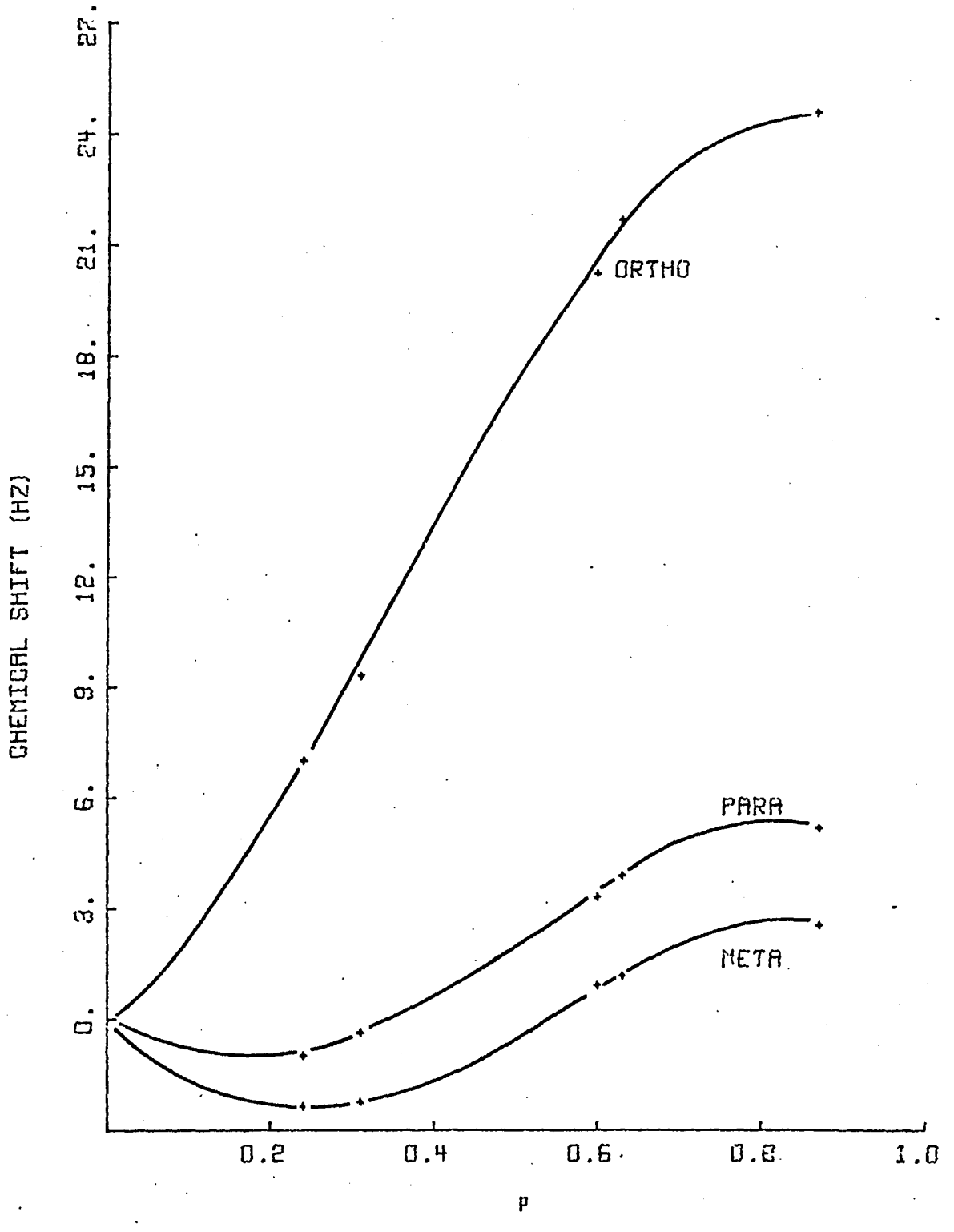

Figure 3 - Chemical Shifts of Pyridine vs. ρ in CCl_4 Solutions.

TABLE 9

Chemical Shifts Induced by $La(dpm)_3$ for Protons in Pyridine Using $CDCl_3$ as Solvent[a].

	Chemical Shifts (in Hz)[b]		
ρ	H_2	H_3	H_4
0.15	2.62	-2.63	-1.75
0.28	4.58	-4.85	-3.53
0.45	6.84	-5.78	-4.16
0.58	9.09	-6.97	-4.74
0.75	10.80	-7.56	-5.63
0[c]	888.69	752.06	792.13

a) [Pyridine] = 0.695M.

b) Relative to the position at ρ = 0 unless other stated.

c) Chemical shifts in Hz relative to TMS.

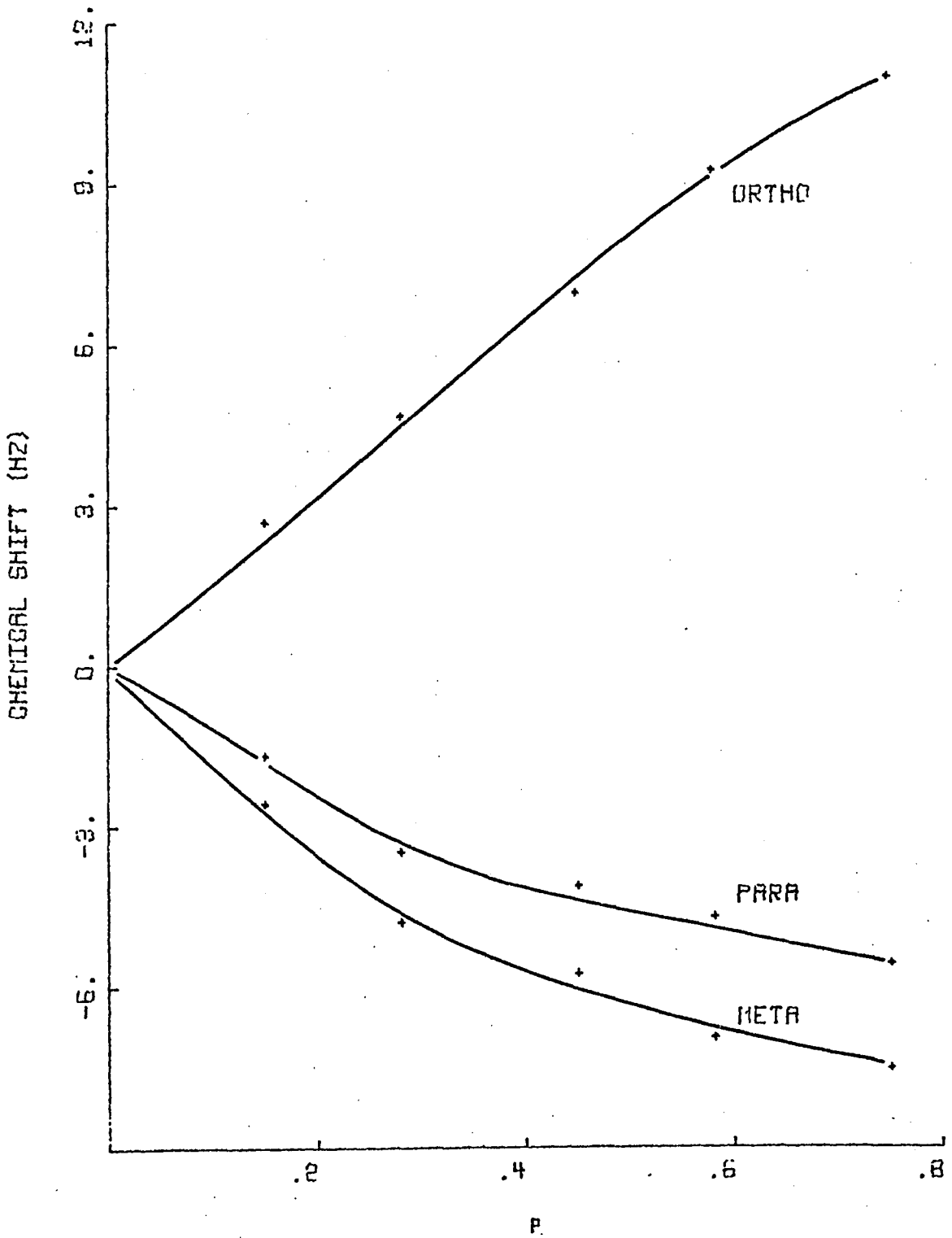

Figure 4 - Chemical Shifts of Pyridine vs. ρ in $CDCl_3$ Solutions.

This observation has been reported previously also by Tori et al.[23] using $La(fod)_3$ as the diamagnetic shift reagent for the CFS in pyridine derivatives. The presence of adducts of different stoichiometry at different ρ[51,72] has been suggested as a possible explanation.

Since the magnitudes of the displacements are relatively low, any quantitative analysis should include:

a) The reaction field of the solvent: CCl_4 is an inert solvent, but subject to polarization by the solute permanent dipoles; this modifies in turn the electron distribution in the surrounding molecules to an extent depending on their polarizability. $CDCl_3$ is not an inert solvent[11], the reaction field is stronger in this medium and furthermore hydrogen bonding is likely to be present:

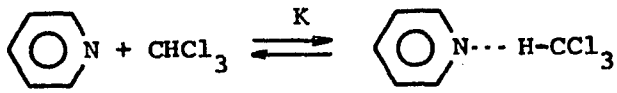

$K = 0.69\ M^{-1}$ (36)

(Isotope effects will tend to decrease the value of the equilibrium constant.)

b) Self-association of pyridine which may occur via charge transfer complexes and/or dipolar attraction.

c) The possibility of adduct formation of different stoichiometry, as suggested by Tori[23].

d) The diamagnetic effect of the $La(dpm)_3$ itself.

Tables 8 and 9 also report the chemical shifts of pyridine in the two solvents at approximately the same concentration, using TMS as the internal reference. The difference between them is of a magnitude comparable to the shifts induced by the diamagnetic shift reagent, clearly indicating that the solvent effect cannot be ignored if a quantitative analysis is to be carried out.

In order to correct the chemical shifts induced by a paramagnetic lanthanide complex for the CFS contribution, probably the best

procedure would be to analyze nmr spectra in the presence of La(III) (or Lu(III)) complexes under the following conditions:

1) Use of the same solvent;

2) Use of the same substrate concentrations;

3) Use of ρ such that the amount of the bounded substrate would be the same in both cases.

While the first two conditions are easily fulfilled, the third one requires the knowledge of equilibrium constant and stoichiometry for the lanthanide complexes/substrate system. From the above considerations, it appears that for a diamagnetic lanthanide complex the nmr is not the best pathway to such determinations. Only as a first approximation may shifts observed with a paramagnetic shift reagent be corrected for the CFS by subtracting the corresponding shifts with La(III) complexes extrapolated to the same value of ρ.

$La(dpm)_3$ and Aliphatic Systems

For statistical reasons, it is convenient to have as many observations as possible for correlations between chemical shifts and geometry; so to discard the data corresponding to the nuclei next to the coordination center in the case of aliphatic systems, would be an undesirable alternative except in the case of large molecules, where many observations are available.

Again, the chemical shifts induced by a diamagnetic shift reagent would be of CFS nature, and an estimation of their magnitude with several Lewis bases is desirable.

Table 10 includes shifts induced by $La(dpm)_3$ on a few aliphatic substrates. For comparative purposes, the reported data correspond to the extrapolation value at $\rho=1$, along with the maximum ρ achievable.

TABLE 10

Chemical Shifts Induced by $La(dpm)_3$ in Aliphatic Systems[a].

Substrate	Solvent	Maximum ρ	Shifts extrapolated to ρ = 1 in ppm
ethanol	$CDCl_3$	0.48	1.06 (OH) 0.13 (CH_2)
dimethyl sulphoxide	CCl_4	1.03	0.14 (CH_3)
2-pentanone	$CDCl_3$	0.22	0.0 (CH_2) 0.0 (CH_3)
camphor	CCl_4	0.31	0.0 (αCH_2)
diethylamine	$CDCl_3$	0.65	0.0 (CH_2) 0.0 (CH_3)
exo,exo-2, 3-camphanediol	CCl_4	0.69	0.33 (C_2H)[b] 0.0 (C_3H)

a) For clarity of the table, the non-shifted signals are omitted in some cases.

b) Extrapolated from measurements at $\rho < 0.3$.

The CFS for ethanol are of the order of 2% of those induced by $Eu(dpm)_3$[61] for the OH and 0.1% for CH_2, while the methyl group remains unchanged. The shift observed in dimethyl sulfoxide[78] is 2.5% of the corresponding shifts with $Eu(dpm)_3$. The pmr signals for 2-pentanone remain unaltered by the addition of $La(dpm)_3$, but it was not possible to dissolve an appreciable amount of the shift reagent in this case. Similarly, no shift is observed for camphor at the maximum ρ achievable of 0.31. The diethylamine signals also remain unaffected by the $La(dpm)_3$, interaction between the two reactants is obviously present since the high value of ρ, so it is surprising that no CFS is observed.

Without implying an explanation for the behavior of this group of substrates, the effect of the solvent, self-association, dielectric constant, and the presence of several species must be included once more in any interpretation. It is recalled[79] that a difference of -4.9 ppm is reported for the chemical shift of the OH in ethanol (in CCl_4 solutions) between the associated molecules and the corresponding value at infinite dilution with a value for the equilibrium constant for self-association of 51 M^{-1}. The self-association in the case of amines is weaker (for diethylamine[11] $K = 2.75\ M^{-1}$). The difference in solvents does not allow a direct comparison with the shifts observed in the present work, since hydrogen bonding will likely occur between the substrate and $CDCl_3$ when this is used as a solvent, but the magnitude is recalled as a basis to state that the CFS do not arise from a single mechanism.

In order to eliminate the possibility of several types of adducts being formed, exo,exo-2,3-camphanediol was also analyzed (see the last entry in Table 10). The protons α to the OH are the only ones affected by the addition of $La(dpm)_3$ to a 2% extent in comparison to the shifts

induced by $Eu(dpm)_3$. Since the molecule contains two sites of coordination, it is expected that only one type of adduct (1:1) will be formed, but a clear non-linearity (Figure 5) is also found for this case, which can only be due to a combination of contributions to the CFS.

$La(dpm)_3$ and Coupling Constants

Shapiro et al.[80] reported that the coupling constant for the α-geminal protons in camphor shows a change of 0.5 Hz (becomes more negative) upon the addition of $Eu(dpm)_3$ ($\rho = 0.3$). Similar observations[61,80-85] have been reported. The mechanism for such effects is still under investigation, but several suggestions have been offered. Among them are conformational changes[81], a contact mechanism[61], chemical-exchange-spin decoupling[82] and the Lewis acid nature[80] of the shift reagent (substituent effect).

Whatever the mechanism is, it must also account for the observation in the present work: of the compounds analyzed and listed in Table 10, only camphor showed a dependence of the coupling constants upon the addition of the $La(dpm)_3$. A change from -17.8 Hz at $\rho = 0$ to -18.7 Hz at $\rho = 0.31$ is observed for the $^2J_{HH}$(C-3) which is comparable to the change induced by $Eu(dpm)_3$ in Shapiro's report[80].

The dependence of the coupling constant of geminal protons on conformational changes is small compared to the substituent effect, especially when π bonds are involved[9], and particularly when the plane containing C_1-C=X is perpendicular to the plane formed by H-C_1-H. Conformational changes,however, are not ruled out by the observation in the present work, even if the magnitude of the change in ^2J is better explained by the Lewis acid nature of the shift reagent. The contact

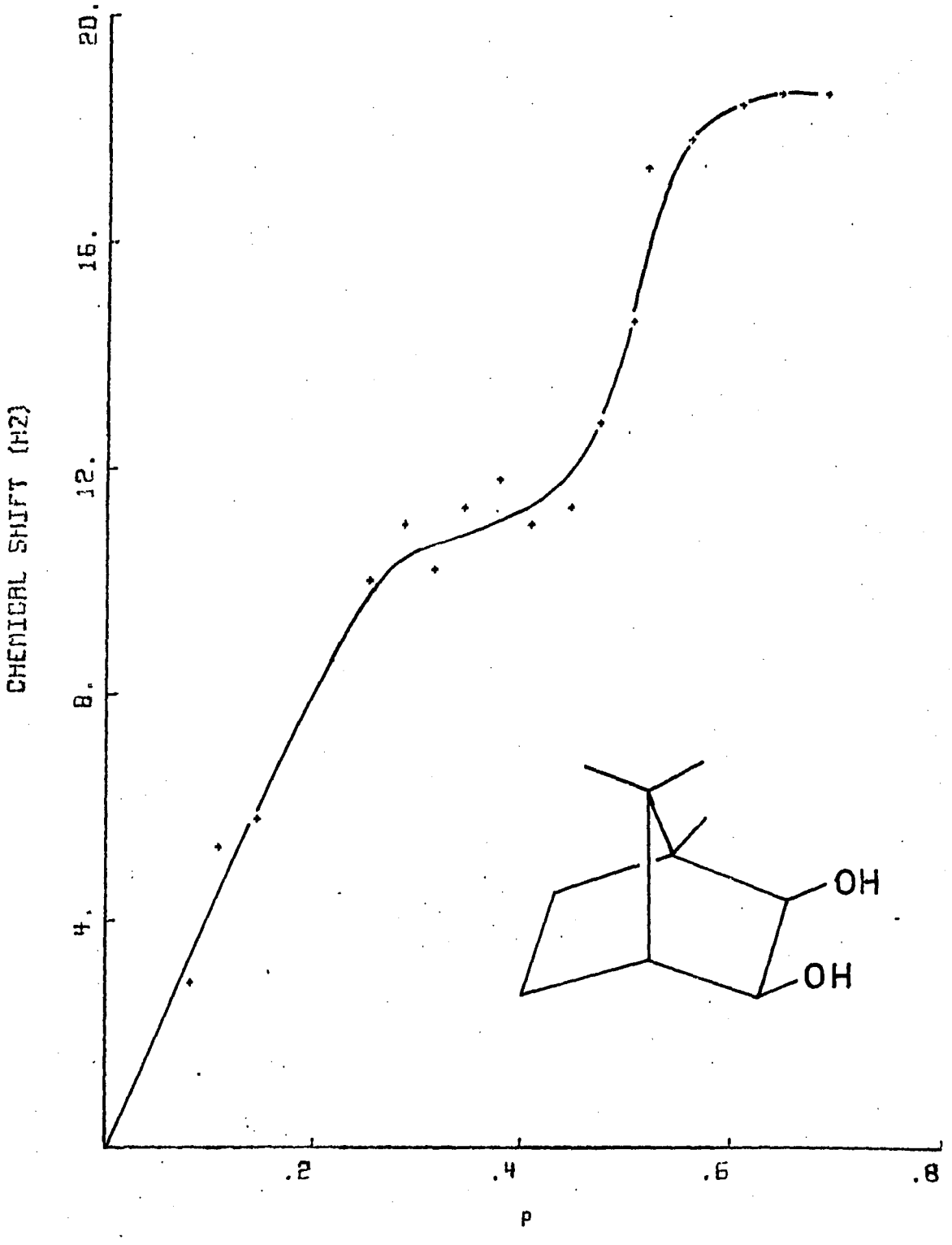

Figure 5 - Chemical Shifts of AB Spectrum in exo,exo-2,3-Camphanediol as a Function of ρ.

mechanism and the chemical exchange-spin decoupling are not likely causes for the change in the coupling constants, since they are associated only with the presence of unpaired electrons.

Analysis of Lanthanide-Induced Shifts (LIS) in Borneol

Because of its rigid structure, borneol has been selected on several occasions for correlations between geometrical structure and chemical shifts induced by lanthanide complexes (dpm and fod).

As already mentioned in the introduction, there are several assumptions made when the McConnell equation is applied to the LIS analysis. Hawkes et al.[84] attempted to determine quantitatively the importance of one such assumption; that is, the orientation of the principal magnetic axis, since generally it is supposed to be colinear with the Ln-O bond. Their conclusion was that deviation of such co-linearity is small (< 2°); $Ln(fod)_3$ (Ln = Eu and Pr) was used as the shift reagent. As will be shown by the study of equilibrium constants and stoichiometry in the present work, fluorinated lanthanide complexes tend to form 2:1 adducts.

We also selected borneol for similar studies, with particular attention to the following:

1) Selection of a geometrical structure for borneol;
2) Use of the LaMar correlation for the C_{2v} point group;
3) Importance of rotamer population distribution;
4) Influence of contact interactions by neglecting the α-proton in the calculations;
5) Colinearity of the magnetic axis and the Ln-O bond;
6) Treatment of the methyl groups.

Chemical shift data were obtained by a direct determination and by competitive systems analysis (see Borneol and $Eu(dpm)_3$). They are summarized in Table 11.

Selection of a Geometrical Structure for Borneol

Since no X-ray analysis has been reported for complexes between borneol and the shift reagent (which is the most common case for other substrates), we chose three similar molecules and used the results reported from their X-ray analysis. The final coordinates for protons in the borneol structure are summarized in Tables 12 - 14 and correspond to the convention represented in Figure 6.

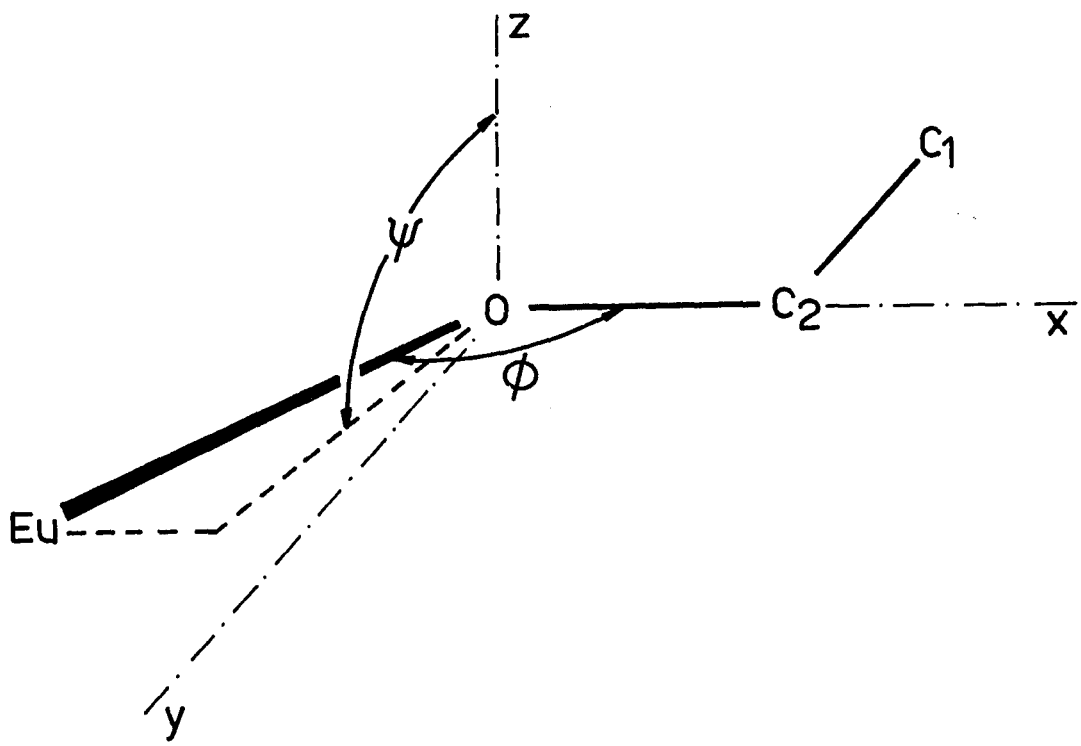

Figure 6 - Orientation of Atoms in the Conventional Coordinate System. The oxygen atom is located along the x axis and C_1 lies on the xy plane. ϕ is the angle Eu-O-C_2. ψ is the angle between the z axis and the projection of the Eu coordinates on the yz plane.

TABLE 11

PMR Chemical Shifts for Borneol (Shift Reagent $Eu(dpm)_3$).

Proton	LIS from Direct[a] Determination	LIS from Competitive[b] Systems	Ratio
2-<u>exo</u>	24.3	21.18	1.14
3-<u>endo</u>	16.63	14.13	1.18
3-<u>exo</u>	8.65	7.63	1.13
4	5.57	4.12	1.35
6-<u>endo</u>	17.36	14.57	1.19
1-CH_3	8.47	7.13	1.19
7-CH_3-<u>anti</u>	3.84	3.24	1.19
7-CH_3-<u>syn</u>	4.22	3.79	1.11

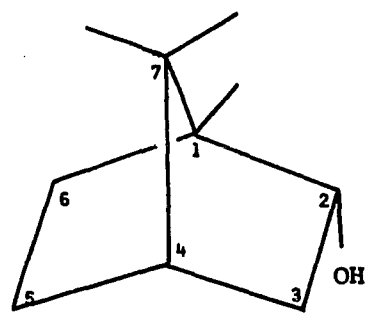

<u>5</u>

a) in CCl_4

b) in $CDCl_3$

TABLE 12

Coordinates for Protons in Borneol from ref 85[a].

Atom	x	y	z
Oxygen	0.	0.	0.
2-<u>exo</u>	1.76 (1.81)	0.60 (0.72)	-0.83 (-0.70)
3-<u>exo</u>	2.66 (2.24)	1.37 (1.32)	0.99 (1.45)
3-<u>endo</u>	1.12 (0.67)	1.05 (0.59)	1.90 (2.00)
4	3.21 (2.81)	-0.30 (-0.47)	2.87 (3.12)
6-<u>endo</u>	0.06 (0.27)	-2.11 (-2.22)	0.81 (0.45)
1-CH_3[b]	2.18 (2.65)	-2.20 (-2.03)	-1.67 (-1.65)
7-CH_3-<u>anti</u>[b]	4.30 (4.15)	-2.80 (-2.78)	1.28 (1.51)
7-CH_3-<u>syn</u>[b]	4.69 (4.56)	-0.31 (0.11)	0.03 (0.57)
	2.83	-1.41	-1.95
1-CH_3[c]	2.56	-3.07	-1.26
	1.15	-2.11	-1.87
	4.49	-2.93	0.26
7-CH_3-<u>anti</u>[c]	4.94	-2.20	1.85
	3.48	-3.26	1.73
	4.79	-1.08	-0.68
7-CH_3-<u>syn</u>[c]	5.24	-0.34	0.92
	4.03	0.49	-0.15

a) Numbers in parentheses are from the prime molecule reported in ref 85 (see text).

b) As a point group along the C-C bond.

c) The three coordinates correspond to each proton in the most stable staggered conformation.

TABLE 13

Coordinates for Protons in Borneol from ref 88.

Atom	x	y	z
Oxygen	0.	0.	0.
2-<u>exo</u>	1.19	0.30	-1.07
3-<u>exo</u>	2.54	1.69	1.21
3-<u>endo</u>	1.15	0.70	1.64
4	3.67	-0.12	2.43
6-<u>endo</u>	0.82	-2.46	1.08
1-CH_3[a]	2.32	-2.12	-1.57
7-CH_3-<u>anti</u>[a]	4.76	-2.18	0.97
7-CH_3-<u>syn</u>[a]	4.47	0.67	-0.32

a) As a point group along the C-C bond.

TABLE 14

Coordinates for Protons in Borneol from ref 89.

Atom	x	y	z
Oxygen	0.	0.	0.
2-<u>exo</u>	1.78	0.61	-0.87
3-<u>exo</u>	2.55	1.54	1.09
3-<u>endo</u>	1.09	0.93	1.96
4	3.64	-0.22	2.66
6-<u>endo</u>	0.12	-1.99	1.03
1-CH_3[a]	2.31	-2.30	-1.62
7-CH_3-<u>anti</u>[a]	4.3	-2.81	1.11
7-CH_3-<u>syn</u>[a]	4.56	-0.11	-0.28
	2.90	-1.50	-1.94
1-CH_3[b]	2.74	-3.11	-1.11
	1.27	-2.29	-1.80
	5.03	-2.26	1.63
7-CH_3-<u>anti</u>[b]	4.42	-3.00	0.09
	3.45	-3.16	1.62
	5.24	-0.11	0.53
7-CH_3-syn[b]	4.62	-0.85	-1.02
	3.82	0.63	-0.33

a) As a point group along the C-C bond.

b) The three coordinates correspond to each proton in the most stable staggered conformation.

A more specific description is necessary in regard to the extrapolation of the proton coordinates from each model molecule.

(±)-10-Bromo-2-chloro-2-nitrosocamphane (6) forms asymmetric crystal units which consist of two crystallographically independent chemical molecules. Two sets of coordinates are therefore available as reported by Ferguson et al.[85]. Since only carbons and heteroatoms are given, extrapolation from each molecule includes:

1) Location of the oxygen atom along the C_2-N bond at 1.43 Å[86] from C_2;

2) Location of proton 2-exo at 1.073 Å[86] from C_2 and along the C_2-Cl bond;

3) Location of hydrogens 3,5, and 6 by the same geometrical distribution as given for norbornane[87];

4) Location of hydrogen 4 at 1.11 Å[87] from C_4 and on a vector perpendicular to the plane C_3-C_7-C_5 which passes through C_4.

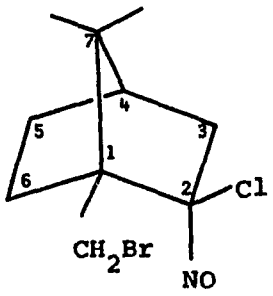

6

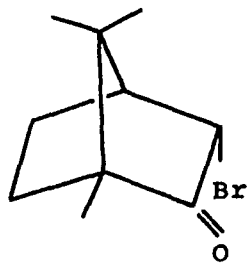

7

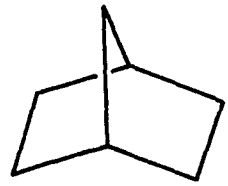

8

As a model for borneol, (±)-3-bromocamphor (7) suffers because of the sp^2 hybridization at C_2, which distorts the geometry with respect to borneol. In order to approximate the borneol structure, the 5 membered ring formed by C_4, C_5, C_6, C_1 and C_7 was projected through C_4, C_1, C_7 plane to simulate the geometrical coordinates for the ethylene bridge.

Proton coordinates were reported by Allen et al.[88] as the result of X-ray analysis, so only the position of the oxygen atom was approximated along the corresponding C-H at 1.43 Å[86] from C_2.

Norbornane itself (8) was a model compound for borneol; electron diffraction studies were reported by Chiang et al.[89]. Inclusion of the necessary methyl and oxygen positions was accomplished as follows:

1) The oxygen atom was located in the same manner as for 6:

2) The C's for the methyl groups were located along the respective C-H bonds at a distance from the atoms of the bicycle at which they are attached as given by Ferguson et al.[85].

The position of hydrogens in the methyl groups were also considered separately, in a staggered conformation, which is included in Tables 12 and 14 (last three entries). Bond angles and distances were standard[86].

Because of the frequent use of framework molecular models, coordinates were also obtained by this method, and are summarized in Table 15.

Classical Approach to the Analysis of LIS

As described in Appendix 1, the straight forward application of the McConnell formulation (equation 10) involves only optimization of three parameters; they are the distance Ln-O and the angles ϕ and ψ of Figure 6. Results for the five molecules with both sets of LIS data are given in Table 16, where R is defined in Appendix 1 as:

$$R^2 = \frac{\sum_{i=1}^{7} (SC_i - SO_i)^2}{\sum_{i=1}^{7} (SO_i)^2} \qquad (37)$$

TABLE 15

Coordinates for Protons in Borneol Using Framework Molecular Models[a].

	x	y	z
Oxygen	0.	0.	0.
2-<u>exo</u>	1.85	0.50	-1.00
3-<u>exo</u>	2.75	-1.65	-1.00
3-<u>endo</u>	1.20	-2.25	0.20
4	3.50	-2.50	1.35
6-<u>endo</u>	0.05	0.00	2.10
1-CH_3[b]	2.05	2.35	1.35
7-CH_3-<u>anti</u>[b]	4.25	0.10	3.10
7-CH_3-<u>syn</u>[b]	4.60	0.25	0.00

a) Convention in the coordinates system is different from Figure 6.

b) As a point group along the C-C bond.

TABLE 16

Least-square Fit of LIS in Borneol to Axial Symmetry Approximation.

Borneol Coordinates derived from	LIS from Direct Determination	LIS from Competitive Systems
Structure 6	Ln-O = 2.98 Å ϕ = 127° ψ = 109° R = 1.3%	Ln-O = 3.04 Å ϕ = 125° ψ = 111° R = 2.02%
Structure 6'	Ln-O = 1.80 Å ϕ = 155° ψ = 110° R = 5.5%	Ln-O = 2.82-2.72 Å[a] ϕ = 116-121° ψ = 111-117° R = 12.5%
Structure 7	Ln-O = 0.75 Å ϕ = 151° ψ = 118° R = 14.2%	Ln-O = 0.76 Å ϕ = 151° ψ = 118° R = 15.1%
Structure 8	Ln-O = 3.05 Å ϕ = 127° ψ = 117° R = 2.9%	Ln-O = 3.14 Å ϕ = 125° ψ = 118° R = 2.5%
Framework Molecular Models	Ln-O = 3.65 Å ϕ = 119° ψ = 187° R = 2.8%	Ln-O = 1.71 Å ϕ = 194° ψ = -29° R = 7.2%

a) No convergence.

One is immediately struck with the large variation in Ln-O, C-O-Ln angle and R from model to model. The importance of a model compound, even for a classical application of equation 10, is clear, and if not selected properly can introduce serious errors in any conclusions.

It would be a tedious procedure to analyze each effect mentioned in the section Analysis of Lanthanide-Induced Shifts in Borneol for each set of data and for each molecule. It appears to be a better procedure to select the best models by the results of Table 16 using the criteria suggested by Hamilton[90] by determining the confidence level according to the R value ratio.

Among the first four entries for the coordinate models, two groups are clearly differentiated, molecules 6 and 8 afford R factors much smaller than 6' and 7. A ratio 5.5/2.9 (that is, the best R among results from 6' and 7 and the worst R among results from 6 and 8) allow acceptance of structure 8 at the 75% confidence level. The confidence level for the model which results in a 2.9% R factor vs. the other entries for 6' and 7 is in the range of 97.5% or higher. Even if a 75% confidence level is not enough to discard coordinates from 6', in order to test the factors mentioned in Analysis of Lanthanide-Induced Shifts in Borneol, the preference was given to the best four fits among Table 16. The selection of coordinates from 6 and 8 over those of 6' and 7 is strengthened by noting the relatively short Ln-O bond distances produced by the latter two models.

Framework molecular models present a special case. The non-selection of this set of coordinates for further analysis is not based principally on the R factors ratio, but rather on the magnitude of the

Ln-O bond distances, which results in high and low values depending on the set of LIS used (comparing with other systems, the Ln-O bond distances generally lie in the range 2.5-3 Å).

The example included in Appendix 1 corresponds to this type of correlations (coordinates from 6 and LIS obtained by direct determination).

Use of LaMar Correlation for C_{2v} Point Group

Since both sets of data for the LIS of Table 11 are obtained using $Eu(dpm)_3$ as the shift reagent, which forms a 1:1 adduct (see Borneol and $Eu(dpm)_3$), the geometric distribution for heptacoordinated complexes will be considered next.

Three geometrical arrangements are known for coordination number 7[19] and, in analogy with X-ray analysis in the case of other substrates, it can be extrapolated that the arrangement of Figure 7 will also be preferred in the present case.

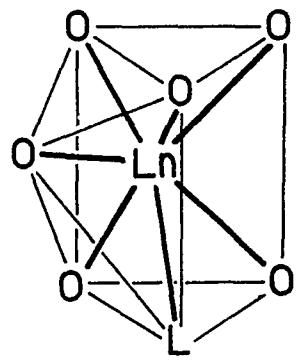

Figure 7 - Geometrical Arrangement for Heptacoordinated Lanthanide Complexes. Addition of the seventh coordination site can be visualized to occur above the center of one of the rectangular faces of a trigonal prism.

Considering only the central ion, the orbital distribution belongs to the C_{2v} point group, so application of equation 14 could be expected to result in a better agreement. Table 17 summarizes such

TABLE 17

Least-square Fit of LIS in Borneol to C_{2v} Point Group[a,b] (1 Rotamer).

Borneol Coordinates derived from	LIS from Direct Determination	LIS from Competitive Systems
Structure 6	Ln-O = 3.01 Å	Ln-O = 3.09 Å
	ϕ = 128°	ϕ = 124°
	ψ = 118°	ψ = 97°
	C_2 = 0.10	C_2 = -0.14
	α = 22°	α = 1.4°
	R = 1.08%	R = 0.8%
Structure 8	Ln-O = 2.67 Å	Ln-O = 3.25 Å
	ϕ = 119°	ϕ = 126°
	ψ = 173°	ψ = 129°
	C_2 = 0.71	C_2 = 0.21
	α = 57°	α = 31°
	R = 0.8%	R = 2.14%

a) $$\frac{\Delta H_i}{H_o} = C_1 \left(\frac{3\cos^2 \Theta_i - 1}{r_i^3} - \frac{3}{2} C_2 \frac{\sin^2 \Theta_i \cos \Omega_i}{r_i^3} \right)$$

where Θ_i, r_i and Ω_i are defined in Figure 25 (Appendix 1).

b) α = angle of rotation around z' axis (see Appendix 1).

results by optimizing the parameters Ln-O distance, the angles ϕ and ψ (Figure 6), the constant C_2 (equation 14) and the rotation through z (see Appendix 1).

The 0.8% value for the R factor is the best fit obtained among Tables 17 to 22. However, the conclusion that a lower symmetry equation better describes the observed LIS should not be taken too literally. In the first place, all entries in Table 17 are the result of 5 parameter optimization with 7 observations; this leaves only 2 degrees of freedom. For this case, Hamilton's statistics provides for accepting the models with a R = 0.8% over the model with R = 2.14% at the 50% confidence level (within the same table).

In the second place, comparing the results from the classical approach (Table 16) with the ones obtained by lower symmetry (Table 17), the following observations can be made: The directly determined LIS and coordinates from 8 result in the higher difference in the R factors among the entries of both tables; using the Hamilton criteria for the confidence level, a 90% is predicted for the accuracy of the C_{2v} model for this group of coordinates and LIS. Since the difference in the R factors for the other data set are lower, it cannot be stated that the C_{2v} model is a better representation for the correlation of LIS with geometrical factors.

Previous attempts to establish the importance of a C_{2v} approximation (LaMar equation), were carried out by Cramer and Dubois[54] for the LIS in 3-picoline using $Eu(dpm)_3$ as the shift reagent. At -115°C, two peaks for each proton in the complexed molecule were observed, which has been explained by the non-axial symmetry. A value of R = 0.337 was obtained with the axial symmetry assumption, while a value of R = 0.038

resulted from a C_{2v} equation. This difference allows the rejection of the axial symmetry assumption with a 99% confidence.

This could be interpreted by either, Huber[33] and Briggs et al.[34] or Dyer et al.[35] arguments. The low temperature could reduce the free rotation around the Ln-N bond and reduce the rate of exchange of free and complexed molecules, that at room temperature were used to justify the axial symmetry approximation.

Importance of Rotamer Population Distribution

Since the Eu ion is not located along the C_2-O bond, the presence of only 1 rotamer could be a simplified model, even if position A in Figure 8 is likely to represent the most stable (and so, the more populated) rotamer, because it is the least sterically crowded.

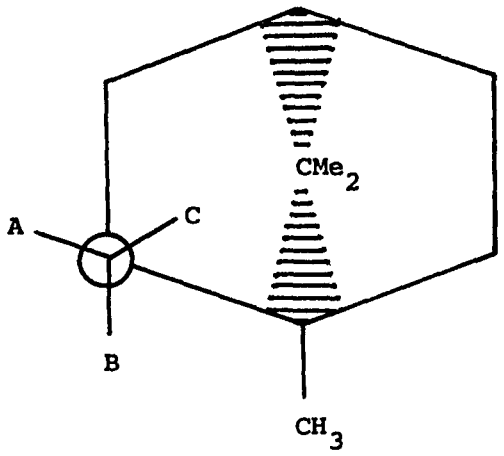

Figure 8 - Staggered Rotamers for Borneol. A, B and C are the three possible conformers for the location of the Eu ion attached to the oxygen atom.

It is understood that analysis for rotamer population distribution could be better performed by including all possible rotamers, but restriction to the three more thermodynamically stable rotamers (at staggered position) should be representative for the total distribution to a first

approximation.

Table 18 includes results for the least square fits, where the angle is fixed to the staggered position defined by A in Figure 8 and the other rotamers are located 120° apart. Because of the presence of the bicycle, the high values for the R factors in this table are probably due to the poor selection for the ψ angle, but attempts to optimize this parameter also were unsuccessful.

Two general conclusions can be drawn; on the one hand, position A always results in the higher populated rotamer, which is in agreement with the result of a single rotamer analysis. On the other hand, the relative population of the rotamers B and C depends on the chosen model. Using directly determinated LIS with model 6, rotamer B is more populated than C, but the opposite results from the same LIS set and coordinates from 8. A 5.36/5.13 ratio for the R factors attributes less than 50% confidence in the model with the lower R factor, and, in both cases, values of bond distances and angles are reasonable. From steric considerations, however, rotamer B should be less sterically crowded than C, so a higher confidence is placed in the analysis that results in this rotamer population distribution.

Analysis of rotamer population was performed by Wing et al.[31] and Armitage et al.[91] on a number of substrates. It appears that such analysis could be of great importance in some cases, since it could account for a wrong assignment of the signals when stereochemical information is desired. In the particular case of bicycles, a series of analyses is presented by Wing et al.[31], that justifies the order of expected population distribution, based on steric considerations.

Similar calculations for the C_{2v} point group affords Table 19. The most important feature in this table is the importance of the accuracy

TABLE 18

Least-square Fit of LIS in Borneol to McConnell Equation (3 Rotamers[a]).

Borneol Coordinates derived from	LIS from Direct Determination	LIS from Competitive Systems
Structure 6[b]	Ln-O = 2.94 Å rot. pop. = 0.89,0.11,0. ϕ = 130° R = 5.13%	Ln-O = 2.96 Å rot. pop. = 0.90,0.10,0. ϕ = 128° R = 5.58%
Structure 8[c]	Ln-O = 2.58 Å rot. pop. = 0.70,0.09,0.21 ϕ = 140° R = 5.36%	Ln-O = 2.91 Å rot. pop. = 0.90,0.10,0. ϕ = 131° R = 7.64%

a) Rotamer population corresponds to positions A, B and C respectively (Figure 8).

b) A fixed at staggered position ψ = 84.27°.

c) A fixed at staggered position ψ = 90.37°.

TABLE 19

Least-square Fit of LIS in Borneol to C_{2v} Point Group (Three Rotamers).

Borneol Coordinates derived from	LIS from Direct Determination	LIS from Competitive Systems
Structure 6	Ln-O = 2.0-2.1 Å[a] rot. pop. = 0.86,0.11,0.03 ϕ = 136-140° C_2 = 0.93-0.94 R = 4.1%	Ln-O = 2.23 Å rot. pop. = 0.85,0.09,0.06 ϕ = 132° C_2 = 0.33 R = 0.94%
Structure 8	Ln-O = 2.94 Å rot. pop. = 0.94,0.07,0.0 ϕ = 130° C_2 = -0.13 R = 5.48%	Ln-O = 2.84 Å rot. pop. = 1.0, 0., 0. ϕ = 119° C_2 = 0.36 R = 3.2%

a) No convergence.

in the LIS, as demonstrated by the fact that no convergence is obtained for the same set of coordinates for LIS arising from a direct determination, while those from the competitive analysis give acceptable parameters at convergence. This does not imply that LIS obtained by the competitive procedure are more accurate than the ones from a direct determination, since, as was stated previously, the optimization of ψ is not performed in these cases.

Influence of the Contact Interaction by Neglecting the α-Proton in the Calculation

If a contact interaction or CFS mechanism is present, their contribution is likely to be most pronounced at the α-proton (H_2)[92]. Rejection of the corresponding data would give an idea of how much error is introduced in approximating the chemical shifts to be of purely dipolar origin. Table 20 reports the results obtained in this case. Optimization of the parameters is analogous to those in Table 16, since one rotamer is considered and axial symmetry is assumed.

Using Hamilton tables again, a 50% confidence for the models in Table 20 over those in Table 16 results for coordinates from 6. No significant improvement is observed for R factors with coordinates from 8.

It appears that the errors due to mechanisms other than dipolar are overcome by the errors in both the geometrical structure and the model used for LIS calculations.

Colinearity of Magnetic Axis and Ln-O Vector

As already attempted by Hawkes et al.[84] with a different set of LIS and using coordinates from 6, an adjustment for the O-Ln-magnetic axis would indicate the degree of confidence for the generally supposed

TABLE 20

Least-square Fit of LIS in Borneol Rejecting Values for H_2.

Borneol Coordinates derived from	LIS from Direct Determination	LIS from Competitive Systems
Structure 6	Ln-O = 2.98 Å	Ln-O = 3.08 Å
	ϕ = 126°	ϕ = 138°
	ψ = 111°	ψ = 87°
	R = 1.68%	R = 1.1%
Structure 8	Ln-O = 3.05 Å	Ln-O = 3.10 Å
	ϕ = 127°	ϕ = 134°
	ψ = 117°	ψ = 106°
	R = 2.9%	R = 2.9%

colinearity between the magnetic axis and the Ln-O bond.

Table 21 summarizes the results from such calculations and, even if the R factors significantly decrease when comparing Tables 21 and 16, the distance of the Ln-O bond also significantly increases. In the case of 8, it is far from any physical meaning (even if there are no X-ray analyses reported for lanthanide complexes and an alcohol, a distance of $\simeq$ 3 Å is generally observed with other substrates[3]). This observation is contrary to Hawkes's results, where an improvement for the Ln-O bond is observed when analogous analyses are attempted. As has already been emphasized in this study, a different data set can produce considerably different results, and in Hawkes's case, ^{13}C data were included. Errors may have been introduced by the presence of 1:1 and 2:1 adducts.

In Table 21, the three angles related to this type of analysis are reported. In order to alter the colinearity of the Ln-O vector and the magnetic axis, rotations through the x and y symmetry coordinates of the lanthanide ion are necessary (see Appendix 1 for details and sign conventions). The magnitude of such rotations are listed in Table 21 as angles β and γ respectively, and the resulting Ln-O-magnetic axis angle is represented by ξ.

Analogously to Hawkes's conclusions, it appears that only a small angle could result from no colinearity considerations.

If this is due to Huber[33], Briggs et al.[34] and/or Dyer et al.[35] justification (see Pseudo-Contact or Dipolar Interaction), then the approximation to axial symmetry will also be valid.

TABLE 21

Least-square Fit of LIS in Borneol Assuming No-Colinearity of Principal Magnetic Axis and Ln-O Vector[a].

Borneol Coordinates derived from	LIS from Direct Determination	LIS from Competitive Systems
Structure 6	Ln-O = 3.34 Å	Ln-O = 2.62 Å
	ϕ = 124°	ϕ = 131°
	ψ = 116°	ψ = 91°
	β = 0.8°	β = -1°
	γ = -2.2°	γ = 3.5°
	ξ = 2°	ξ = 4°
	R = 1.04%	R = 0.99%
Structure 8	Ln-O = 3.8 Å	Ln-O = 3.42 Å
	ϕ = 120°	ϕ = 124°
	ψ = 123°	ψ = 116°
	β = 0.8°	β = 1.5°
	γ = 3.2°	γ = -1.3°
	ξ = 5°	ξ = 2°
	R = 1.88%	R = 1.6%

a) ξ represents the angle O-Ln-magnetic axis, for β and γ see Appendix 1.

Treatment of Methyl Group

A final consideration regarding methyl groups is believed appropriate.

Since a free rotation along the C-C bond is present for $C-CH_3$ at room temperature, methyl groups have been considered as a point group along the C-C bond at a distance that results from projecting each H on such a vector. The real situation, however, should be better represented by a weighted average of all possible conformations. As a first approximation, the location of the three hydrogens at a staggered position is expected to give an indication of the errors introduced when considering the methyl groups as point groups.

Table 22 summarizes results obtained when fitting the LIS to the McConnell equation, considering the coordinates for H in CH_3 as given in Tables 12 and 14 (last three entries).

Before jumping to any conclusions, let us analyze how sensitive the three methyl groups in borneol are to such changes. A simple approach to such an analysis is:

1) Choose a model for geometrical arrangements and LIS;

2) Perform an optimization of the parameters considering methyl as point groups;

3) Calculate chemical shifts for the three independent H's in each methyl group;

4) Average the values from step 3 and compare them with the respective calculated shifts for methyl as a point group.

The results of such operations are given in Table 23 for axial symmetry (McConnell equation fits); coordinates are from 6 and LIS from a direct determination. The difference between the two values in Table 23

TABLE 22

Least-square Fit of LIS in Borneol Considering Staggered Methyl Groups.

Borneol Coordinates derived from	LIS from Direct Determination	LIS from Competitive Systems
Structure 6	Ln-O = 2.99 Å	Ln-O = 3.04 Å
	ϕ = 128°	ϕ = 125°
	ψ = 108°	ψ = 109°
	R = 1.5%	R = 2.21%
Structure 8	Ln-O = 3.06 Å	Ln-O = 3.16 Å
	ϕ = 128°	ϕ = 125°
	ψ = 115°	ψ = 117°
	R = 3.3%	R = 2.98%

are of a magnitude comparable to the difference between the observed and the calculated shifts after convergence is reached (see Figure 26 in Appendix 1).

TABLE 23

Comparison of Results for Each Methyl Group as a Point Group and as Three Independent Hydrogens.

Group	Θ_i	LIS calculated from	
		Point appr.	Staggered Me
1-CH_3	24.13°	8.232	7.976
7-CH_3-syn	30.29°	4.303	4.202
7-CH_3-anti	11.19°	4.153	3.993

Furthermore, considering the converged parameters for methyl as a point group (Table 16) and staggered methyl (Table 22), no appreciable difference is observed for the same model. It appears in this case, that methyl groups could be treated as point groups without introducing a serious deviation from the real model.

Methyl groups have been the subject of previous studies and the results in the present work partially support the previous conclusions. Caution has been suggested[31], however, when the methyl groups lie in a region close to $\Theta = 54.7°$, for which a change in sign[93] is predicted for the chemical shifts from McConnell equation 10. The Θ_i angles for methyls as point groups are included in Table 23 for comparison purposes.

Introduction to Competitive Systems

The determination of equilibrium constants and stoichiometry by nmr techniques has been reviewed in the Introduction. From previous work, the following general conclusions can be listed:

1) Shift reagents of high purity are generally required[47] (for precise analyses, the purification of the shift reagent just prior to use is recommended);

2) Impurities from other sources must be eliminated[56], since they can act as "scavengers," thus altering the effective concentration of the shift reagent;

3) The determination of stoichiometry is not a direct consequence from the chemical shifts analysis. Most authors, who devoted their attention to this study, were aware of high adduct formation (2:1 type mainly) or mixtures of adducts. However, the determination of this factor, by direct analysis of the chemical shifts, is based principally on better agreement between the calculated and the observed values[51-52].

Alternatives to such determinations are desirable, and are the subject of the last study in this thesis.

Williams[94] in 1972 presented an elegant start to a possible solution, by considering the competition of several independent substrates in combining with shift reagents present in solution. Assuming only a 1:1 type of adduct to be formed, equation 38 was derived, where the subscripts A and B refer to the reference and the competing substrate

$$\frac{1}{\delta_A - \delta_{A\ free}} = \frac{K_B}{K_A}\frac{\Delta_B}{\Delta_A}\frac{1}{\delta_B - \delta_{B\ free}} + \left(1 - \frac{K_B}{K_A}\right)\frac{1}{\Delta_A} \qquad (38)$$

respectively; K is the equilibrium constant, Δ the chemical shift for the 1:1 adducts (taking the free shift as reference), δ the observed chemical

shifts with respect to a chosen reference (generally TMS), and δ free the chemical shift for the non-bound substrate with respect to the same reference as for δ.

It follows that if the behavior of A in the presence of a shift reagent is totally known, then the corresponding equilibrium for B can be totally established by simply adding B to a sample of A and the shift reagent and/or vice versa. The observed shifts for both substrates are recorded and a plot of $1/\delta$ vs. $1/\delta$ should result in a straight line, whose intercept and slope are used in the determination of K_B and Δ_B. It is obvious that the use of equation 38 greatly simplifies the problem, since the concentration of the shift reagent is immaterial (also its purity), and no precuations are necessary in the purification of solvents and substrates, not even their concentrations are relevant.

Williams also attempted to experimentally demonstrate the use of equation 38, and chose a mixture of simple alcohols and esters for such purposes. As will be shown later, however, this system does not present ideal properties for such an analysis.

Independently, we also derived equation 38 (see Appendix 2), but applied different criteria in its use. The reference substrate A must present the following characteristics:

1) The pmr signals from A should be singlets, since it facilitates their chemical shifts measurements and minimizes interference with the signals from substrate B;

2) More than one signal is desirable since application of equation 38 could be checked among a larger number of observations from the same reference;

3) A must form only 1:1 type of adducts.

Dimethoxyethane (DME, 9) displays the above characteristics based

$$CH_3\text{-}O\text{-}CH_2\text{-}CH_2\text{-}O\text{-}CH_3$$

9

on the observation at a low temperature pmr by Grotens et al.[55] with a series of shift reagents. Separation of the free and bound shifts was successful at -63.4°C and corresponded to 1:1 type of adducts based on the relative intensity. Additional evidence that DME forms only 1:1 adducts at room temperature as well will be presented.

Theoretical Analysis Including 2:1 Type of Adduct for B

A further consideration must be made regarding the possible formation of adducts of different stoichiometry for substrate B. While A shows a 1:1 adduct formation behavior, substrate B is generally a monodentate compound, so if a coordination number 8 is preferred by the shift reagent, then 2:1 type of adducts can occur with B. The justification for coordination number 8 (and not higher) will also be presented during this work.

Theoretical analysis for equation 39, where R stands for the shift reagent, is presented in Appendix 4.

$$\begin{aligned} A + R &\overset{K_A}{\rightleftharpoons} A\cdot R \\ B + R &\overset{K_{B1}}{\rightleftharpoons} B\cdot R \\ B + B\cdot R &\overset{K_{B2}}{\rightleftharpoons} B_2\cdot R \end{aligned} \qquad (39)$$

Since a $1/\delta$ vs. $1/\delta$ plot is used for a 1:1 adduct analysis, it is convenient to construct similar plots for the case depicted by equation 39

as well. Figures 9 to 12 represent theoretical plots predicted for a few values of K's and Δ's chosen arbitrarily. For comparative purposes, all relative concentrations of A, B, and R are identical in the four figures. The following observations are important·

1) A clear deviation from linearity is shown. This by itself is a useful probe for the presence of complexes of higher stoichiometry.

2) There is a strong dependence on concentration factors, a clear curvature results from adding the substrate B to an original solution of A and the shift reagent, but not vice versa.

3) A comparison of Figures 11 with 12,and 9 with 10, clearly shows that the extent of curvature is highly dependent on the value of the equilibrium constants.

To understand the curvature mentioned in the second observation, a plot of the concentration of 1:1 vs. concentration of 2:1 adducts for B is represented in Figure 13. Values are obtained from the 0.2 M solutions whose complete analysis is given as an example in Appendix 4. Clearly, while a quasi-linear relationship is observed when the reference A is added to an original solution of the substrate B and R, a pronounced curvature results when the mode of mixing is inverted. This is also the case for the other concentrations and at different K's.

Description of the System DME-$Eu(dpm)_3$

The pmr for DME were recorded at different concentrations of $Eu(dpm)_3$ and DME, using $CDCl_3$ as the solvent. A plot for the CH_2 pmr signals vs. shift reagent and DME concentrations is represented in Figure 14.

It would be anticipated that extrapolation to $Eu(dpm)_3 = 0$

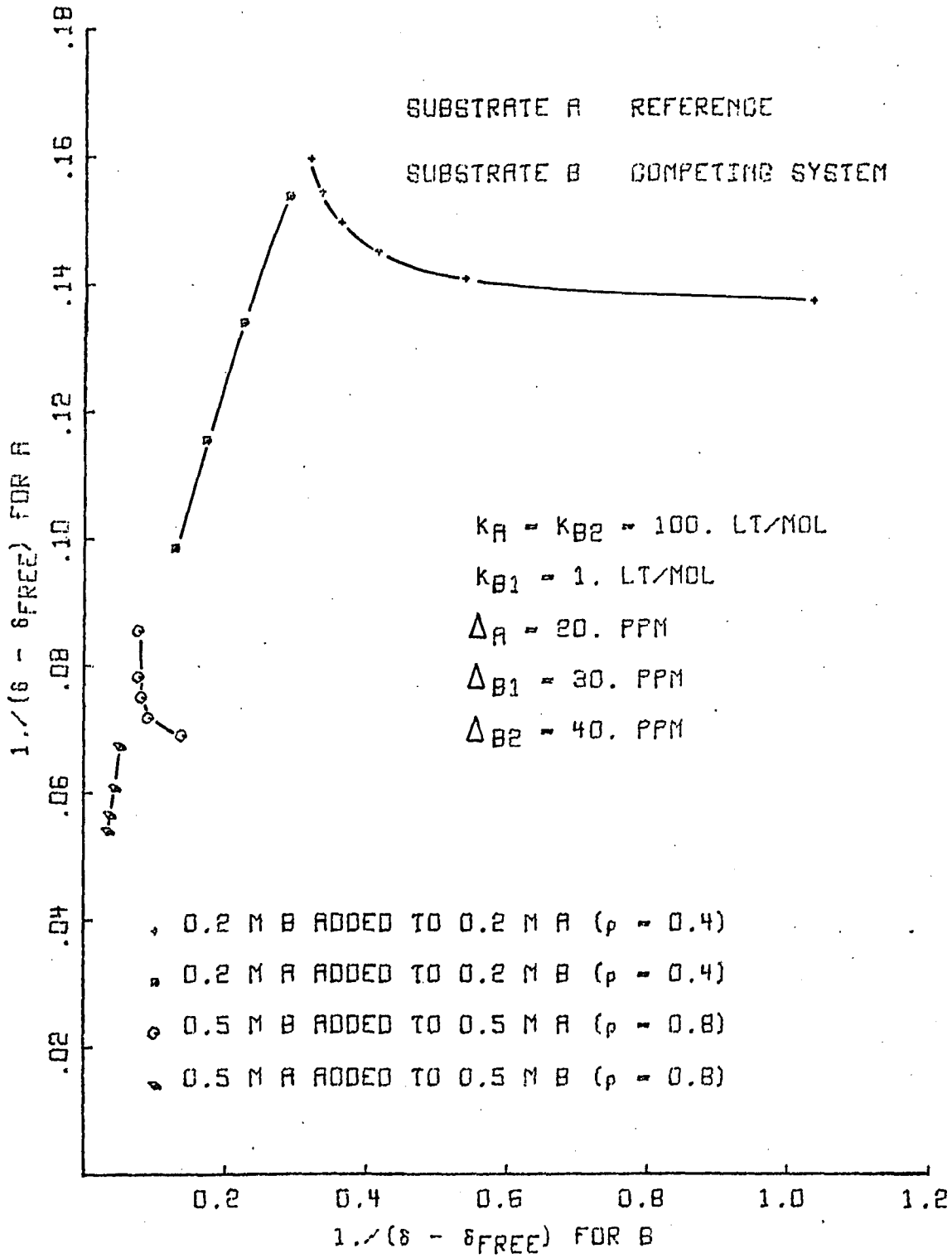

Figure 9 - Theoretical Analysis of 1:1 and 2:1 Adduct Formation for B in Competition Experiments.

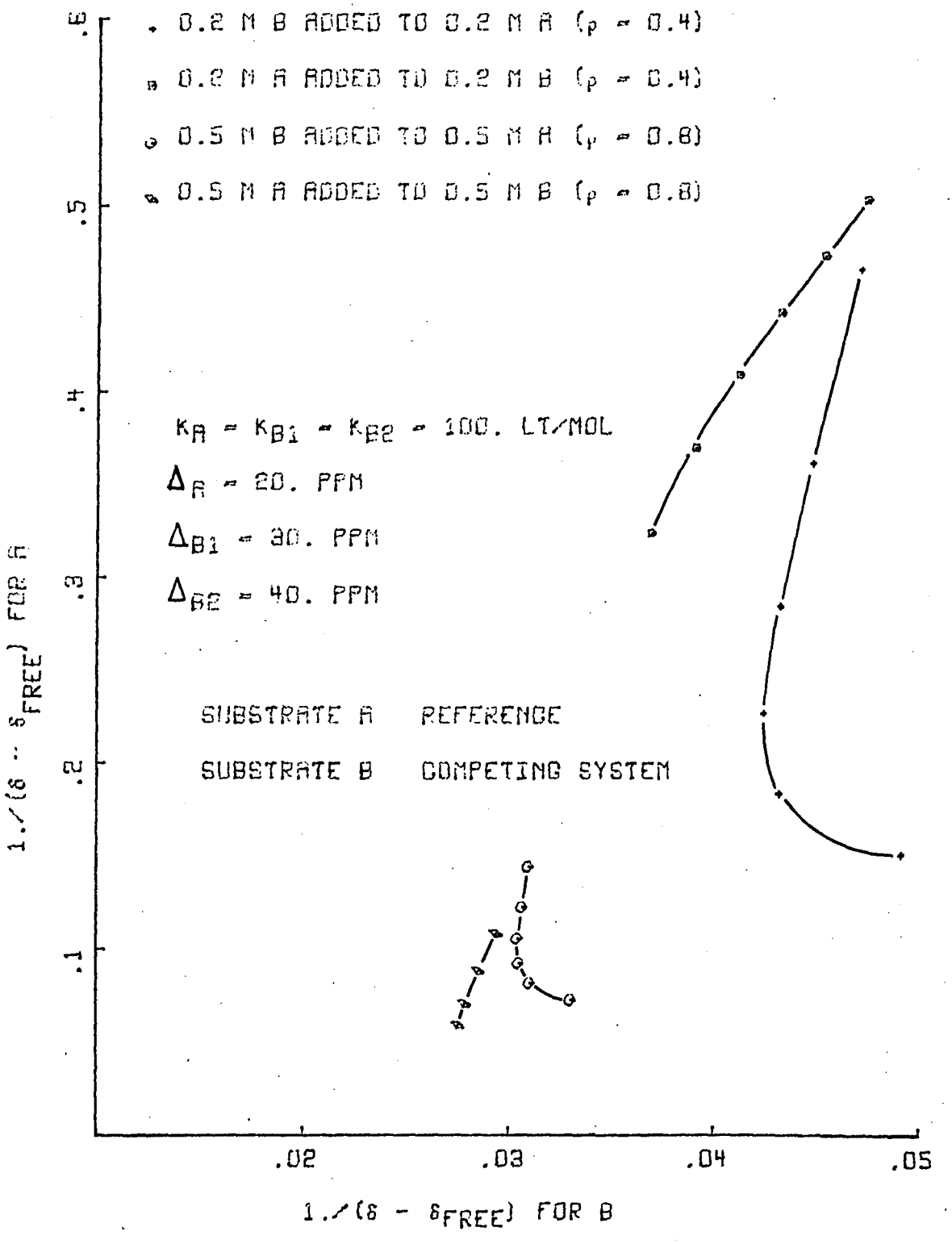

Figure 10 - Theoretical Analysis of 1:1 and 2:1 Adduct Formation for B in Competition Experiments.

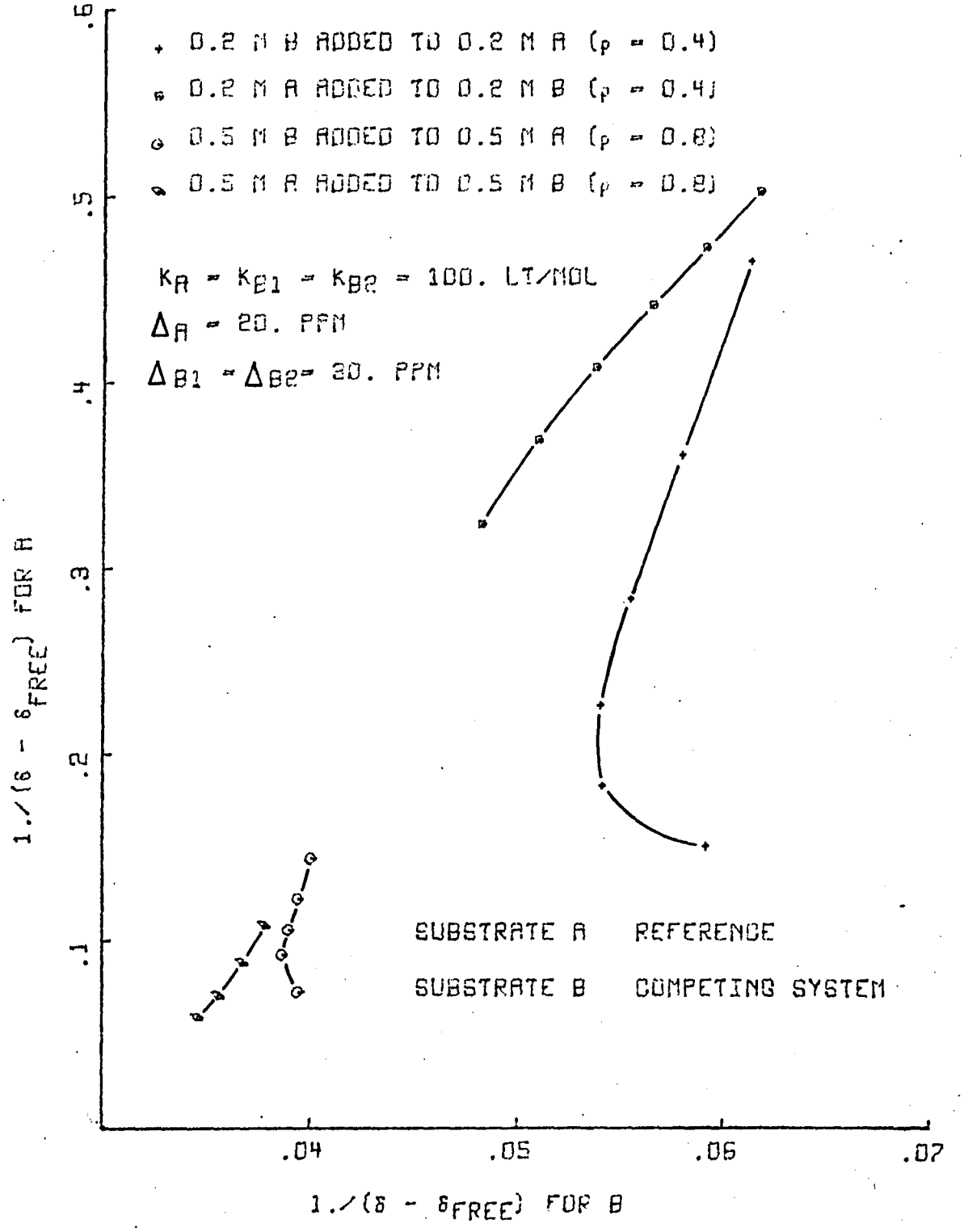

Figure 11 - Theoretical Analysis of 1:1 and 2:1 Adduct Formation for B in Competition Experiments.

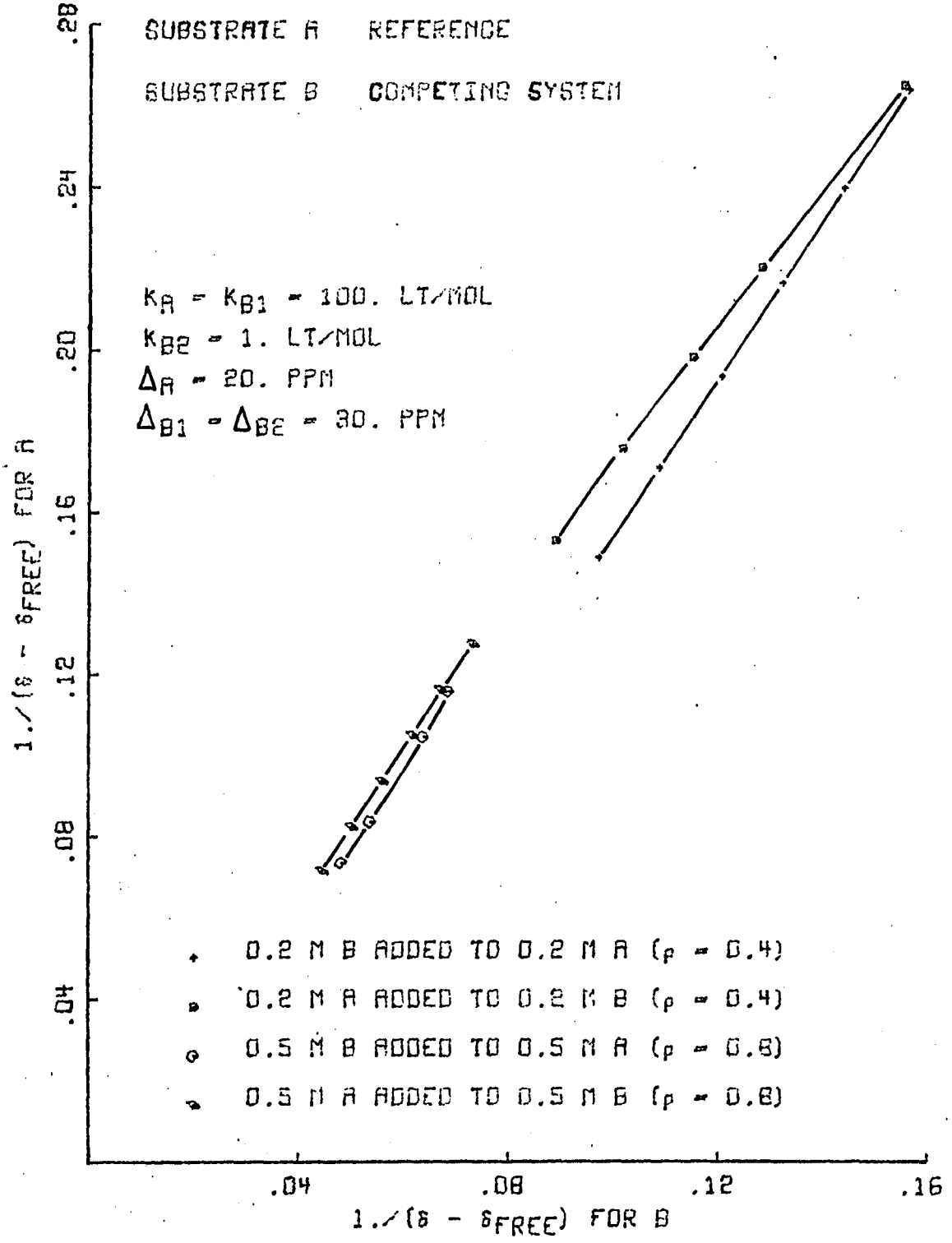

Figure 12 - Theoretical Analysis of 1:1 and 2:1 Adduct Formation for B in Competition Experiments.

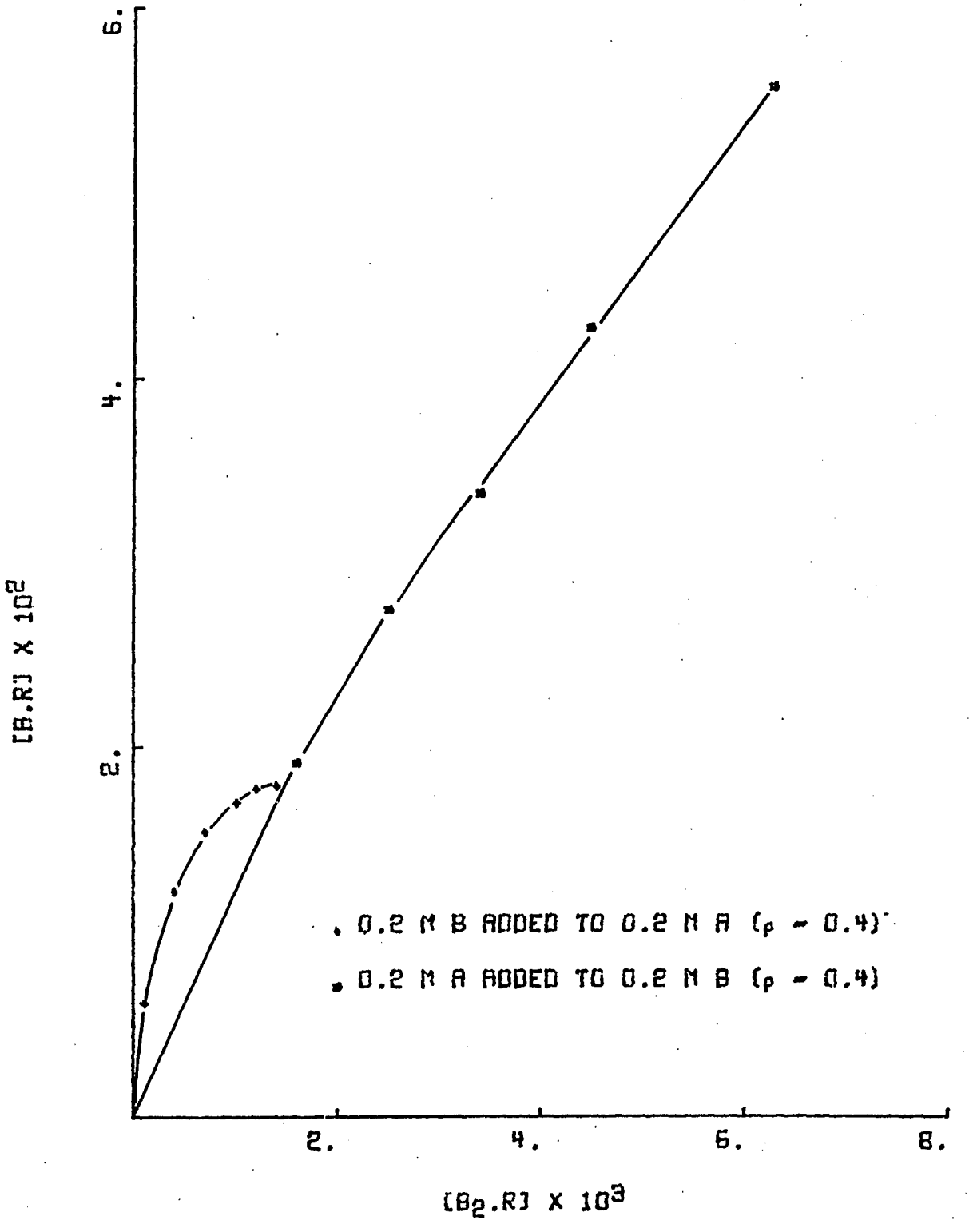

Figure 13 - [B•R] vs. [B_2•R] from Theoretical Analysis. Tabulated values in Figure 27 (Appendix 4) from the 0.2 M solutions mixture.

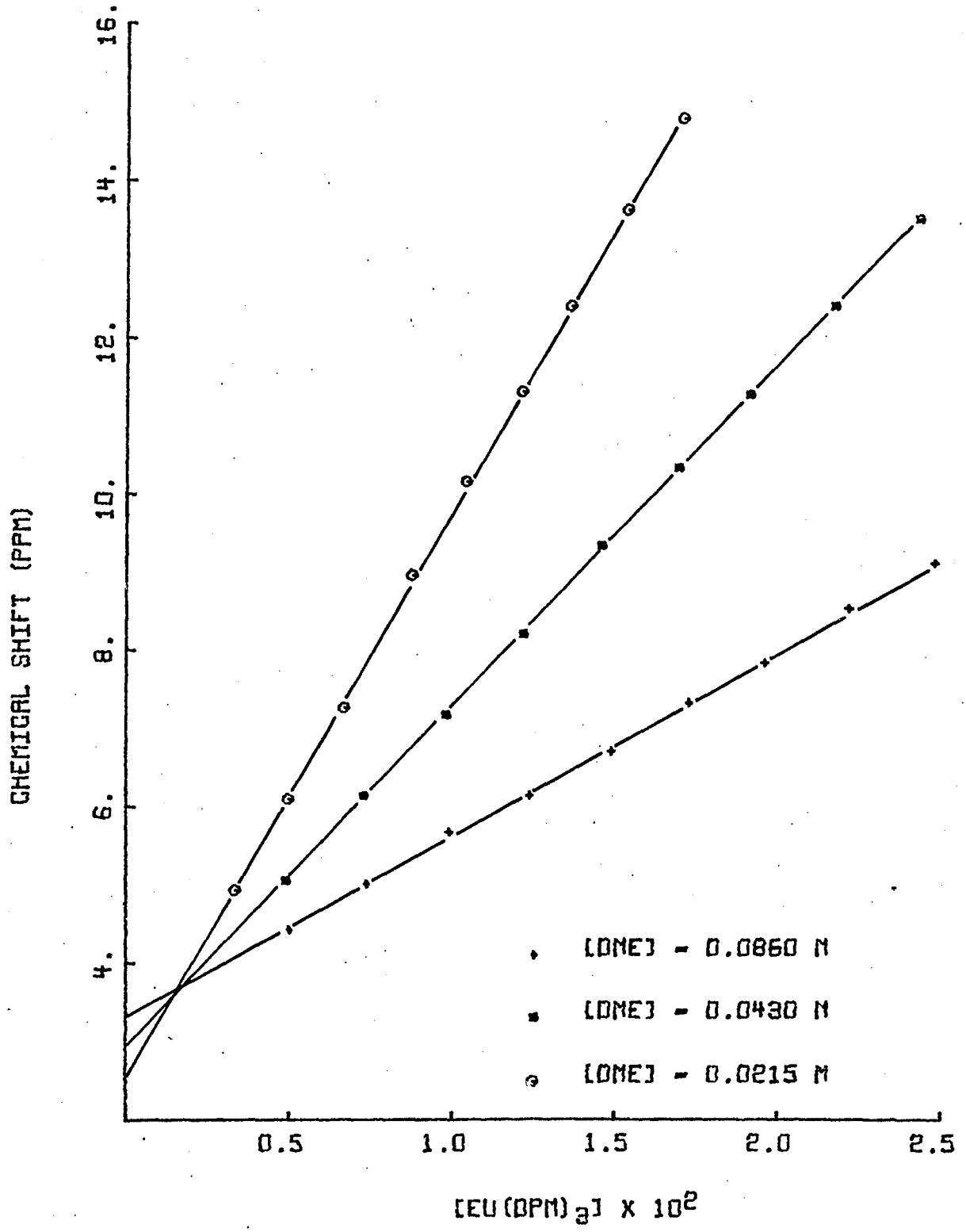

Figure 14 - Chemical Shifts of CH_2 in DME *vs.* DME and $Eu(dpm)_3$ Concentrations.

should yield the chemical shifts for the free substrate, which is not the case as clearly shown in Figure 14. The experimental value for the free shift agrees, however, with the value in the y coordinate where the three lines intercept. This behavior has been observed in previous reports, and its origin has not been determined. It has been attributed to the presence of "scavengers"[95] and to "inactive"[47] concentration of the shift reagent, and the general attitude adopted has been to shift the x-axis scale such that the intercept of the three lines corresponds to the zero in the concentration of the shift reagent.

Since not many alternatives are left, the shifting of the x-axis procedure was also adopted in the present work, and analysis of the observed pmr signals was performed as described in Appendix 5. Tables 24 and 25 summarize the results from such analysis. The low standard deviations in both, the converged parameters and the observed chemical shifts, affords some confidence. However, the experimental values for the chemical shifts in the DME (in the absence of the shift reagent) are δ 3.56 (CH_2), 3.39 (CH_3). From Tables 24 and 25, where the free shifts were also optimized, a small discrepancy exists between these values and the experimental ones.

Analysis of Possible Interfering Equilibria

It is useful to consider the factors that may affect a direct determination of K and Δ.

Reuben[5] analyzed some equilibria other than adduct formation, and their effect on the determination of equilibrium constants and shifts, when such values are calculated by L_o *vs.* $1/\delta$ plots. Since a different procedure is used in the present case, theoretical values (represented

TABLE 24

Computer Output from a Direct Determination of Equilibrium Constant and Δ for CH_2 in DME [Shift Reagent: $Eu(dpm)_3$].

CONCENTRATION OF SUBSTRATE	CONCENTRATION OF LANTHANIDE	1:1 COMPLEX	CALCULATED CHEMICAL SHIFT (SC)	OBSERVED CHEMICAL SHIFT (SO)	SO-SC
0.0860	0.0235	0.0214	9.1372	9.0600	-0.0572
0.0860	0.0209	0.0191	8.5072	8.5000	-0.0072
0.0860	0.0182	0.0168	7.8677	7.8000	-0.0677
0.0860	0.0160	0.0147	7.3077	7.2900	-0.0177
0.0860	0.0135	0.0125	6.7099	6.6800	-0.0299
0.0860	0.0111	0.0102	6.0939	6.1200	0.0261
0.0860	0.0086	0.0080	5.4748	5.6600	0.1852
0.0860	0.0061	0.0057	4.8529	5.0100	0.1571
0.0860	0.0036	0.0034	4.2282	4.4200	0.1918
0.0430	0.0229	0.0183	13.2848	13.4400	0.1552
0.0430	0.0204	0.0165	12.2978	12.3300	0.0322
0.0430	0.0178	0.0146	11.2599	11.2100	-0.0499
0.0430	0.0155	0.0129	10.3296	10.2900	-0.0396
0.0430	0.0132	0.0110	9.3143	9.2800	-0.0343
0.0430	0.0107	0.0091	8.2475	8.1600	-0.0875
0.0430	0.0083	0.0071	7.1615	7.1500	-0.0115
0.0430	0.0058	0.0050	6.0500	6.1200	0.0700
0.0430	0.0034	0.0030	4.9196	5.0400	0.1204
0.0215	0.0158	0.0102	14.4210	14.7100	0.2890
0.0215	0.0140	0.0093	13.4509	13.5600	0.1091
0.0215	0.0122	0.0083	12.3904	12.3300	-0.0604
0.0215	0.0107	0.0074	11.4010	11.2500	-0.1510
0.0215	0.0090	0.0064	10.2613	10.1200	-0.1413
0.0215	0.0073	0.0053	9.0677	8.9300	-0.1377
0.0215	0.0052	0.0039	7.5211	7.2400	-0.2811
0.0215	0.0036	0.0027	6.2539	6.0800	-0.1739
0.0215	0.0019	0.0015	4.9178	4.9300	0.0122

	CHEMICAL SHIFT OF FREE SUBSTRATE	CHEMICAL SHIFT OF 1:1 COMPLEX	EQUILIBRIUM CONSTANT
	3.3119	23.3900	162.4438
STANDARD DEVIATIONS	0.0460	0.3572	8.5594
DERIVATIVES	0.0006	0.0002	0.0000

STANDARD DEVIATION OF AN OBSERVATION OF UNIT WEIGHT 0.1018

PERCENTAGE OF STANDARD DEVIATION 0.5809

TABLE 25

Computer Output from a Direct Determination of Equilibrium Constant and Δ for CH_3 in DME [Shift Reagent: $Eu(dpm)_3$].

CONCENTRATION OF SUBSTRATE	CONCENTRATION OF LANTHANIDE	1:1 COMPLEX	* CALCULATED * CHEMICAL * SHIFT (SC) *	* OBSERVED * CHEMICAL * SHIFT (SO) *	SO-SC
0.0860	0.0235	0.0214	5.4694	5.4400	-0.0294
0.0860	0.0209	0.0191	5.2348	5.2100	-0.0248
0.0860	0.0182	0.0168	4.9967	4.9600	-0.0367
0.0860	0.0160	0.0147	4.7882	4.7800	-0.0082
0.0860	0.0135	0.0125	4.5656	4.5600	-0.0056
0.0860	0.0111	0.0102	4.3363	4.3500	0.0137
0.0860	0.0086	0.0080	4.1058	4.1800	0.0742
0.0860	0.0061	0.0057	3.8742	3.9400	0.0658
0.0860	0.0036	0.0034	3.6416	3.7100	0.0684
0.0430	0.0229	0.0183	7.0137	7.0600	0.0463
0.0430	0.0204	0.0165	6.6462	6.6700	0.0238
0.0430	0.0178	0.0146	6.2597	6.2400	-0.0197
0.0430	0.0155	0.0129	5.9133	5.8900	-0.0233
0.0430	0.0132	0.0110	5.5353	5.5000	-0.0353
0.0430	0.0107	0.0091	5.1381	5.1000	-0.0381
0.0430	0.0083	0.0071	4.7338	4.7200	-0.0138
0.0430	0.0058	0.0050	4.3199	4.3500	0.0301
0.0430	0.0034	0.0030	3.8990	3.9600	0.0610
0.0215	0.0158	0.0102	7.4367	7.5600	0.1233
0.0215	0.0140	0.0093	7.0755	7.1400	0.0645
0.0215	0.0122	0.0083	6.6807	6.6600	-0.0207
0.0215	0.0107	0.0074	6.3123	6.2700	-0.0423
0.0215	0.0090	0.0064	5.8879	5.8200	-0.0679
0.0215	0.0073	0.0053	5.4435	5.3800	-0.0635
0.0215	0.0052	0.0039	4.8676	4.7600	-0.1076
0.0215	0.0036	0.0027	4.3958	4.3400	-0.0558
0.0215	0.0019	0.0015	3.8984	3.9200	0.0216

	CHEMICAL SHIFT OF FREE SUBSTRATE	CHEMICAL SHIFT OF 1:1 COMPLEX	* EQUILIBRIUM * CONSTANT
	3.3004	8.7089	162.4438
STANDARD DEVIATIONS	0.0416	0.1981	8.5594
DERIVATIVES	0.0002	0.0001	0.0000

STANDARD DEVIATION OF AN OBSERVATION OF UNIT WEIGHT 0.1018

PERCENTAGE OF STANDARD DEVIATION 0.5809

EXECUTION TERMINATED. EXECUTION TIME 9.849 SECONDS.

in Figure 15 for the 0.025 M solutions of a substrate) were calculated for each of the following assumptions:

1) A 0.1% of impurity is considered in the shift reagent. Besides changing the actual concentration of this species, it was assumed that the impurity could also form 1:1 adducts with a high equilibrium constant ($K = 1000\ M^{-1}$).

2) Analogous assumptions for impurity in the substrate (0.1%) were considered. Their influence will be to alter the calculated concentration of the substrate and form 1:1 adducts with $K = 1000\ M^{-1}$. In Figure 15, this case is very similar to the first one and is eliminated for clarity.

3) The solvent ($CDCl_3$) could act as a Lewis base, and form adducts with the shift reagent. Even if the equilibrium constant is assumed low ($K = 0.5\ M^{-1}$), the high concentration of the solvent introduces a drastic change on the observed shifts.

4) Ethers can also form weak hydrogen bonding with $CHCl_3$. In deuterated chloroform, this effect will also be low, but again the concentration of the solvent will be high. Assuming that the substrate bound to the chloroform is inactive toward the shift reagent, even for a value of $K = 0.5\ M^{-1}$ for the hydrogen bonding association[11], the calculated shifts result in a drastic change. In Figure 15, this case is eliminated for clarity, since it is similar to the results from case 3.

5) In several occasions, dimerization of the shift reagent has been postulated[48,52], which is assumed in the present analysis to occur with an equilibrium constant of $40\ M^{-1}$ and form inactive species.

6) Self-association for ethers occurs in very low extent, so

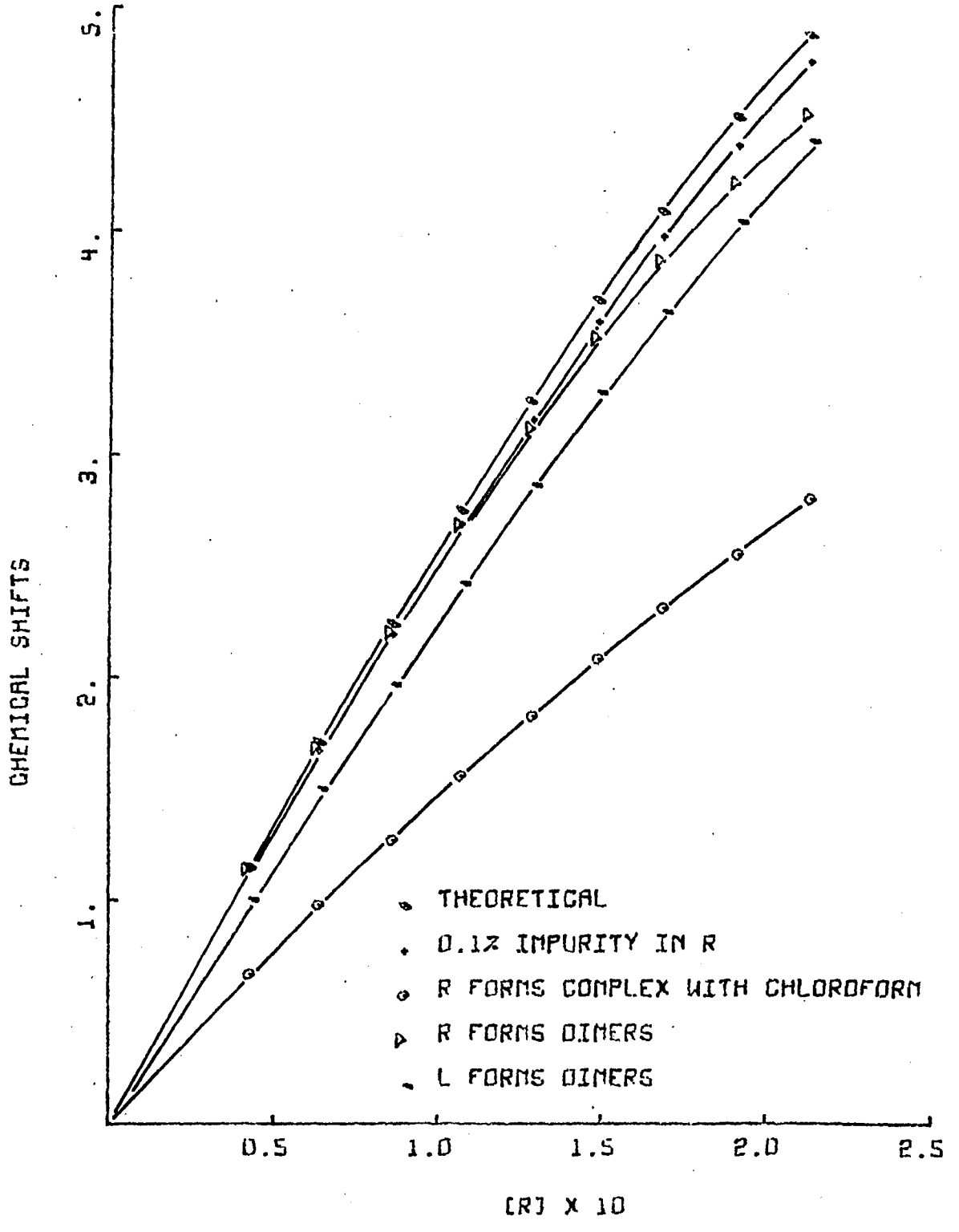

Figure 15 - Influence of Interfering Equilibria in the Chemical Shift of A.

this last consideration will not probably affect the system DME-R. However, alcohols were also used in later studies, and they do display a strong tendency for self-association[79]. This consideration is therefore included, and a $K = 40\ M^{-1}$ is assumed. The associated species are considered not to bind to the shift reagent.

Calculated values of the chemical shifts by each of the previous considerations at different substrate and shift reagent concentrations were used as data in the calculation of K and Δ, by the method described in Appendix 5 (direct determination). The results are summarized in Table 26 from which one important observation can be drawn: the Δ values are not influenced to a great extend in any case.

It is understood that none of the above considerations are expected to be present independently and that the assumed inactivity toward adduct formation of each considered species is only an approximation to the real situation. The analysis is done merely for the purpose of building some knowledge about the deviations which may occur in the determination of K and Δ by the present method.

The theoretical analysis for the equilibrium concentrations of adducts and interfering adduct formation is not presented since it is similar to the analysis in Appendix 4.

Description of the System DMB-Eu(dpm)$_3$

Before proceeding to use DME as a reference substrate, the following points need to be demonstrated:

1) DME forms only 1:1 adducts at room temperature;

2) The K and Δ's properly describe the system.

To achieve these goals, a second bidentate ligand is chosen,

TABLE 26

Theoretical Calculation for Interfering Equilibria.

	K (in M^{-1})	Δ
Theoretical	250.	8.00
0.1% impurity in R[a] K = 1000 M^{-1}	254.	7.76
0.1% impurity in A[a] K = 1000 M^{-1}	268.	7.88
$CHCl_3$ forms complexes with R[b] K = 0.5 M^{-1}	42.4	7.98
$CHCl_3$ forms complexes with A[a] K = 0.5 M^{-1}	41.7	8.02
R dimerizes K = 40 M^{-1}	185.	8.02
A dimerizes K = 40 M^{-1}	243.	7.2

a) The equilibrium constant refers to the adduct formation between the shift reagent and the impurity.

b) $[CHCl_3]$ = 10. M

that is dimethoxybenzene (DMB, 10); if the presence of two coordination

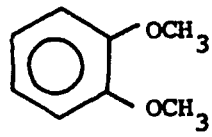

10

centers in each substrate would restrict the adduct stoichiometry to a 1:1 type, then equation 38 should be followed by DME and DMB as competing substrates. Furthermore, from such expected straight lines, values for K and Δ's for DMB could be predicted and an independent determination (by the same procedure used by DME) should result in an agreement (see DME and DMB in Competition for $Eu(dpm)_3$).

A procedure similar to the one described in the case of DME was carried out using DMB as the binding substrate, with similar treatment of data. Figure 16 represents chemical shifts for the ortho protons as a function of the shift reagent and DMB concentrations. Tables 27-29 report results after adjusting the values on the x-axis as described previously.

Again, the experimental shifts in DMB (in the absence of shift reagent) and the ones obtained from the analysis of the adducts result in some difference [pmr: δ 6.92 (aromatic), 3.87 (CH_3)].

DME and DMB in Competition for $Eu(dpm)_3$

Under the conditions specified in the Experimental section, DME and DMB were allowed to compete for $Eu(dpm)_3$. Results are presented in Table 30, and a graphical representation for 1/δ vs. 1/δ for the system CH_3 in DME vs. DMB is given in Figure 17.

From a least square fitting to a straight line, the constants of

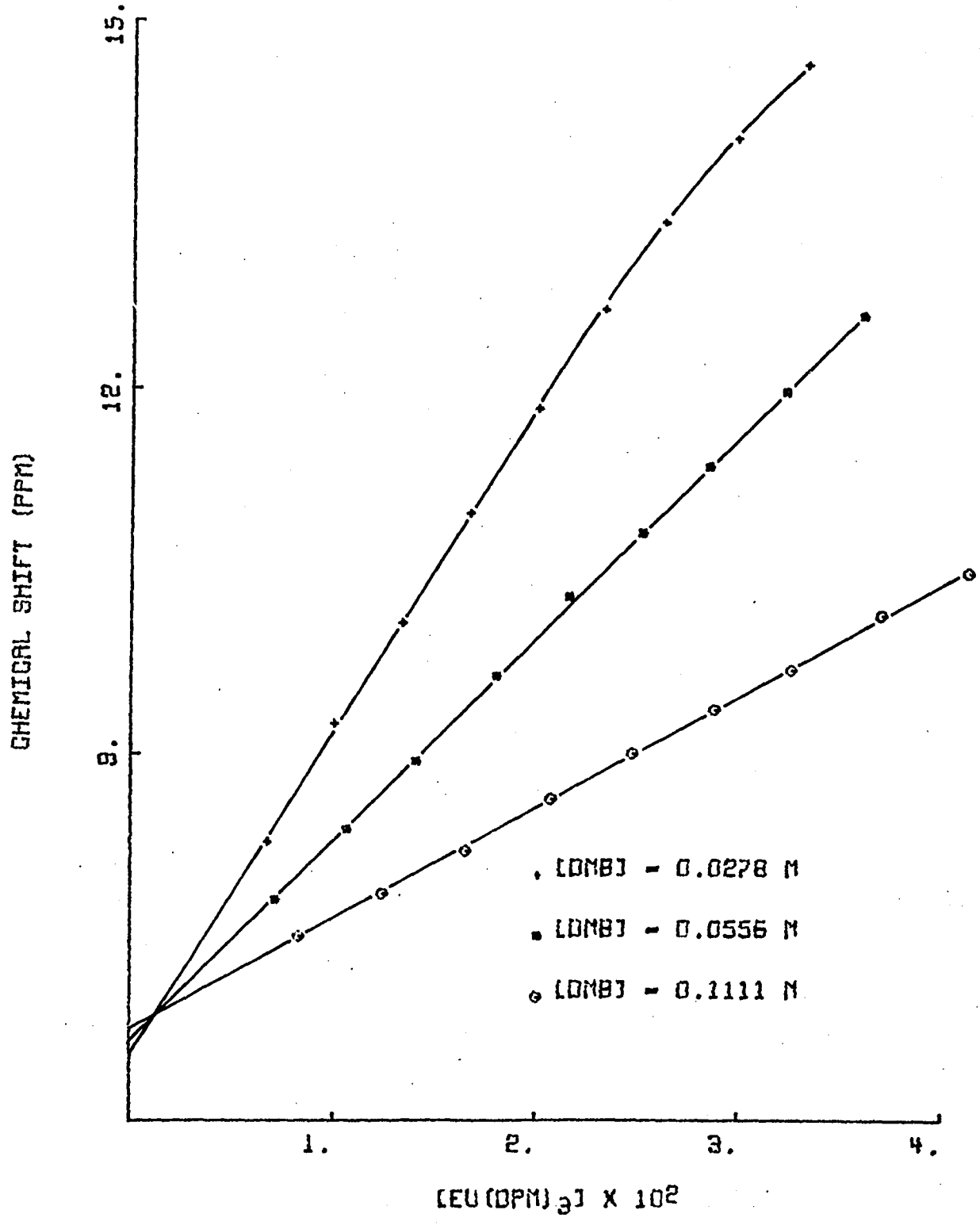

Figure 16 - Chemical Shifts of ortho Protons in DMB vs. DMB and $Eu(dpm)_3$ Concentrations.

TABLE 27

Computer Output from a Direct Determination of Equilibrium Constant and Δ for meta Proton in DMB [Shift Reagent: $Eu(dpm)_3$].

CONCENTRATION OF SUBSTRATE	CONCENTRATION OF LANTHANIDE	1:1 COMPLEX	* CALCULATED CHEMICAL SHIFT (SC)	* OBSERVED CHEMICAL SHIFT (SO)	SO-SC
0.0278	0.0056	0.0041	7.6492	7.6179	-0.0313
0.0278	0.0090	0.0063	8.1500	8.0853	-0.0647
0.0278	0.0123	0.0084	8.6151	8.4930	-0.1221
0.0278	0.0157	0.0103	9.0447	8.9406	-0.1041
0.0278	0.0190	0.0121	9.4343	9.3682	-0.0661
0.0278	0.0222	0.0136	9.7778	9.7262	-0.0516
0.0278	0.0253	0.0149	10.0667	10.1041	0.0374
0.0278	0.0288	0.0162	10.3622	10.4621	0.0999
0.0278	0.0323	0.0174	10.6154	10.7804	0.1650
0.0556	0.0061	0.0052	7.3090	7.3792	0.0702
0.0556	0.0095	0.0080	7.6291	7.6576	0.0286
0.0556	0.0129	0.0108	7.9370	7.9361	-0.0009
0.0556	0.0170	0.0140	8.2966	8.2742	-0.0224
0.0556	0.0206	0.0167	8.6040	8.5825	-0.0215
0.0556	0.0241	0.0193	8.8945	8.8610	-0.0335
0.0556	0.0274	0.0217	9.1575	9.1395	-0.0180
0.0556	0.0313	0.0243	9.4478	9.4378	-0.0100
0.0556	0.0350	0.0267	9.7191	9.7262	0.0071
0.1111	0.0072	0.0067	7.1062	7.2002	0.0939
0.1111	0.0114	0.0104	7.3170	7.3991	0.0820
0.1111	0.0155	0.0142	7.5264	7.5582	0.0318
0.1111	0.0196	0.0179	7.7348	7.7770	0.0422
0.1111	0.0238	0.0216	7.9409	7.9560	0.0151
0.1111	0.0278	0.0252	8.1403	8.1350	-0.0053
0.1111	0.0316	0.0285	8.3265	8.3041	-0.0224
0.1111	0.0360	0.0323	8.5387	8.5129	-0.0258
0.1111	0.0403	0.0360	8.7453	8.6720	-0.0733

	CHEMICAL SHIFT OF FREE SUBSTRATE	CHEMICAL SHIFT OF 1:1 COMPLEX	EQUILIBRIUM CONSTANT
	6.7332	6.2098	111.4736
STANDARD DEVIATIONS	0.0451	0.1780	7.4128
DERIVATIVES	0.0004	0.0001	0.0000

STANDARD DEVIATION OF AN OBSERVATION OF UNIT WEIGHT 0.1036

PERCENTAGE OF STANDARD DEVIATION 0.4110

TABLE 28

Computer Output from a Direct Determination of Equilibrium Constant and Δ for ortho Proton in DMB [Shift Reagent: $Eu(dpm)_3$].

CONCENTRATION OF SUBSTRATE	CONCENTRATION OF LANTHANIDE	1:1 COMPLEX	* CALCULATED CHEMICAL SHIFT (SC)	* OBSERVED CHEMICAL SHIFT (SO)	SO-SC
0.0278	0.0056	0.0041	8.3652	8.2742	-0.0910
0.0278	0.0090	0.0063	9.3715	9.2389	-0.1326
0.0278	0.0123	0.0084	10.3061	10.0643	-0.2418
0.0278	0.0157	0.0103	11.1692	10.9494	-0.2198
0.0278	0.0190	0.0121	11.9521	11.8147	-0.1374
0.0278	0.0222	0.0136	12.6423	12.6103	-0.0321
0.0278	0.0253	0.0149	13.2228	13.3164	0.0936
0.0278	0.0288	0.0162	13.8166	14.0026	0.1860
0.0278	0.0323	0.0174	14.3252	14.5993	0.2741
0.0556	0.0061	0.0052	7.6818	7.7969	0.1151
0.0556	0.0095	0.0080	8.3249	8.3737	0.0488
0.0556	0.0129	0.0108	8.9436	8.9207	-0.0229
0.0556	0.0170	0.0140	9.6662	9.6168	-0.0494
0.0556	0.0206	0.0167	10.2838	10.2732	-0.0106
0.0556	0.0241	0.0193	10.8674	10.7903	-0.0771
0.0556	0.0274	0.0217	11.3959	11.3274	-0.0685
0.0556	0.0313	0.0243	11.9792	11.9439	-0.0352
0.0556	0.0350	0.0267	12.5244	12.5605	0.0361
0.1111	0.0072	0.0067	7.2744	7.4985	0.2242
0.1111	0.0114	0.0104	7.6979	7.8466	0.1487
0.1111	0.0155	0.0142	8.1186	8.1947	0.0760
0.1111	0.0196	0.0179	8.5373	8.6124	0.0751
0.1111	0.0238	0.0216	8.9515	8.9903	0.0388
0.1111	0.0278	0.0252	9.3520	9.3483	-0.0037
0.1111	0.0316	0.0285	9.7262	9.6665	-0.0596
0.1111	0.0360	0.0323	10.1526	10.1240	-0.0286
0.1111	0.0403	0.0360	10.5678	10.4621	-0.1056

	CHEMICAL SHIFT OF FREE SUBSTRATE	CHEMICAL SHIFT OF 1:1 COMPLEX	EQUILIBRIUM CONSTANT
	6.5248	12.4772	111.4736
STANDARD DEVIATIONS	0.0492	0.2776	7.4128
DERIVATIVES	0.0006	0.0002	0.0000

STANDARD DEVIATION OF AN OBSERVATION OF UNIT WEIGHT 0.1036

PERCENTAGE OF STANDARD DEVIATION 0.4110

TABLE 29

Computer Output from a Direct Determination of Equilibrium Constant and Δ for Methyl in DMB [Shift Reagent: $Eu(dpm)_3$].

CONCENTRATION OF SUBSTRATE	CONCENTRATION OF LANTHANIDE	1:1 COMPLEX	* CALCULATED * CHEMICAL * SHIFT (SC) *	* OBSERVED * CHEMICAL * SHIFT (SO) *	SO-SC
0.0278	0.0056	0.0041	4.9742	4.9128	-0.0614
0.0278	0.0090	0.0063	5.7317	5.6189	-0.1128
0.0278	0.0123	0.0084	6.4353	6.2256	-0.2097
0.0278	0.0157	0.0103	7.0850	6.9018	-0.1832
0.0278	0.0190	0.0121	7.6744	7.5681	-0.1062
0.0278	0.0222	0.0136	8.1940	8.1450	-0.0490
0.0278	0.0253	0.0149	8.6309	8.6820	0.0510
0.0278	0.0288	0.0162	9.0780	9.2290	0.1510
0.0278	0.0323	0.0174	9.4608	9.7063	0.2455
0.0556	0.0061	0.0052	4.4597	4.5648	0.1051
0.0556	0.0095	0.0080	4.9438	4.9824	0.0386
0.0556	0.0129	0.0108	5.4095	5.3902	-0.0194
0.0556	0.0170	0.0140	5.9536	5.9173	-0.0363
0.0556	0.0206	0.0167	6.4185	6.3747	-0.0438
0.0556	0.0241	0.0193	6.8578	6.8024	-0.0554
0.0556	0.0274	0.0217	7.2557	7.2101	-0.0455
0.0556	0.0313	0.0243	7.6948	7.6875	-0.0073
0.0556	0.0350	0.0267	8.1052	8.1450	0.0397
0.1111	0.0072	0.0067	4.1530	4.3360	0.1830
0.1111	0.0114	0.0104	4.4718	4.5846	0.1128
0.1111	0.0155	0.0142	4.7885	4.8532	0.0646
0.1111	0.0196	0.0179	5.1037	5.1615	0.0578
0.1111	0.0238	0.0216	5.4155	5.4499	0.0344
0.1111	0.0278	0.0252	5.7170	5.7184	0.0013
0.1111	0.0316	0.0285	5.9987	5.9670	-0.0317
0.1111	0.0360	0.0323	6.3197	6.2753	-0.0444
0.1111	0.0403	0.0360	6.6322	6.5538	-0.0785

	CHEMICAL SHIFT OF FREE SUBSTRATE	CHEMICAL SHIFT OF 1:1 COMPLEX	* EQUILIBRIUM * CONSTANT
	3.5887	9.3928	111.4736
STANDARD DEVIATIONS	0.0469	0.2257	7.4128
DERIVATIVES	0.0005	0.0002	0.0000

STANDARD DEVIATION OF AN OBSERVATION OF UNIT WEIGHT 0.1036

PERCENTAGE OF STANDARD DEVIATION 0.4110

EXECUTION TERMINATED. EXECUTION TIME 11.599 SECONDS.

TABLE 30

DME and DMB in Competition for $Eu(dpm)_3$[a].

	δ in DME (in ppm)		δ in DMB (in ppm)		
Mixing Procedure	CH_2	CH_3	CH_3	o	m
	12.15	6.54	6.45	10.32	8.59
	13.09	6.88	6.76	10.71	8.80
0.15 M DME added	14.24	7.27	7.16	11.26	9.07
to 0.15 M DMB	15.57	7.77	7.63	11.87	9.37
	16.88	8.24	8.12	12.53	9.68
	17.95	8.63	8.52	13.08	9.95
	19.06	9.03	8.94	13.64	10.23
	10.79	6.03	5.98	9.64	8.27
	11.73	6.39	6.30	10.06	8.48
	12.19	6.55	6.40	10.25	8.57
	12.94	6.82	6.64	10.60	8.72
	13.64	7.07	6.90	10.91	8.89
0.15 M DMB added	14.20	7.28	7.08	11.17	9.01
to 0.15 M DME	14.86	7.52	7.32	11.50	9.16
	15.63	7.80	7.60	11.84	9.34
	16.50	8.12	7.93	12.28	9.56
	17.50	8.48	8.32	12.80	9.80
	18.60	8.88	8.76	13.36	10.10
free shift:	3.55	3.39	3.87	6.92	6.92

a) Shifts have to be corrected by 0.69%.

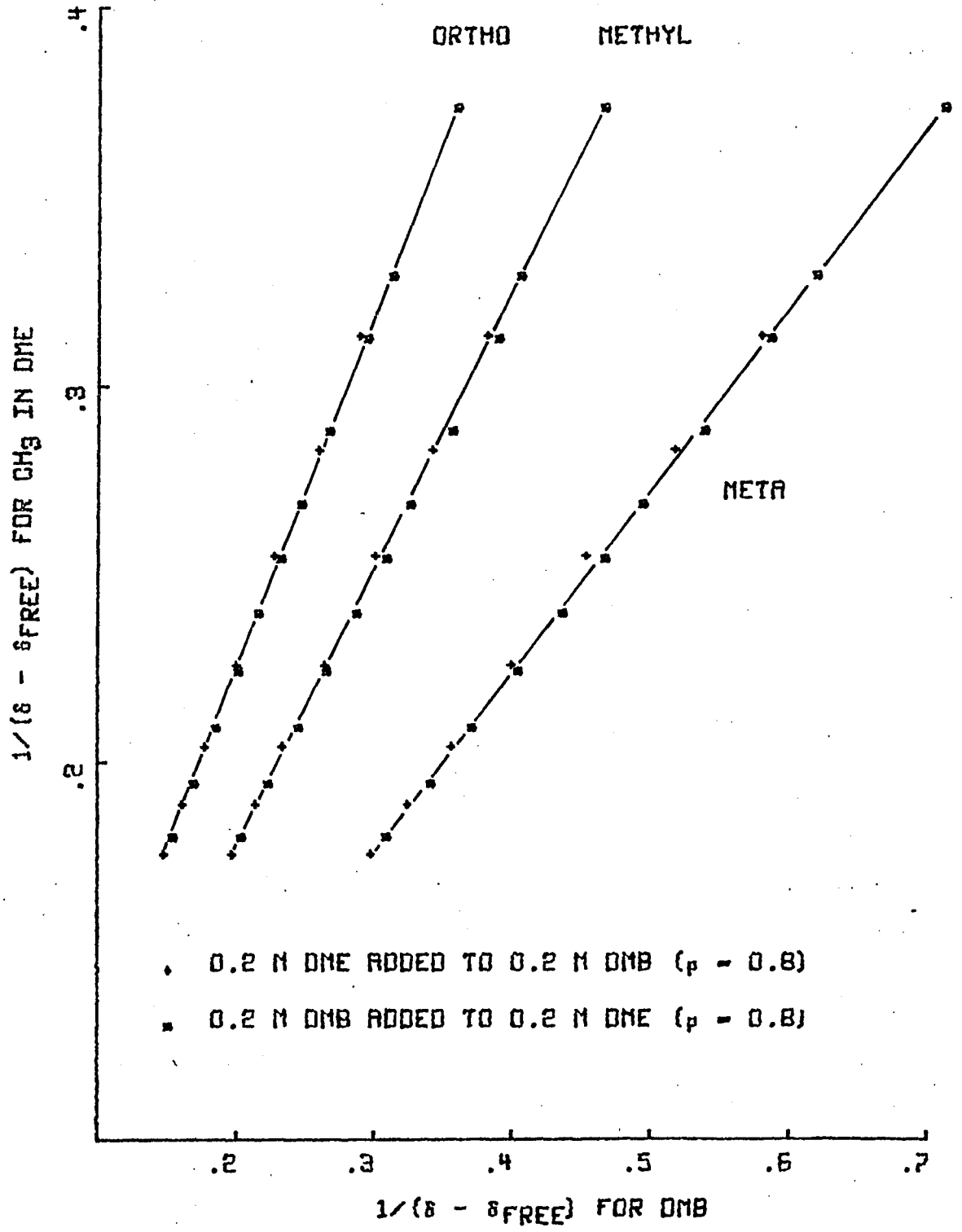

Figure 17 - 1/δ (DME) vs. 1/δ (DMB) in the Presence of $Eu(dpm)_3$.

Table 31 result with a value of K in a good agreement with the value obtained from a direct determination (Tables 27-29).

Interpretation of these results leads to the conclusion that, with $Eu(dpm)_3$ as the shift reagent, DME and DMB form only 1:1 type of adduct and the precautions taken to avoid contamination in determining equilibrium constants from a direct analysis, were effective.

No theoretical treatment was done to introduce the effect of equilibria other than substrate-shift reagent adduct formation in the competing system method. By reanalyzing Table 26, however, only the presence of complexes between $CHCl_3$ with A (or B) and the dimerization of A (or B) could be possible interfering mechanisms. The other would not alter the ratio [A]/[A·R] (or equivalent expression for B) and so should not affect in the application of equation 38.

It is realized that the agreement in the equilibrium constant for DMB-$Eu(dpm)_3$ by the two methods is not a proof for the accuracy of K for DME-$Eu(dpm)_3$. If $CHCl_3$ binds to the shift reagent (which produces a strong effect from Table 26), the ratio of K's from competitive experiments will still agree with the values of a direct determination since in this last case, the K's will be affected in the same extension.

Description of the System DME-$Eu(fod)_3$

$Eu(fod)_3$ has been frequently used as a shift reagent. Its solubility in organic solvents is much higher than $Eu(dpm)_3$, which therefore avoids tedious and careful procedures to achieve a homogeneous solution. Observations over the wider range of concentrations, which this reagent makes possible, has provided evidences for higher adduct formation[7,51].

Again, motivated by the low temperature pmr with DME as the

TABLE 31

Least-square Fit to $1/\delta$ *vs.* $1/\delta$ for DME-DMB in the Presence of $Eu(dpm)_3$.

	CH_2 in DME *vs.*			CH_3 in DME *vs.*		
	CH_3	*o* proton in DMB	*m* proton	CH_3	*o* proton in DMB	*m* proton
Slope	0.2689	0.3470	0.1769	0.7267	0.9376	0.4781
σ_{slope}	0.0024	0.0029	0.0015	0.0068	0.0084	0.0044
Intercept	0.0114	0.0132	0.0115	0.0333	0.0381	0.0336
$\sigma_{interc.}$	0.0007	0.0007	0.0007	0.0021	0.0020	0.0021
Corr. Coeff.	0.9994	0.9995	0.9994	0.9993	0.9994	0.9993
K_{DMB}	119.1	112.3	118.7	115.3	108.5	114.9
σ_K	9.6	9.4	9.6	10.2	9.8	10.1
Δ	8.58	11.74	5.66	8.91	12.22	5.89
σ_Δ	0.03	0.08	0.02	0.03	0.07	0.02

Average values for DMB - $Eu(dpm)_3$

$K = 115.\ M^{-1}$ ($\pm 4.$)

$\Delta_{CH_3} = 8.75$ ppm (± 0.02)

$\Delta_{\underline{ortho}} = 12.01$ ppm (± 0.05)

$\Delta_{\underline{meta}} = 5.78$ ppm (± 0.01)

substrate[55], only 1:1 type of adducts are expected for this system at room temperature. The already mentioned procedure of a direct determination of K and Δ's was applied for DME-Eu(fod)$_3$. One main problem arose. Severe broadening of the pmr signals was observed of such a magnitude that made it impossible to obtain chemical shift data. It was noted that addition of traces of water greatly sharpened such signals, but caused no shifting, that is water acts as a catalyst to the interchange between the free and the complex substrate molecules, but does not interfere as "scavenger." This may appear strange at this point, but an explanation will be offered in the section DME and Neopentanol (11) in Competition for Eu(fod)$_3$.

Using as solvent deuterated chloroform saturated with water, the observed chemical shifts for DME-Eu(fod)$_3$ are given in Tables 32-33; Figure 18 is a representation of the chemical shifts for CH_2 as a function of Eu(fod)$_3$ and DME concentrations.

DMB and DME in Competition for Eu(fod)$_3$

In a similar manner as for Eu(dpm)$_3$, the presence of only 1:1 type of adducts with the fluorinated shift reagent must be demonstrated. DMB was again the choice with results similar to the previous reported. Tables 34 and 35 summarize observed chemical shifts and least square analysis to the straight line predicted by equation 38. Figure 19 is an example of such correlation.

It may appear that the magnitude of the equilibrium constant for the system DMB-Eu(fod)$_3$ is low compared to the respective value for DME, and no further attempt to demonstrate the accuracy by a direct determination was carried out, since the major concern was the stoichiometry of the adducts. The apparent relative instability of Eu(fod)$_3$·DMB *vs.*

TABLE 32

Computer Output from a Direct Determination of Equilibrium Constant and Δ for CH_3 in DME [Shift Reagent: $Eu(fod)_3$].

CONCENTRATION OF SUBSTRATE	CONCENTRATION OF LANTHANIDE	CONCENTRATION OF 1:1 COMPLEX	CALCULATED CHEMICAL SHIFT (SC)	OBSERVED CHEMICAL SHIFT (SO)	SO-SC
0.1076	0.1191	0.1035	11.4812	11.5175	0.0363
0.1076	0.1066	0.0993	11.1472	11.0757	-0.0716
0.1076	0.0940	0.0907	10.4710	10.3627	-0.1083
0.1076	0.0831	0.0812	9.7216	9.6096	-0.1120
0.1076	0.0714	0.0703	8.8634	8.7661	-0.0973
0.1076	0.0595	0.0588	7.9583	7.8925	-0.0658
0.1076	0.0476	0.0471	7.0408	7.0591	0.0183
0.1076	0.0357	0.0354	6.1167	6.1554	0.0387
0.1076	0.0238	0.0236	5.1894	5.2316	0.0422
0.0538	0.1191	0.0533	11.7273	11.7384	0.0111
0.0538	0.1066	0.0532	11.7092	11.7083	-0.0009
0.0538	0.0940	0.0530	11.6800	11.6982	0.0182
0.0538	0.0831	0.0527	11.6365	11.6681	0.0317
0.0538	0.0714	0.0521	11.5422	11.6079	0.0656
0.0538	0.0649	0.0515	11.4334	11.4773	0.0439
0.0538	0.0595	0.0504	11.2670	11.2765	0.0095
0.0538	0.0510	0.0469	10.7087	10.7142	0.0055
0.0538	0.0476	0.0446	10.3566	10.2322	-0.1244
0.0538	0.0408	0.0392	9.4981	9.4690	-0.0291
0.0538	0.0357	0.0346	8.7785	8.7461	-0.0324
0.0538	0.0286	0.0279	7.7243	7.6917	-0.0325
0.0538	0.0238	0.0233	7.0047	7.0591	0.0544
0.0538	0.0179	0.0176	6.0932	6.2056	0.1123
0.0269	0.1110	0.0267	11.7446	11.7083	-0.0363
0.0269	0.0476	0.0262	11.5682	11.7284	0.1602
0.0269	0.0376	0.0256	11.3895	11.4572	0.0677
0.0269	0.0332	0.0250	11.2101	11.2765	0.0664
0.0269	0.0286	0.0238	10.8293	10.8648	0.0354
0.0269	0.0260	0.0227	10.4684	10.4631	-0.0052
0.0269	0.0238	0.0214	10.0715	10.1016	0.0301
0.0269	0.0255	0.0224	10.3911	10.3125	-0.0786
0.0269	0.0216	0.0199	9.5942	9.5795	-0.0147
0.0269	0.0179	0.0168	8.6281	8.6155	-0.0126
0.0269	0.0143	0.0137	7.6281	7.6214	-0.0067
0.0269	0.0119	0.0114	6.9347	6.9185	-0.0162

	CHEMICAL SHIFT OF FREE SUBSTRATE	CHEMICAL SHIFT OF 1:1 COMPLEX	EQUILIBRIUM CONSTANT
	3.3266	8.4801	1608.8735
STANDARD DEVIATIONS	0.0622	0.0816	92.9064
DERIVATIVES	0.0058	0.0047	0.0000

STANDARD DEVIATION OF AN OBSERVATION OF UNIT WEIGHT 0.1063

PERCENTAGE OF STANDARD DEVIATION 0.2866

TABLE 33

Computer Output from a Direct Determination of Equilibrium Constant and Δ for CH_2 in DME [Shift Reagent: $Eu(fod)_3$].

CONCENTRATION OF SUBSTRATE	CONCENTRATION OF LANTHANIDE	1:1 COMPLEX	* CALCULATED * CHEMICAL * SHIFT (SC) *	* OBSERVED * CHEMICAL * SHIFT (SO) *	SO-SC
0.1076	0.1191	0.1035	19.5689	19.6209	0.0520
0.1076	0.1066	0.0993	18.9050	18.7473	-0.1578
0.1076	0.0940	0.0907	17.5609	17.3114	-0.2495
0.1076	0.0831	0.0812	16.0714	15.8252	-0.2461
0.1076	0.0714	0.0703	14.3656	14.1483	-0.2172
0.1076	0.0595	0.0588	12.5665	12.4212	-0.1453
0.1076	0.0476	0.0471	10.7427	10.8347	0.0920
0.1076	0.0357	0.0354	8.9058	8.9971	0.0913
0.1076	0.0238	0.0236	7.0626	7.1696	0.1070
0.0538	0.1191	0.0533	20.0581	20.0828	0.0247
0.0538	0.1066	0.0532	20.0221	20.0426	0.0205
0.0538	0.0940	0.0530	19.9641	20.0125	0.0484
0.0538	0.0831	0.0527	19.8775	19.9623	0.0848
0.0538	0.0714	0.0521	19.6902	19.8318	0.1416
0.0538	0.0649	0.0515	19.4739	19.5707	0.0968
0.0538	0.0595	0.0504	19.1432	19.1791	0.0359
0.0538	0.0510	0.0469	18.0333	18.0143	-0.0191
0.0538	0.0476	0.0446	17.3335	17.0904	-0.2431
0.0538	0.0408	0.0392	15.6271	15.5541	-0.0730
0.0538	0.0357	0.0346	14.1966	14.1182	-0.0784
0.0538	0.0286	0.0279	12.1012	12.0296	-0.0716
0.0538	0.0238	0.0233	10.6710	10.7242	0.0532
0.0538	0.0179	0.0176	8.8592	9.0975	0.2383
0.0269	0.1110	0.0267	20.0925	20.0426	-0.0498
0.0269	0.0476	0.0262	19.7418	19.9924	0.2506
0.0269	0.0376	0.0256	19.3867	19.5707	0.1840
0.0269	0.0332	0.0250	19.0300	19.1891	0.1591
0.0269	0.0286	0.0238	18.2732	18.3657	0.0925
0.0269	0.0260	0.0227	17.5557	17.5423	-0.0134
0.0269	0.0238	0.0214	16.7669	16.8695	0.1026
0.0269	0.0255	0.0224	17.4022	17.2511	-0.1511
0.0269	0.0216	0.0199	15.8182	15.7449	-0.0733
0.0269	0.0179	0.0168	13.8978	13.8471	-0.0507
0.0269	0.0143	0.0137	11.9101	11.8890	-0.0211
0.0269	0.0119	0.0114	10.5318	10.5234	-0.0084

	CHEMICAL SHIFT OF FREE SUBSTRATE	CHEMICAL SHIFT OF 1:1 COMPLEX	* EQUILIBRIUM * CONSTANT
	3.3599	16.8561	1608.8735
STANDARD DEVIATIONS	0.0623	0.0885	92.9064
DERIVATIVES	0.0127	0.0105	0.0000

STANDARD DEVIATION OF AN OBSERVATION OF UNIT WEIGHT 0.1063

PERCENTAGE OF STANDARD DEVIATION 0.2866

EXECUTION TERMINATED. EXECUTION TIME 9.649 SECONDS.

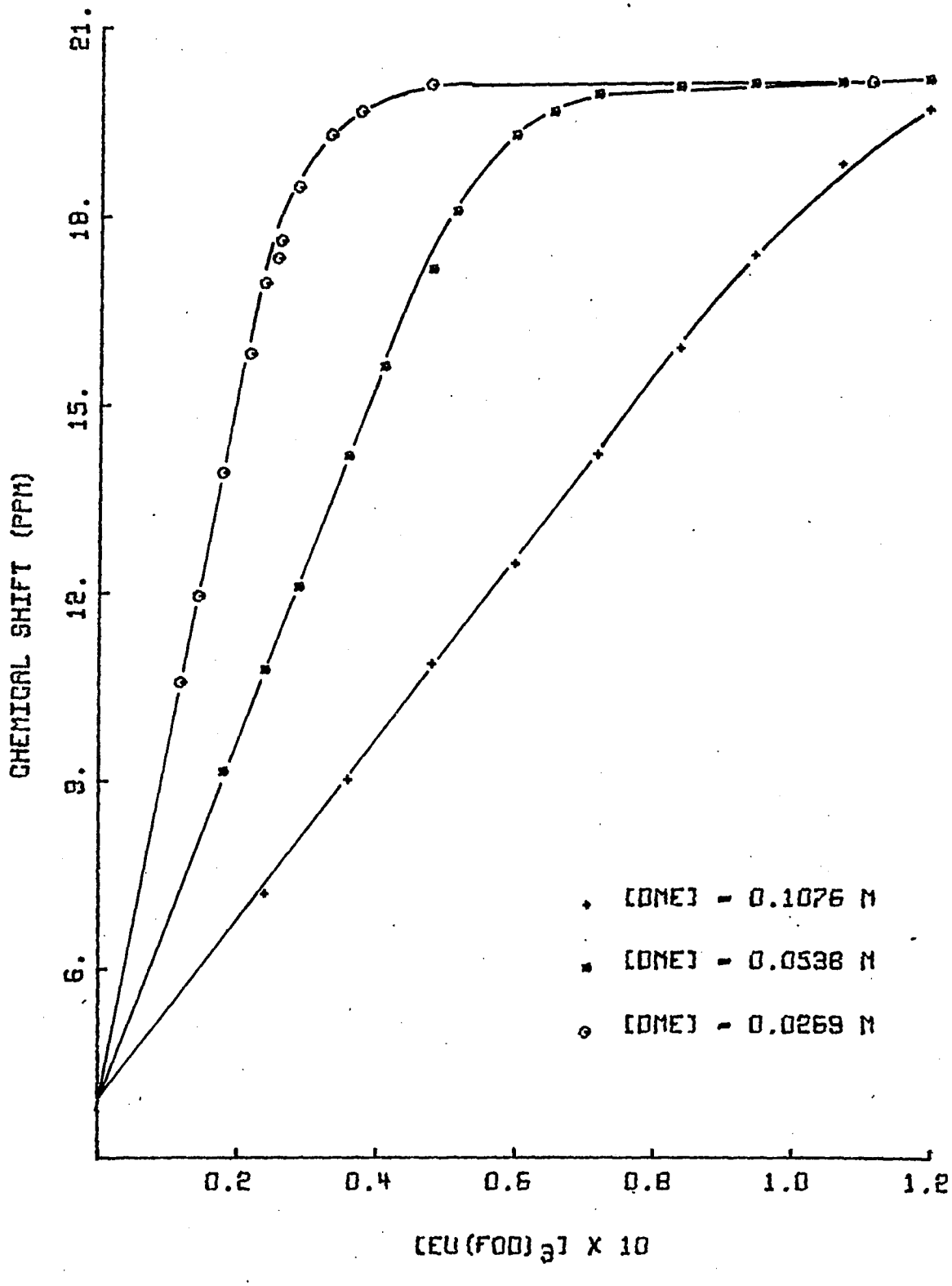

Figure 18 - Chemical Shifts of CH_2 in DME vs. DME and $Eu(fod)_3$ Concentrations.

TABLE 34

DME and DMB in Competition for Eu(fod)$_3$[a].

	δ in DME (in ppm)		δ in DMB (in ppm)		
Mixing Procedure	CH_2	CH_3	CH_3	o	m
	16.62	9.98	5.03	8.26	7.54
	17.70	10.53	5.55	8.88	7.84
	18.27	10.79	6.06	9.52	8.13
0.2 M DME added to	18.73	11.03	6.68	10.27	8.48
0.2 M DMB	19.07	11.20	7.39	11.03	8.88
	19.39	11.34	8.13	12.02	9.31
	19.59	11.45	8.92	12.98	9.74
	19.68	11.51	9.59	13.78	10.12
	17.07	10.20	5.22	8.50	7.64
	17.36	10.36	5.37	8.66	7.72
0.2 M DMB added to	17.65	10.51	5.54	8.86	7.81
0.2 M DME	17.90	10.62	5.76	9.10	7.93
	18.22	10.78	6.06	9.49	8.11
free shift	3.55	3.39	3.87	6.92	6.92

a) Shifts must be corrected by 0.69%.

TABLE 35

Least-square Fit to $1/\delta$ *vs.* $1/\delta$ for DME-DMB in the Presence of $Eu(fod)_3$

	CH_2 in DME *vs.*			CH_3 in DME *vs.*		
	CH_3	*o* proton in DMB	*m* proton	CH_3	*o* proton in DMB	*m* proton
Slope	0.0217	0.0252	0.0120	0.0421	0.0489	0.0234
σ_{slope}	0.0001	0.0002	0.0001	0.0005	0.0006	0.0003
Intercept	0.0577	0.0578	0.0578	0.1148	0.1151	0.1150
$\sigma_{interc.}$	0.0001	0.0001	0.0001	0.0002	0.0002	0.0002
Corr. Coeff.	0.9997	0.9997	0.9997	0.9994	0.9993	0.9993
K_{DMB}	44.1	41.4	41.4	42.6	38.5	39.9
σ_K	13.5	13.4	13.4	6.7	6.4	6.5
Δ	13.35	16.51	7.86	13.47	17.31	8.00
σ_Δ	3.19	4.17	1.98	1.16	1.66	0.73

Average values for DMB-$Eu(fod)_3$

K = 41. M^{-1} (±3.)

Δ_{CH_3} = 13. ppm (±1.)

$\Delta_{\underline{ortho}}$ = 17. ppm (±2.)

$\Delta_{\underline{meta}}$ = 8.0 ppm (±0.7)

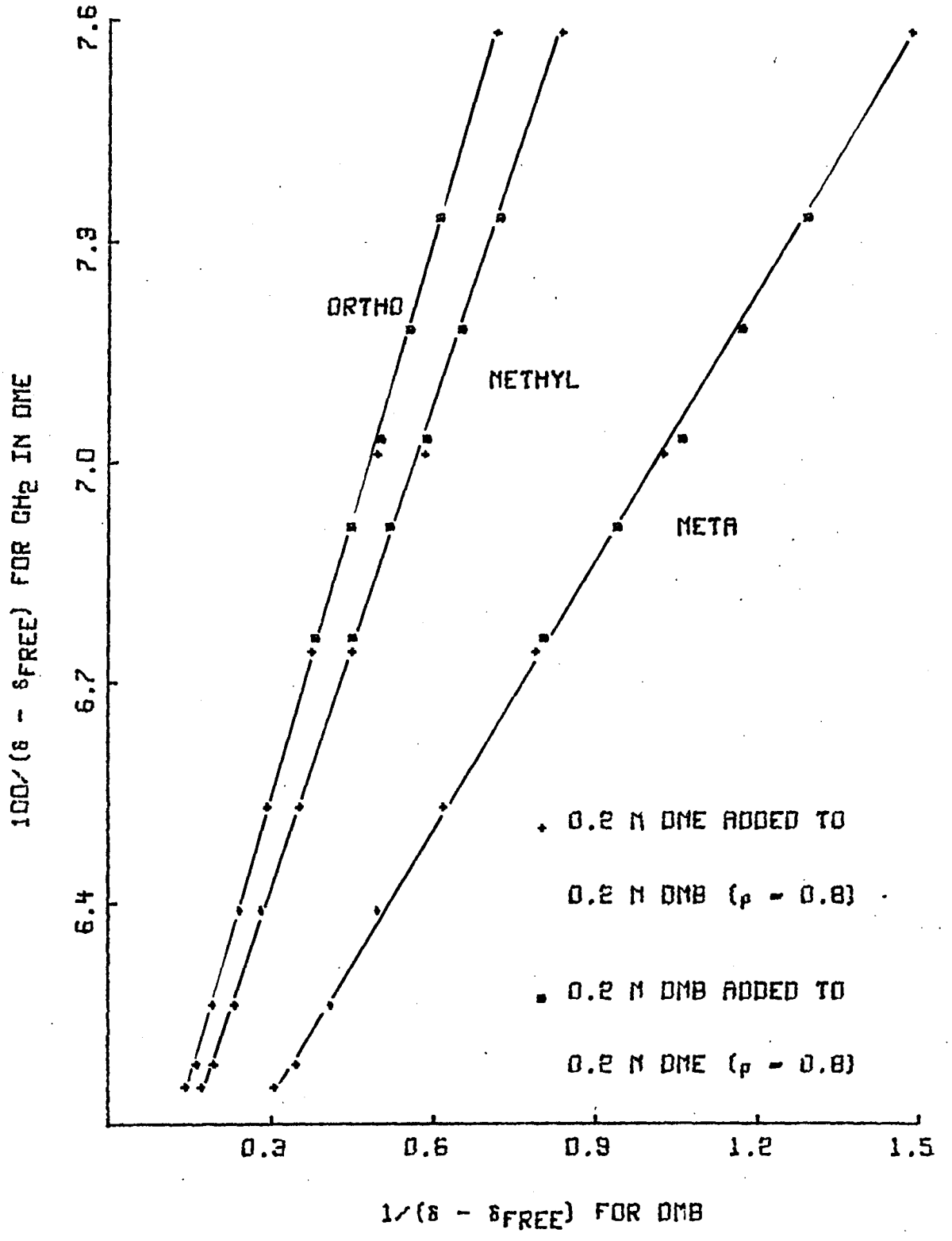

Figure 19 - 1/δ (DME) vs. 1/δ (DMB) in the Presence of $Eu(fod)_3$.

$Eu(fod)_3 \cdot DME$ could be due to different spatial arrangements and angle stress in the formation of the adducts. As a first approximation, the higher value for $\Delta(CH_3)$ in DMB [compared to $\Delta(CH_3)$ in DME] could be interpreted as a smaller Ln-O bond, which could result in a more unstable five-membered ring in the chelate.

Independently of the relative equilibrium constants, the straight lines with a high correlation coefficient are the basis for believing that at room temperature the preferred stoichiometry for the adduct formation between $Eu(dpm)_3$ and DME (and DMB) is 1:1. Even if a coordination number 9 has been detected for some lanthanides, it appears from the previous results that with these particular shift reagents, the higher coordination number will be 8 since a clear deviation from linearity would otherwise be expected for the competitive systems described here and in previous sections. Theoretical analysis for a higher coordination number of 9 was not carried out, but the above statement is extrapolated from the difference between the 1:1 analysis and 1:1 and 2:1 adduct formation analysis (compare sections Introduction to Competitive Systems with Theoretical Analysis Including 2:1 Type of Adduct for B).

DME and Neopentanol (11) in Competition for $Eu(dpm)_3$

Table 36 gives experimental data for the system neopentanol (11) and DME in the presence of $Eu(dpm)_3$, Figure 20 is a graphical example of the $1/\delta$ vs. $1/\delta$ plots.

If the approximation to a straight line of equation 38 is made, the values reported in Table 37 result. Particular attention is called to the magnitude of the resulting equilibrium constant, since a drastic difference exists with previously reported values[47,49] (see Table 4, $K = 10\text{-}6.3\ M^{-1}$).

TABLE 36

Neopentanol and DME in Competition for $Eu(dpm)_3$[a].

	δ in DME (in ppm)		δ in neopentanol (in ppm)	
	CH_2	CH_3	CH_2	CH_3
	7.13	4.77	7.80	2.65
	7.46	4.88	8.20	2.80
0.2 M DME added to	7.90	5.05	8.78	3.03
0.2 M neopentanol.	8.36	5.22	9.37	3.25
	9.02	5.45	10.14	3.56
	9.66	5.72	11.00	3.90
	7.45	4.88	8.14	2.77
	7.87	5.04	8.57	2.96
0.2 M neopentanol	8.28	5.19	8.98	3.13
added to 0.2 M DME.	8.89	5.41	9.64	3.37
	9.62	5.67	10.33	3.65
	10.37	5.95	11.27	3.97
	10.04	5.85	11.06	3.98
	10.50	5.97	11.57	4.14
0.5 M DME added to	10.98	6.19	12.09	4.42
0.5 M neopentanol.	11.79	6.50	12.91	4.73
	13.00	6.95	14.00	5.18
	14.44	7.56	15.32	5.69
	10.00	5.81	11.06	3.97
	10.68	6.07	11.56	4.17
0.5 M neopentanol	11.66	6.48	12.29	4.49
added to 0.5 M DME.	12.62	6.79	12.92	4.72
	13.85	7.24	13.75	5.02
	15.33	7.77	14.69	5.42
free shift	3.56	3.42	3.31	0.92

a) Shifts must be corrected by -2.94%.

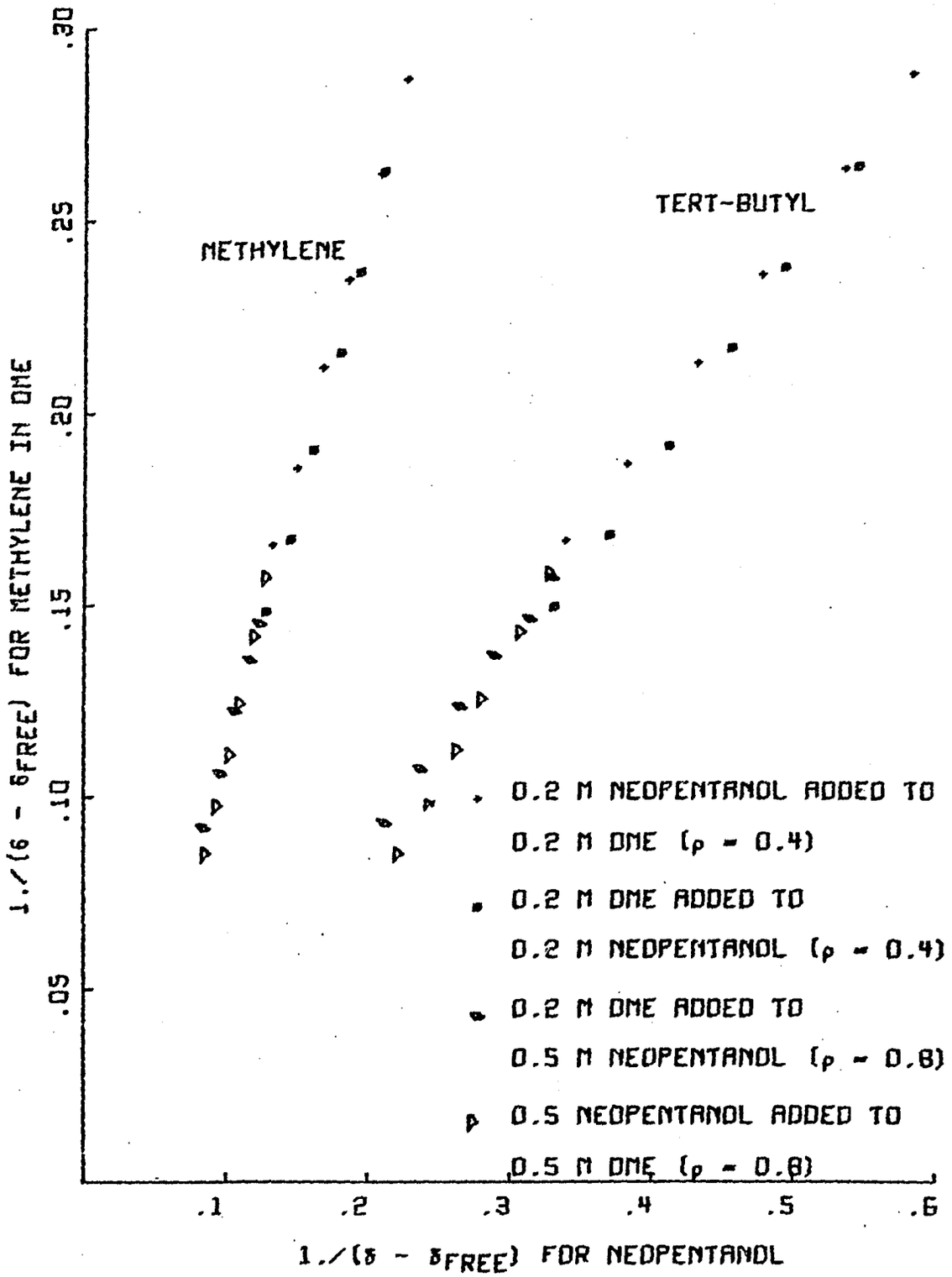

Figure 20 - 1/δ (DME) vs. 1/δ (Neopentanol) in the Presence of $Eu(dpm)_3$

TABLE 37

Least-square Fit to $1/\delta$ *vs.* $1/\delta$ for DME - Neopentanol in the Presence of $Eu(dpm)_3$.

	CH_2 in DME *vs.*		CH_3 in DME *vs.*	
	CH_2 in Neopentanol	CH_3 in Neopentanol	CH_2 in Neopentanol	CH_3 in Neopentanol
Slope	1.3916	0.5314	3.8323	1.4636
σ_{slope}	0.0280	0.0107	0.0758	0.0283
Intercept	-0.0277	-0.0223	-0.0808	-0.0659
$\sigma_{interc.}$	0.0041	0.0040	0.0111	0.0106
Corr. Coeff.	0.9956	0.9956	0.9957	0.9959
$K_{\underline{11}}$	267.6	247.1	276.7	255.6
σ_K	28.1	27.0	27.7	26.4
Δ	19.75	8.17	19.59	8.10
σ_Δ	0.33	0.17	0.09	0.06

Average values for **11** - $Eu(dpm)_3$

$K_{\underline{11}} = 260.\ M^{-1}$ ($\pm 14.$)

$\Delta_{CH_2} = 19.60$ ppm (± 0.09)

$\Delta_{CH_3} = 8.11$ ppm (± 0.06)

Because of different ambient conditions and treatment of data, it was desirable to estimate once more K and Δ's for 11 by a direct determination as performed with the DME and DMB. Tables 38 and 39 give results by applying the method described in Appendix 5. Even though this procedure affords a value for K which is considerably higher than that reported in the literature ($K = 150\ M^{-1}$), a significant difference exists between it and the $K = 260\ M^{-1}$ from the competition analysis.

There are two possible explanations for such a behavior:

1) The direct determination of K and Δ for an alcohol could be affected by interfering equilibria (Table 26) to a different extent than the ether. For example, self-association for alcohols occurs to a considerable extent (see $La(dpm)_3$ and Aliphatic Systems), and so the association with $CHCl_3$ (this last possibility will tend to decrease K from a direct determination method). Furthermore, these two effects are the only ones that could influence the results of the competitive system analysis and they probably do not occur to the same extent in DME. A deviation from linearity could result, but no further attempts to include these effects were made.

2) Reexamination of Figure 20 shows a close similarity with Figure 12, where competing 2:1 and 1:1 equilibria are plotted. An attempt is made to analyze the data of Table 36 by the procedure described in Appendix 6, where 2:1 and 1:1 adducts are assumed to be formed by the substrate B and the shift reagent. Such analysis is, however, generally unsuccessful, since no convergence is reached. For the 0.2 M data set, using the chemical shifts of tert-butyl of 11 and methyl and methylene of DME, a convergence is obtained with the results summarized in Table 40.

TABLE 38

Computer Output from a Direct Determination of Equilibrium Constant and Δ for CH_2 in Neopentanol [Shift Reagent: $Eu(dpm)_3$].

CONCENTRATION OF SUBSTRATE	CONCENTRATION OF LANTHANIDE	1:1 COMPLEX	CALCULATED CHEMICAL SHIFT (SC)	OBSERVED CHEMICAL SHIFT (SO)	SO-SC
0.1375	0.0176	0.0166	6.4460	6.3100	-0.1360
0.1375	0.0156	0.0148	6.0921	6.0000	-0.0921
0.1375	0.0137	0.0130	5.7320	5.6600	-0.0720
0.1375	0.0120	0.0114	5.4212	5.3500	-0.0712
0.1375	0.0102	0.0097	5.0878	5.0500	-0.0378
0.1375	0.0084	0.0080	4.7465	4.7200	-0.0265
0.1375	0.0065	0.0062	4.4048	4.4600	0.0552
0.1375	0.0047	0.0045	4.0644	4.1000	0.0356
0.1375	0.0029	0.0027	3.7217	3.8000	0.0783
0.0687	0.0172	0.0153	9.1904	9.3200	0.1296
0.0687	0.0152	0.0136	8.5190	8.6200	0.1010
0.0687	0.0132	0.0119	7.8319	7.8800	0.0481
0.0687	0.0115	0.0103	7.2327	7.2700	0.0373
0.0687	0.0096	0.0087	6.5916	6.6300	0.0384
0.0687	0.0078	0.0070	5.9325	5.9200	-0.0125
0.0687	0.0059	0.0053	5.2660	5.3000	0.0340
0.0687	0.0040	0.0036	4.5994	4.7400	0.1406
0.0687	0.0021	0.0019	3.9258	4.1000	0.1742
0.0344	0.0184	0.0139	14.0540	14.2600	0.2060
0.0344	0.0163	0.0125	12.9758	13.0000	0.0242
0.0344	0.0142	0.0110	11.8299	11.7400	-0.0899
0.0344	0.0124	0.0097	10.8051	10.6900	-0.1151
0.0344	0.0104	0.0083	9.6793	9.6700	-0.0093
0.0344	0.0084	0.0068	8.4975	8.3500	-0.1475
0.0344	0.0064	0.0052	7.2787	7.0800	-0.1987
0.0344	0.0044	0.0036	6.0381	5.9000	-0.1381
0.0344	0.0024	0.0020	4.7656	4.8100	0.0444

	CHEMICAL SHIFT OF FREE SUBSTRATE	CHEMICAL SHIFT OF 1:1 COMPLEX	EQUILIBRIUM CONSTANT
	3.1883	26.9122	150.4342
STANDARD DEVIATIONS	0.0364	0.5202	12.6414
DERIVATIVES	0.0006	0.0001	0.0000

STANDARD DEVIATION OF AN OBSERVATION OF UNIT WEIGHT 0.0812

PERCENTAGE OF STANDARD DEVIATION 0.6841

TABLE 39

Computer Output from a Direct Determination of Equilibrium Constant and Δ for tert-butyl in Neopentanol [Shift Reagent: $Eu(dpm)_3$].

CONCENTRATION OF SUBSTRATE	CONCENTRATION OF LANTHANIDE	1:1 COMPLEX	* CALCULATED CHEMICAL SHIFT (SC)	* OBSERVED CHEMICAL SHIFT (SO)	SO-SC
0.1375	0.0176	0.0166	2.1256	2.0800	-0.0456
0.1375	0.0156	0.0148	1.9895	1.9600	-0.0295
0.1375	0.0137	0.0130	1.8510	1.8300	-0.0210
0.1375	0.0120	0.0114	1.7315	1.7100	-0.0215
0.1375	0.0102	0.0097	1.6032	1.6000	-0.0032
0.1375	0.0084	0.0080	1.4720	1.4700	-0.0020
0.1375	0.0065	0.0062	1.3405	1.3600	0.0195
0.1375	0.0047	0.0045	1.2096	1.2400	0.0304
0.1375	0.0029	0.0027	1.0778	1.1000	0.0222
0.0687	0.0172	0.0153	3.1812	3.2300	0.0488
0.0687	0.0152	0.0136	2.9229	2.9600	0.0371
0.0687	0.0132	0.0119	2.6586	2.6800	0.0214
0.0687	0.0115	0.0103	2.4282	2.4500	0.0218
0.0687	0.0096	0.0087	2.1816	2.1900	0.0084
0.0687	0.0078	0.0070	1.9281	1.9200	-0.0081
0.0687	0.0059	0.0053	1.6718	1.6800	0.0082
0.0687	0.0040	0.0036	1.4154	1.4700	0.0546
0.0687	0.0021	0.0019	1.1563	1.2100	0.0537
0.0344	0.0184	0.0139	5.0517	5.1400	0.0883
0.0344	0.0163	0.0125	4.6371	4.6600	0.0229
0.0344	0.0142	0.0110	4.1963	4.1700	-0.0263
0.0344	0.0124	0.0097	3.8022	3.7400	-0.0622
0.0344	0.0104	0.0083	3.3692	3.3300	-0.0392
0.0344	0.0084	0.0068	2.9146	2.8500	-0.0646
0.0344	0.0064	0.0052	2.4459	2.3800	-0.0659
0.0344	0.0044	0.0036	1.9687	1.9100	-0.0587
0.0344	0.0024	0.0020	1.4793	1.4900	0.0107

	CHEMICAL SHIFT OF FREE SUBSTRATE	CHEMICAL SHIFT OF 1:1 COMPLEX	* EQUILIBRIUM CONSTANT
	0.8727	10.3508	150.4342
STANDARD DEVIATIONS	0.0285	0.2445	12.6414
DERIVATIVES	0.0001	0.0000	0.0000

STANDARD DEVIATION OF AN OBSERVATION OF UNIT WEIGHT 0.0812

PERCENTAGE OF STANDARD DEVIATION 0.6841

EXECUTION TERMINATED. EXECUTION TIME 7.949 SECONDS.

TABLE 40

Analysis of tert-Butyl Shifts in Neopentanol [Shift Reagent: $Eu(dpm)_3$].[a]

		K_{B1}	K_{B2}	Δ_{B1}	Δ_{B2}
From competition	CH_3	170. (8.)	1.30 (2)	10.27 (2)	5.93 (5)
with DME[b]	CH_2	186. (8.)	0.32 (7)	9.45 (7)	15. (2.)
From theoretical	CH_3	154. (1.)	-	10.51 (2)	-
K above[c]	CH_2	136. (4.)	-	10.16 (8)	-

a) The σ are given in parenthesis for the last significant figure; K's are given in M^{-1} and Δ's in ppm.

b) Chemical shifts from mixing of 0.2 M solutions.

c) Chemical shifts calculated from the first two entries in the table and treated as a 1:1 adduct formation. Compare with Table 39.

An argument against this second possibility is the large difference (especially in the Δ values) that results from such fits (it will be shown with $Eu(fod)_3$ that converged parameters are very similar), but even if a 2:1 complex is present, this species forms to a very small extent and the precision in the observed chemical shifts is not sufficient to allow accurate calculations.

In favor of the 2:1 adduct formation, is the theoretical analysis with values of K's and Δ's from Table 40. Theoretical chemical shifts were calculated (see Appendix 7) using K_{B1}, K_{B2}, Δ_1, and Δ_2 from the competition runs at the concentrations (Table 39) used for the determination of K by the direct method. The resulting chemical shifts were used as input in the calculation of K and Δ assuming that only 1:1 adducts were formed (Appendix 5). In both cases, low values of equilibrium constants result, which were included in Table 40.

Even if the 2:1 adduct formation would not be the responsible for the non-colinearity in Figure 20, the present analysis clearly shows that equilibrium constants could be erroneously determined by the direct method. From observed shifts reported in Tables 38 and 39, there is absolutely no indication that equilibria other than the 1:1 adduct formation are involved.

Attempts to analyze the chemical shifts of Tables 38 and 39 as 1:1 and 2:1 adducts (Appendix 8) failed, which could be attributed to the small range in the shift reagent concentrations.

Borneol and $Eu(dpm)_3$

Since the competitive experiments provide an alternative estimation of LIS, it is useful to compare results from a direct determination

and competitive analysis in a structure correlation. Borneol was chosen for such analysis and chemical shifts obtained by both methods are summarized in Table 11.

The problem of determining the free shift had to be overcome in this case, since, except for the CH_3 groups and the H_2 proton, these data cannot be obtained directly from the spectrum of borneol.

When observed shifts of high magnitude (*e.g.* > 100 Hz) are analyzed by using equation 38, one finds that the results are not very sensitive to the value of the free shift (see Appendix 2).

The chemical shifts for the methyl groups and the H_2 proton display a linear relationship with the total ρ (= $[Eu(dpm)_3]/\Sigma[Substrate]$), and the extrapolation to $\rho = 0$ for this case does result in a good agreement with the experimental values. It is expected that similar extrapolations would result in a close determination for the free shifts of the other protons, and they were so estimated. $1/\delta$ *vs.* $1/\delta$ plots for DME and borneol in the presence of $Eu(dpm)_3$ result in a linear relationship, thus indicating the formation of 1:1 adducts between borneol and the shift reagent as the main contributors to the observed shifts.

The ratio between the Δ's calculated by both methods is relatively constant for all protons, except for the bridgehead proton 4. The corresponding signals, however, are often superimposed with the signals from H_5 and H_{6exo}, producing in both determinations a poor evaluation of Δ.

A direct comparison between the equilibrium constants by the two methods cannot be made in this case, since they were determined in two different solvents:

1) By a direct determination (in CCl_4), K_B = 121. ± 15. M^{-1}

2) By the competitive experiment (in $CDCl_3$), K_B = 194. ± 5 M^{-1}

However, a higher value in a CCl_4 medium is generally found[96] (compared with $CDCl_3$ by the same method). Since a higher equilibrium constant value is found by the competitive experiments in $CDCl_3$, the previously used arguments for neopentanol could also be applied to this case.

DME and Neopentanol (11) in Competition for $Eu(fod)_3$

Table 41 gives experimental values for the concentrations and chemical shifts for DME and 11 mixtures in the presence of $Eu(fod)_3$ as the shift reagent. There is no doubt about a 2:1 adduct formation for 11 and $Eu(fod)_3$, as can be seen by inspection of Figure 21, where $1/\delta$ vs. $1/\delta$ plots are presented for the CH_3 (in DME) vs. CH_2 (in 11).

Appendix 6 describes the procedure used to extract values of K's and Δ's from the experimental chemical shifts, and the results for this system are summarized in Table 42. It has to be kept in mind that interference from other possible equilibria could also be present. No attempt was made to refine the analysis in this case either, since it is considered that the primary contribution of the competitive method is to unequivocally establish the stoichiometry of the adducts.

Nevertheless, despite the high standard deviations, values for the equilibrium constants are quite consistent among the four possible analysis. Unfortunately, there are not many reports in the literature concerning the formation of adducts of different stoichiometry. Isopropyl alcohol was analyzed by Reuben[52] by recording its spectra at a constant substrate concentration and varying the concentration of the shift reagent. This analysis is also the only report in the literature that can be compared with the results in the present work, using $Eu(fod)_3$ as the shift

TABLE 41

Neopentanol and DME in Competition for $Eu(fod)_3$.

Concentrations		δ in DME (in ppm)		δ in neopentanol (in ppm)	
DME	Neopentanol	CH_2	CH_3	CH_2	CH_3
0.0952	0.0804	8.87	6.04	4.07	1.20
0.1122	0.0609	8.95	6.17	4.02	1.20
0.1366	0.0329	9.12	6.26	3.88	1.13
0.0792	0.0986	9.96	6.70	4.50	1.38
0.0785	0.1068	11.16	7.32	4.90	1.54
0.0602	0.1164	12.31	7.89	5.37	1.73
0.0478	0.1280	14.03	8.76	6.22	2.07
0.0326	0.1422	16.02	9.76	7.61	2.64
0.0138	0.1598	17.85	10.59	9.78	3.51
0.2172	0.2409	13.08	8.34	8.30	2.95
0.1934	0.2611	14.51	9.06	9.36	3.39
0.1653	0.2851	15.71	9.63	10.32	3.77
0.1314	0.3139	17.09	10.351	11.55	4.28
0.0900	0.3491	18.63	11.08	13.18	4.91
0.0380	0.3933	19.98	11.75	15.53	5.81
0.2364	0.2284	11.88	7.70	7.42	2.60
0.2566	0.2036	12.45	7.96	7.46	2.62
0.2806	0.1742	12.78	8.15	7.48	2.63
0.3095	0.1388	13.26	8.37	7.43	2.59
0.3451	0.0952	13.77	8.64	7.30	2.56
0.3899	0.0404	14.38	8.96	6.70	2.30
free shift		3.56	3.42	3.31	0.92

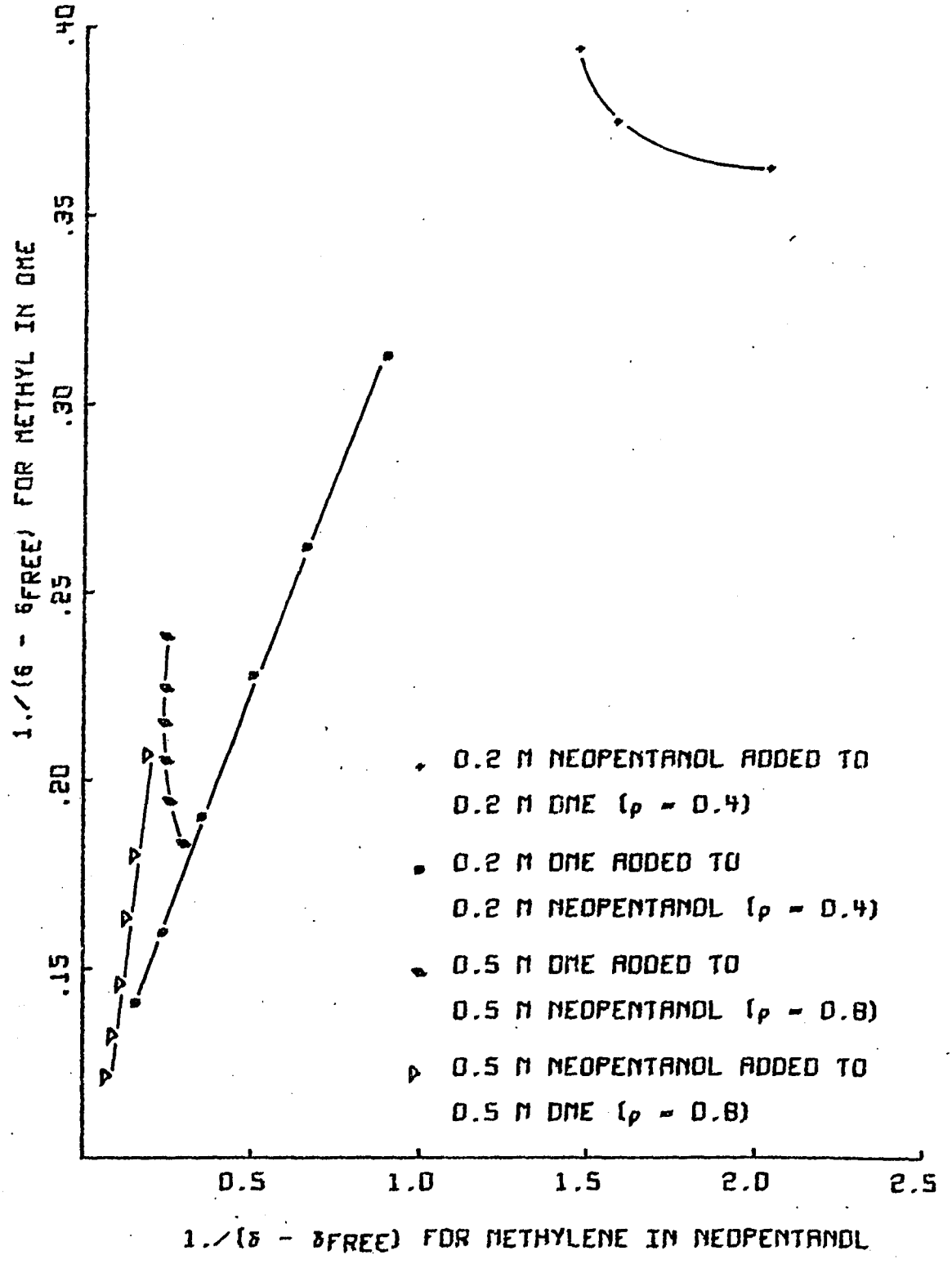

Figure 21 - 1/δ (DME) vs. 1/δ (Neopentanol) in the Presence of $Eu(fod)_3$

TABLE 42

Neopentanol - DME - $Eu(fod)_3$ Analysis.

	CH_2 in DME vs.		CH_3 in DME vs.	
	CH_2 in Neopentanol	CH_3	CH_2 in Neopentanol	CH_3
K_{B1}	83.	83.	82.	79.
σ	950.	433.	807.	373.
K_{B2}	17.	17.	17.	18.
σ	267,	122.	233.	115.
Δ_{B1}	11.	4.1	11.	4.4
σ	34.	6.7	22.	4.6
Δ_{B2}	15.	6.3	15.	6.0
σ	31.	5.9	23.	4.3

Average values for Neopentanol - $Eu(fod)_3$

$K_{B1} = 81.\ M^{-1}$ ($\pm 257.$)

$K_{B2} = 17.\ M^{-1}$ ($\pm 76.$)

	CH_2 (in ppm)	CH_3 (in ppm)
Δ_{B1} =	11. ± 18.	4.3 ± 3.8
Δ_{B2} =	15. ± 18.	6.1 ± 3.5

reagent. Values for K's and Δ's were given in Table 5 (from Reuben calculations), and are in agreement with those of Table 42 (from competitive systems).

The opportunity presents itself to explain the non-scavenger characteristic for the D_2O in the direct determination of K and Δ's for the system DME-Eu(fod)$_3$.

The percentage of H_2O in a saturated solution of $CHCl_3$ at 23°C is 0.072% by weight[97], which corresponds to a concentration of 0.06 M. Even if no data was found in the literature for this particular deuterated binary mixture, isotope effects are expected to greatly reduce the solubility of D_2O in $CDCl_3$ (in fact, the solubility[98] of D_2O in $CHCl_3$ is reduced by 15% by isotope effects).

From Figure 21, when aliquots of an alcohol are added to an original 0.2 M solution of DME, the 1/δ values for the reference signals are not affected significantly. Even if D_2O and an alcohol probably have different equilibrium constants for the adduct formation, a behavior similar to Figure 21 for D_2O should not be surprising.

DME and 2-Butanone (12) in Competition for Eu(dpm)$_3$

Ketones are known to bind weakly with shift reagents. With Eu(dpm)$_3$ and DME as the reference, the chemical shifts of 2-butanone and DME from competitive runs are reported in Table 43. 1/δ *vs.* 1/δ plots afford values of intercepts and slopes of Table 44, from which the values for K and Δ's were calculated. Good straight lines result from this system, as illustrated in Figure 22 for the CH_2 (in DME) *vs.* the methyl groups in 12.

The data from ketone 12 provide further confidence in the K

TABLE 43

2-Butanone and DME in Competition for $Eu(dpm)_3$[a].

	δ in DME (in ppm)		δ in 2-butanone (in ppm)		
Mixing Procedure	CH_2	CH_3	CH_3(s)	CH_2	CH_3(t)
	13.66	7.04	2.64	2.94	1.45
	15.09	7.56	2.79	3.08	1.55
0.1 M DME added to	16.56	8.08	2.99	3.29	1.71
0.4 M 2-butanone	18.28	8.72	3.32	3.63	1.96
	19.68	9.24	3.71	4.01	2.24
	20.74	9.60	4.17	4.50	2.60
	15.02	7.54	2.79	3.09	1.55
	15.58	7.76	2.85	3.16	1.62
0.4 M 2-butanone	16.16	7.96	2.93	3.24	1.67
added to 0.1 M DME	16.88	8.22	3.04	3.34	1.74
	17.66	8.50	3.17	3.47	1.84
	18.59	8.84	3.39	3.70	2.00
free shift	3.55	3.39	2.13	2.44	1.05

a) Shifts must be corrected by 4.1%.

TABLE 44

Least-square Fit to $1/\delta$ *vs.* $1/\delta$ for 2-Butanone and DME in the Presence of $Eu(dpm)_3$.

	CH_2 in DME *vs.*			CH_3 in DME *vs.*		
	CH_3(s)	CH_2	CH_3(t)	CH_3(s)	CH_2	CH_3(t)
	in 2-butanone			in 2-butanone		
Slope	0.0328	0.0332	0.0241	0.0881	0.0890	0.0646
σ_{slope}	0.0004	0.0005	0.0004	0.0012	0.0013	0.0010
Intercept	0.0398	0.0399	0.0401	0.1094	0.1095	0.1101
$\sigma_{interc.}$	0.0004	0.0005	0.0005	0.0012	0.0013	0.0015
Corr. Coeff.	0.9994	0.9990	0.9987	0.9991	0.9989	0.9987
$K_{\underline{12}}$	11.2	10.8	10.1	7.7	7.5	6.7
σ_K	4.4	4.8	4.8	5.7	5.8	6.1
Δ	11.1	11.6	9.1	16.3	16.8	13.7
σ_Δ	3.5	4.2	3.5	10.6	11.4	11.2

Average values for $\underline{12}$ - $Eu(dpm)_3$

$K_{\underline{12}} = 9.\ M^{-1}\ (\pm 2.)$

$\Delta_{CH_3(s)} = 12.$ ppm $(\pm 3.)$

$\Delta_{CH_2} = 12.$ ppm $(\pm 4.)$

$\Delta_{CH_3(t)} = 10.$ ppm $(\pm 3.)$

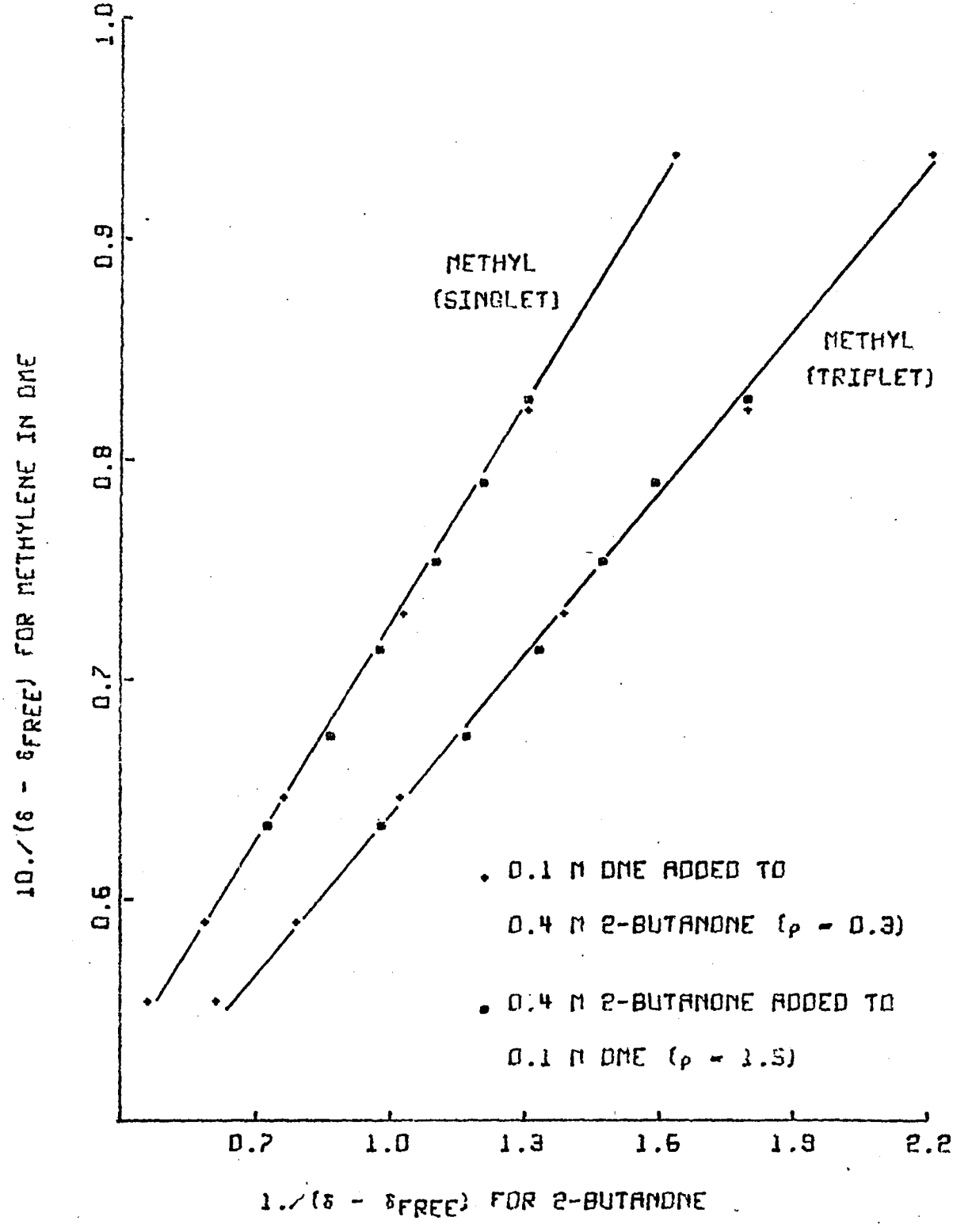

Figure 22 - 1/δ (DME) vs. 1/δ (2-Butanone) in the Presence of $Eu(dpm)_3$

and Δ's of DME obtained by the direct determination method. From Table 26 it was evident that interference from other equilibria tends to decrease the value for Δ, so $\Delta(CH_2)$ and $\Delta(CH_3)$ for DME could possibly be higher than those previously determined (Tables 24 and 25). However, such higher Δ values are clearly unacceptable because their use in determining K for 12 leads to negative equilibrium constant ratio, which has no physical meaning.

Literature values[50b] for similar systems (propiophenone-Eu(dpm)$_3$ in $CDCl_3$) were reported in Table 4, the differences with the present work are small and could be attributed to the different substrate.

DME and 2-Butanone (12) in Competition for Eu(fod)$_3$

This competitive system in the presence of Eu(fod)$_3$ represents an example for the limit of the application of this method. The ketone is a very poor competitive compound to DME because of the relatively high equilibrium constant for DME-Eu(fod)$_3$. Even at high concentrations of 12 and low concentrations of DME (in the ratio 8:1 in the starting solutions), relatively small shifts are observed when 12 is added to an original solution of DME and the shift reagent.

Experimental chemical shifts and concentrations are reported in Table 45. Attempts to apply the procedure of Appendix 6 for the system described by equation 39 (1:1 and 2:1 equilibria) failed to converge. Taking CH_2 in DME as the reference, values of equilibrium constants tend to $K_{B1} \simeq 5.\ M^{-1} \pm 1500.$ and $K_{B2} \simeq 2.\ M^{-1} \pm 1000.$; not only standard deviations are high, but also a very poor correlation exists between observed and calculated chemical shifts.

However, since a superimposition of the $1/\delta$ plots for the two methods of mixing does not result, it is concluded that a 2:1 complex

TABLE 45

2-Butanone and DME in Competition for $Eu(fod)_3$[a].

Concentrations		δ in DME (in ppm)		δ in 2-butanone (in ppm)		
DME	2-butanone	CH_2	CH_3	CH_3(s)	CH_3(t)	CH_2
0.0237	0.5226	19.08	11.16	4.78	2.84	4.90
0.0344	0.4676	19.06	11.16	4.36	2.56	4.51
0.0431	0.4231	18.86	11.06	3.93	2.28	4.12
0.0503	0.3863	18.78	11.02	3.55	2.02	3.76
0.0564	0.3554	18.58	10.93	3.21	1.79	3.45
0.0890	0.0688	20.03	11.75	4.02	2.36	4.27
0.0781	0.1610	19.71	11.59	3.45	1.96	3.71
0.0697	0.2332	19.46	11.47	3.21	1.79	3.48
0.0628	0.2912	19.24	11.36	3.08	1.69	3.35
0.0572	0.3388	19.05	11.27	2.99	1.62	3.25
0.0525	0.3787	18.94	11.21	2.92	1.58	3.18
free shifts		3.55	3.40	2.18	1.02	2.49

a) Chemical shifts should be corrected by -3.3%.

is formed, probably with low equilibrium constants.

DME could be a better choice for the determination of equilibrium constants between a ketone and $Eu(fod)_3$, since it shows a much lower K for the reference-$Eu(fod)_3$ system. No attempts at such an analysis were made.

n-Propylamine (13) and DME in Competition for $Eu(dpm)_3$

By the already familiar competitive procedure, spectra of n-propylamine (13) and DME mixtures were recorded in the presence of $Eu(dpm)_3$. Results are reported in Table 46, and an example of $1/\delta$ vs. $1/\delta$ plots is given in Figure 23 with the calculated values of K and Δ's from the straight line of equation 38 summarized in Table 47.

Armitage et al.[47,49] previously reported a value of K = 43-12 M^{-1} (Table 4) for the n-propylamine-$Eu(dpm)_3$ adducts formation. It is realized that the previous discrepancy in the case of neopentanol was high, but is much worse in the case of the amine. On the other hand, the superimposition of the $1/\delta$ values for the two methods of mixing, indicates no interference from other equilibria, since they would be dependent on the concentration of the substrates (DME and 13).

From the previously analyzed systems, great confidence is given to the competitive system technique. Besides, if $K \simeq 8000\ M^{-1}$ is a closer value for the adduct formation $Eu(dpm)_3 \cdot 13$, the method used previously for the determination of equilibrium constants would not be valid with this substrate, since it is based on an approximate formula assuming that the concentration of the adduct is low compared to the concentration of the other species in solution.

TABLE 46

n-Propylamine and DME in Competition for $Eu(dpm)_3$

	δ in DME (in ppm)		δ in n-propylamine (in ppm)		
Mixing Procedure	CH_2	CH_3	CH_3	$\underline{CH_2}CH_3$	$\underline{CH_2}NH_2$
	4.85	3.88	6.00	10.53	17.65
	5.28	4.04	6.34	11.09	18.72
	5.64	4.16	6.53	11.40	19.23
0.15 M DME added to	5.85	4.24	6.60	11.54	19.47
0.15 M n-propylamine	6.39	4.45	6.77	11.83	19.95
	6.80	4.59	6.86	12.01	20.25
	7.34	4.79	6.96	12.16	20.49
	8.17	5.09	7.07	12.34	20.78
	5.14	3.98	6.25	10.93	18.44
0.15 M n-propylamine	6.11	4.36	6.75	11.80	19.91
added to 0.15 M DME	7.65	4.92	7.15	12.51	21.11
	9.65	5.65	7.43	13.03	22.01
free shifts	3.55	3.40	0.91	1.46	2.67

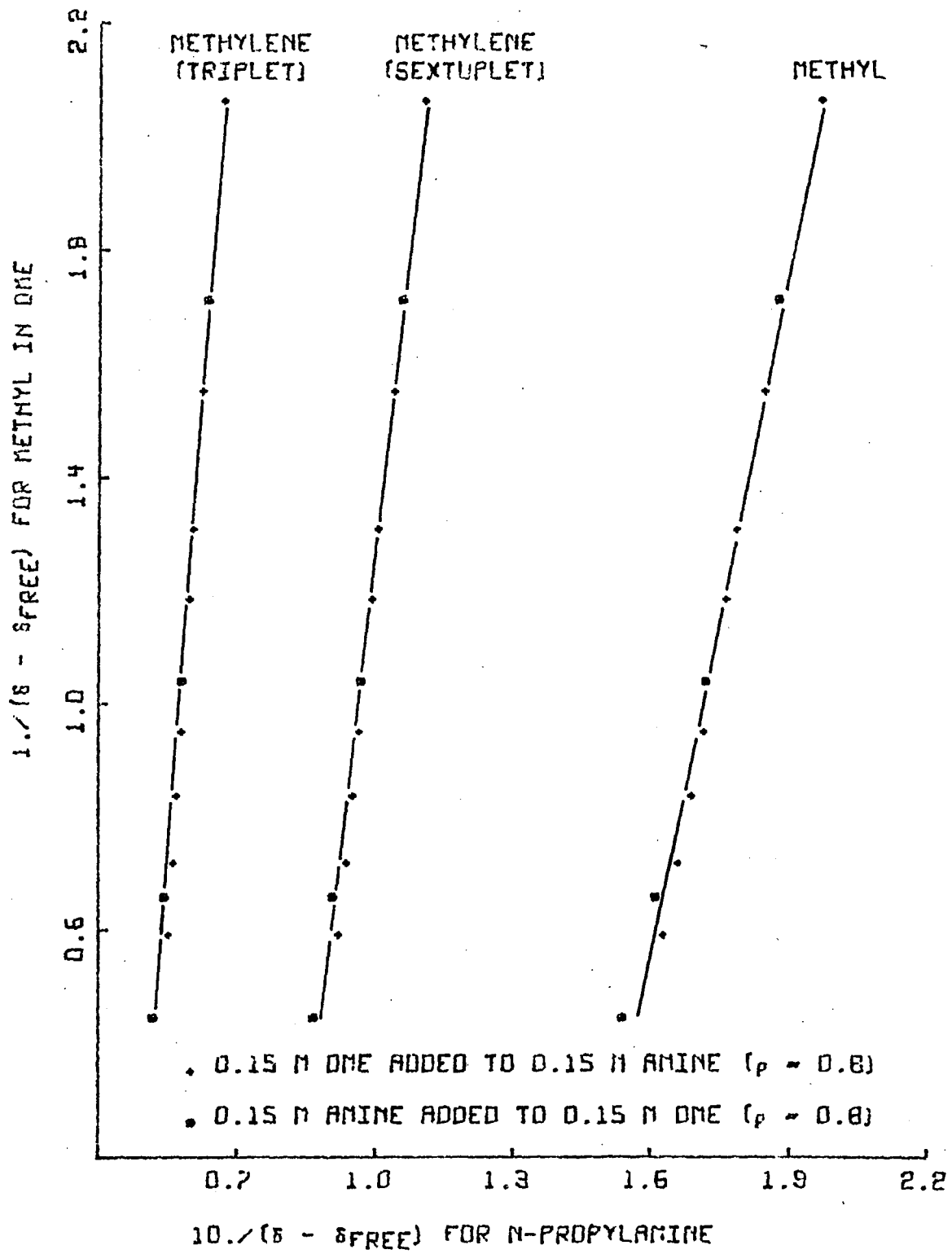

Figure 23 - 1/δ (DME) vs. 1/δ (n-Propylamine) in the Presence of $Eu(dpm)_3$.

TABLE 47

Least-square Fit to $1/\delta$ vs. $1/\delta$ for n-Propylamine and DME in the Presence of $Eu(dpm)_3$.

	CH_2 in DME vs.			CH_3 in DME vs.		
	CH_3	$\underline{CH_2}CH_3$	$\underline{CH_2}$-NH_2	CH_3	$\underline{CH_2}CH_3$	$\underline{CH_2}NH_2$
	in n-propylamine			in n-propylamine		
Slope	14.73	26.56	42.88	39.78	71.75	115.83
σ_{slope}	0.63	1.28	2.10	1.64	3.33	5.54
Intercept	-2.14	-2.19	-2.11	-5.79	-5.91	-5.69
$\sigma_{interc.}$	0.11	0.13	0.12	0.28	0.33	0.32
Corr. Coeff.	0.9911	0.9885	0.9882	0.9916	0.9893	0.9888
$K_{\underline{13}}$	8291.	8481.	8177.	8352.	8522.	8211.
σ_K	732.	815.	765.	650.	726.	703.
Δ	6.75	11.90	19.92	6.74	11.91	19.95
σ_Δ	0.15	0.24	0.47	0.26	0.44	0.76

Average values for 13 - $Eu(dpm)_3$

$K_{\underline{13}}$ = 8300. M^{-1} (±300.)

Δ_{CH_3} = 6.8 ppm (±0.1)

$\Delta_{\underline{CH_2}CH_3}$ = 11.9 ppm (±0.2)

$\Delta_{\underline{CH_2}NH_2}$ = 19.9 ppm (±0.4)

n-Propylamine (13) and DME in Competition for $Eu(fod)_3$

The final system analyzed bears the title of this section. Tables 48 and 49 represent experimental data and results respectively, and Figure 24 is a graphical example for $1/\delta$ vs. $1/\delta$ type of plots.

No precedent for the 1:1 and 2:1 adducts formation analysis was found in the literature for an aliphatic amine and $Eu(fod)_3$. The magnitude of the equilibrium constants determined in the present work, are reasonable when compared with the results from the other substrates, which are generally bound to the shift reagent in a lesser extent than amines.

In previous determinations, and when necessary, correction for the volume change of the solution caused by the introduction of the shift reagent was achieved by measuring the solutions height in a previously calibrated nmr tube. It was noted, however, that for the analysis of equation 39, high precision is required, and correction for the volume change was performed in this last system by a different method (described in the Experimental section).

Comments on the Competitive Methods

In a final overall review of the competitive method, it seems appropriate to make a few remarks.

The convenience of the method was already expressed in the previous section, when the competitive technique was introduced. Compared with other methods, very few inconveniences are found, especially since in most of the cases, such inconveniences still represent an improvement.

The errors calculated from standard procedures (given in Appendix 2)

TABLE 48

n-Propylamine and DME in Competition for $Eu(fod)_3$.

Concentrations		δ in DME (in ppm)		δ in n-propylamine (in ppm)		
DME	n-propyl-amine	CH_2	CH_3	CH_3	$\underline{CH_2}CH_3$	$\underline{CH_2}NH_2$
0.0341	0.1074	3.68	3.46	2.79	4.74	7.77
0.0417	0.1007	3.81	3.53	3.25	5.56	9.04
0.0536	0.0903	4.42	3.85	3.96	6.83	11.01
0.0625	0.0824	5.49	4.39	4.32	7.45	11.97
0.0590	0.0726	9.64	6.50	4.64	8.02	12.80
0.0652	0.658	11.34	7.37	4.67	8.04	12.82
0.0728	0.0575	13.14	8.30	4.60	7.97	12.60
0.0823	0.0470	15.12	9.31	4.48	7.74	12.15
0.0948	0.0333	17.13	10.19	4.15	7.20	10.91
0.1118	0.0147	19.96	11.69	3.55	6.13	9.12
0.1223	0.0290	5.02	4.16	3.52	6.04	9.69
0.1147	0.0354	5.34	4.32	3.73	6.42	10.30
0.1028	0.0455	5.87	4.59	4.00	6.90	10.99
0.0939	0.0531	6.30	4.81	4.15	7.16	11.41
0.0757	0.0687	7.33	5.34	4.46	7.72	12.29
0.0679	0.0752	7.90	5.65	4.55	7.90	12.58
0.0587	0.0830	8.84	6.10	4.64	8.04	12.80
0.0473	0.0926	10.24	6.83	4.75	8.24	13.10
0.0329	0.1048	13.04	8.26	4.89	8.48	13.46
	free shifts:	3.54	3.39	0.91	1.46	2.67

TABLE 49

n-Propylamine - DME - $Eu(fod)_3$ Analysis.

	CH_2 in DME vs.			CH_3 in DME vs.		
	CH_3	$\underline{CH_2}CH_3$	$\underline{CH_2}NH_2$	CH_3	$\underline{CH_2}CH_3$	$\underline{CH_2}NH_2$
	in n-propylamine			in n-propylamine		
K_{B1}	3848.	3832.	4133.	3792.	3768.	4097.
σ	170.	402.	1144.	289.	591.	1478.
K_{B2}	256.	251.	221.	265.	261.	226.
σ	35.	55.	106.	48.	76.	137.
Δ_{B1}	2.50	4.43	6.05	2.51	4.45	6.09
σ	0.07	0.19	0.73	0.09	0.24	0.88
Δ_{B2}	4.621	8.15	12.89	4.58	8.09	12.81
σ	0.06	0.17	0.73	0.08	0.22	0.92

Average values for 13 - $Eu(fod)_3$

K_{B1} = 3800. M^{-1} (±100.)

K_{B2} = 260. M^{-1} (±20.)

	CH_3 (in ppm)	CH_2CH_3 (in ppm)	CH_2NH_2 (in ppm)
Δ_{B1} =	2.50 ± 0.06	4.4 ± 0.1	6.1 ± 0.6
Δ_{B2} =	4.61 ± 0.05	8.1 ± 0.1	12.9 ± 0.6

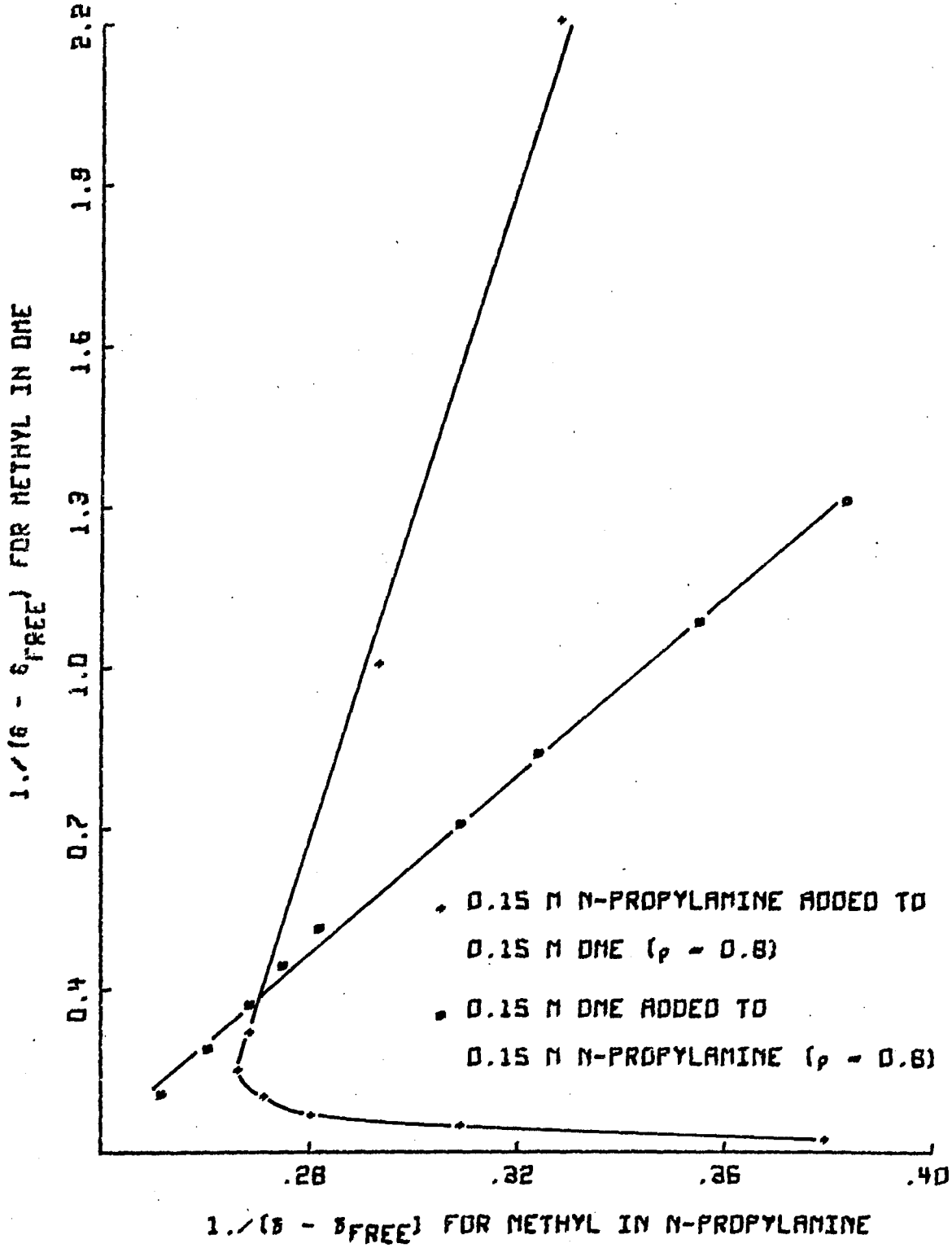

Figure 24 - 1/δ (DME) vs. 1/δ (n-Propylamine) in the Presence of $Eu(fod)_3$.

for the case of a 1:1 adduct formation are in the order of 10% for all the substrates chosen in this study. It is true that this is also the precision reported[47] for L_o *vs.* $1/\delta$ plots, but the presence of other equilibria are not easily detected for such cases, sometimes introducing great errors in the accuracy. It is apparent that study of such equilibria is necessary in order to improve the determination of K and Δ's.

Furthermore, special attention must be directed to the concentration of the substrates if adducts of different stoichiometry are formed, and any effort in this direction will be compensated by a higher precision. This also requires the purification of the substrates, but impurities in the shift reagent are irrelevant since at this point there is no need to know the concentration of this species. However, one complication can arise, that is the competitive system analysis is based on the assumption that shifts in a given substrate are produced by formation of 1:1 and 2:1 adducts for B (equation 39). If species such as $Eu(fod)_3 \cdot DME \cdot B$ or $Eu(fod)_3 \cdot B \cdot Impurity$ are present[7], they would lead to erroneous conclusions. Further investigation is required to determine the importance of such factors, especially when $Eu(fod)_3$ is used as the shift reagent.

The use of two references for the pmr spectra are recommended ($CHCl_3$ and TMS were used in the present work) since a change in the bulk magnetic susceptibility is produced by the presence of the shift reagent in solution. Corrections can be easily performed if two references are used and will be proportional to the deviation in the separation of the two reference signals in the presence and absence of the shift reagent.

CONCLUSIONS

Complex Formation Shifts (CFS)

The shifts induced by $La(dpm)_3$ (complex formation shifts, CFS) in a series of substrates are generally small and could be ignored in many cases. The propagation through a saturated chain in the substrates is limited to 2 bonds, but in the presence of π bonds, the influence can be extended to the fourth atom in the molecule, as is the case in pyridine.

Changes in coupling constants by adduct formation were observed by other authors[61,80-85], and several mechanisms had been proposed. In the present work, and particularly for the case camphor-$La(dpm)_3$, such mechanisms can be limited to two possibilities: substituent effects and conformational changes.

Even if CFS for $La(dpm)_3$ are small, they should be checked for other shift reagents. The corresponding shifts induced by $La(fod)_3$ have been shown by Tori *et al.*[23] to be significant, and are obviously due to the different (more electronegative) ligand fod.

Correlation Between Structure and LIS

The importance of both reliable LIS and accurate structure is illustrated in several sections. The LIS for the protons in borneol, using $Eu(dpm)_3$ as the shift reagent, were determined by two different methods. Structural parameters were derived from X-ray analysis of similar molecules.

The present analysis suggests that the McConnell derivation (equation 10) predicts the observed LIS to a satisfactory degree of

approximation, without the need to consider other factors such as lower symmetry, non-colinearity of Ln-O vector and magnetic axis, and averaging of the methyl groups from independent coordinates for each proton.

The quality of the correlation was found to be quite dependent on the structural parameters. Such parameters obtained from X-ray analysis of related compounds or from molecular models gave widely varying results. The use of several similar models is recommended, so a comparison among the results from each is possible and the selection of the best representation of these structural parameters can be performed by either the use of Hamilton tables and/or the physical meaning of bond distances and angles at convergence.

It has also been shown that CFS does not influence significantly the correlation analysis, since for the case of a structural model (not derived from X-ray of the adducts), the uncertainties in the coordinates of each atom overcome the errors introduced by the CFS.

It is understood that a more complete analysis should include also combinations of the several factors independently analyzed in the present work. This would require the optimization of a considerably higher number of parameters, which is limited by the number of observations.

Equilibrium Analysis

The last study concerns with the equilibrium analysis for the adduct formation between a substrate and a shift reagent. The competition method is shown to provide a convenient pathway to unequivocally establishing the stoichiometry of the adducts.

For the 1:1 adducts, the method is apparently most effective if the two equilibrium constants involved are similar in magnitude. For example, in the case of n-propylamine/DME system in the presence of

$Eu(dpm)_3$, the relatively small equilibrium constant for DME•$Eu(dpm)_3$ formation (compared to the n-propylamine), makes the ether a poor competitor in the presence of the amine. As a consequence, the range of observed chemical shifts for n-propylamine is relatively small. The extrapolation to $1/\delta_{\text{n-propylamine}} = 0.$ is therefore very large (since negative values of $1/\delta$ have no physical meaning and so cannot be experimentally evaluated). On the other hand, when the equilibrium constant for the reference is larger than the one of the competing substrate (as in the case of 2-butanone), the extrapolated value (b) times Δ_A is very close to 1. Since the ratio of the equilibrium constants is given by $1-b\Delta_A$ (see Appendix 2), high precision and accuracy are required in both, b and Δ_A, in order to reduce the standard deviation in the equilibrium constant and Δ of the competing substrate.

For the 2:1 adducts, the competitive analysis for the determination of K's and Δ's are highly sensitive to the precision with which the concentrations are determinated. Nevertheless, the procedure that involves low concentrations in the substrates and high values of ρ appears to be very convenient, since a wide range in the total ρ, and therefore in the observed chemical shifts, is obtained.

As a general conclusion, $Eu(dpm)_3$ will form mainly 1:1 adducts with aliphatic Lewis bases, while $Eu(fod)_3$ will prefer a coordination number 8. In relation to previous works, where fluorinated shift reagents were used to obtain chemical shifts for structural correlation purposes, it is noted that the Δ's for the 1:1 and 2:1 adducts are in a ratio that is closely constant for all the protons in the same molecule. Since C in equation 10 is just a scale factor such that:

$$\frac{\sum_i SO_i}{\sum_i SC_i} = C$$

the almost constant ratio for the two types of adducts justifies the relatively good agreements obtained using these data.

EXPERIMENTAL

General

All pmr spectra were recorded in a JOEL JNH-MH-100 or Varian A-60 spectrophotometers. Unless otherwise stated, all chemical shifts are reported in ppm from TMS, with a precision of ± 0.02 ppm. When calibration with a second reference was necessary, the $CHCl_3$ signals were used for this purpose with a displacement from TMS of 7.27 ppm[9]. The temperature of the probe was determined from the separation of the signals in a MeOH sample to be 36.5°.

All materials were commercially available, unless otherwise specified.

An IBM 360-50 digital computer was used for the computational work.

Preparation of Nopol Tosylate

The general procedure described in Org. Syntheses[99] was followed. Nopol (3.9 g) and pyridine (7.05 g) were mixed in a flask provided with a magnetic stirrer and surrounded by an ice bath. p-Toluenesulfonyl chloride (4.9 g) was added at such a rate to keep the temperature below 10°. The mixture was stirred for four hours at the same temperature, during which time a second layer forms. The excess of p-toluenesulfonyl chloride was hydrolyzed with 13.9 ml of concd HCl diluted with 46 ml of iced water. Ether was added and the ethereal solution separated, dried ($CaCl_2$), filtered, and evaporated to give 6.2 g of product as an oil (82.5%): pmr (CCl_4)δ 7.3 (m,4), 4.95 (s,1), 3.82 (t, 2, $\underline{CH_2}O$), 2.13 (s, 3, CH_3-Ar), ≃ 2 (m, 7), 1.83 (m, 1), 0.98 (s, 3, $\underline{CH_3}$-trans), 0.5 (s, 3, $\underline{CH_3}$-cis).

Reduction of 2-Phenylbutyric Acid

The technique of Birtwistle[100] was used for the reduction with $LiAlH_4$. To a suspension of $LiAlH_4$ (1.56 g) in ether (30 ml), previously dried over sodium wire, a solution of 2-phenylbutyric acid (5 g) in ether was added dropwise, at a rate sufficient to maintain a gentle reflux. The suspension was stirred for an additional four hours and the excess of $LiAlH_4$ destroyed by the addition of water. The suspension was filtered and the ether evaporated to yield 3.2 g of 2-phenylbutanol. The white slurry from the filtration was dissolved in dilute HCl and extracted with ether. After drying ($MgSO_4$), filtering, and evaporating the solvent, an additional 1 g of the alcohol was obtained (92%): pmr (neat) δ 6.84 (s, 5, aromatic), 3.89 (broad, 1, OH), 3.30 (d, 2, $\underline{CH_2}OH$), 2.8 (m, 1, $\underline{CH}$), 1.35 (m, 2, $\underline{CH_2}CH_3$), 0.45 (t, 3, CH_3).

Preparation of 2-Phenylbutyl Tosylate

The same procedure used to prepare nopol tosylate was followed with a total yield of 92%. The 2-phenylbutyl tosylate was recrystallized from methanol as white needles: mp 44-44.5°, (lit.[101] mp 35-41°).

Preparation of 2-Phenylbutyl Iodide

The general preparation of the iodide from the corresponding alcohol described in Org. Syntheses[102] was followed. 2-Phenylbutanol (6 g) was mixed with triphenyl phosphite (11.5 ml) and methyl iodide (3.5 ml). The solution was refluxed in a flask provided with a condenser and a calcium chloride drying tube. The initial reflux temperature of 75-80° rose after a few hours to 135°. After cooling overnight, the reaction mixture was distilled under reduced pressure, and the fraction boiling below 115° (1.5 mm) collected. The distillate

was diluted with ether, washed with three portions of 1 N NaOH followed by water. The ether layer was dried ($CaCl_2$) and distilled. The 2-phenylbutyl iodide was collected at 74-80° (4 mm) (5.1 g, 51.5%): pmr (CCl_4) δ 6.85 (m, 5, aromatic), 3.00 (d, 2, CH_2I), 2.48 (m, 1, CH), 1.50 (m, 2, CH_2CH_3), 0.50 (t, 3, CH_3).

Attempted Alkylation under Basic Conditions

The conditions were similar to the ones described in Org. Syntheses[103]. Analytical reagent grade acetone was used as the solvent and potassium carbonate was dried at 100° overnight. 2-Phenylbutyl tosylate (5.5 g) (or 6.3 g of nopol tosylate) was dissolved in acetone (10 ml) and redistilled acetylacetone (1.5 g) and potassium carbonate (2.1 g) added. A white solid precipitated (potassium acetylacetonate). The reaction mixture was refluxed for 8 hours (decomposition occurred), filtered, and the solid washed several times with acetone. The solvent was evaporated and the crude solid (or oil from nopol tosylate) identified as the original tosylate (reisolated in ≈ 60% yield).

A similar procedure was used with dimethylsulfoxide as the solvent and 2-phenylbutyl iodide. The mixture was allowed to stand at 50° for three days. The pmr spectrum of the crude ethereal extract, after evaporation of the solvent, presented strong bands at 4.7-5 ppm, indicative of elimination products of the original iodide [lit.[104] pmr δ 5.0-5.1 (= CH_2)].

Attempted Alkylation under Acid Conditions

Acetylacetone (2 g) was mixed with nopol (3 g) (or 2.9 g of 2-phenylbutanol), the temperature lowered to -10° with an ice-salt bath. Through an inlet tube, BF_3 (dried in concd H_2SO_4) was bubbled

into the mixture, until white fumes sharply increased at the end of the outlet tube. The dark colored mixture was allowed to stand at 0° for 24 hours, then warmed to room temperature and poured into a solution of $NaOAc \cdot 3H_2O$ (10 g in 20 ml of water), and allowed to stand at room temperature overnight. The mixture was extracted with ether, dried ($NaSO_4$), filtered and the solvent evaporated:

1) In the case of 2-phenylbutanol, 80% of unreacted starting materials were recovered. The residue from evaporation of the ether was identified as a mixture of acetylacetone and the alcohol, by comparing the pmr spectrum of a mixture of the two components and by integration of CH_3 vs. $\underline{CH_2}OH$ in the alcohol.

2) In the case of nopol, the pmr spectrum showed decomposition of this reactant, by the complete disappearance of the geminal methyl absorption

Attempted Alkylation by Anion Extraction

Tetrabutylammonium hydrogen sulfate (3.4 g) was added to a cold solution of NaOH (0.8 g in 10 ml of water); to this acetylacetone (1 g) was added and the mixture extracted with chloroform. The two layers were separated and a double excess of 2-phenylbutyl iodide (or tosylate) added to the organic solution. The mixture was allowed to reflux for one hour, then evaporated and ether added to the residue. A white precipitate appeared in both cases, The ether solution was filtered and the solvent evaporated:

1) The pmr spectrum of the extract from the iodide showed a high percentage of α-ethylstyrene from bands at 5.4 ppm [lit.[104] pmr δ 5.0-5.1 ($=CH_2$)], and a very weak band for the CH_3 α to the carbonyl at ≃ 2 ppm.

2) The extract from the tosylate was diluted with methanol to precipitate the excess of 2-phenylbutyl tosylate (reisolated in a 80% yield), the solvent was again evaporated after filtration and the pmr spectrum of the extract showed a very weak band corresponding to the $COCH_3$ at ≃ 2 ppm.

Synthesis of $La(dpm)_3$

Lanthanum oxide was purchased from Alfa Inorganic Co. and the dipivaloylmethane (dpmH) from Aldrich. The synthetic procedure described in Inorganic Syntheses[6] was followed: La_2O_3 (1.06 g) was dissolved in 17 ml of concd HNO_3 on a steam bath. Elimination of excess HNO_3 was achieved by addition of water and repeated evaporation until the vapors were neutral. To a solution of dpmH (3.72 g in 95% ethanol) were added 17 ml of a 4.8% solution of NaOH in 50% ethanol. The $La(NO_3)_3$ was dissolved in 17 ml of 50% ethanol and added to the basic solution of dpmH, with vigorous stirring. Evaporation of the solvent was immediately started by connecting the flask to a vacuum pump. Precipitation of the complex started immediately and increased with the reduction in the volume. When the original solution was reduced by half, the vacuum was removed and 120 ml of water added. The solid was filtered, dried (60°, 0.6 mm) for one hour, and sublimed (190°, 0.5 mm) to yield 3.6 g (81%) of a white powder, mp 242-3° (lit.[7] 238-248°).

Measurement of Complex Formation Shifts (CFS) in Pyridine

All spectra for CFS measurements were recorded at SW 270 Hz, with a precision of ± 0.005 ppm.

Pyridine was distilled from NaOH and kept over 4A molecular sieves. Pyridine (0.0550 g) was diluted to 1 ml with $CDCl_3$ ([Pyridine] = 0.695 M),

and portions of approximately 0.05 g of $La(dpm)_3$ were added. To avoid evaporation of the solvent, the flask was sealed with parafilm and magnetically stirred. The concentration of $La(dpm)_3$ was determined by integration of the pmr spectra, the volume change of the solution by the introduction of $La(dpm)_3$ was considered negligible, so the concentration of the pyridine was assumed closely constant.

A stock solution was prepared by dissolving 0.1301 g of pyridine in CCl_4 (final volume 3 ml, [Pyridine] = 0.548 M). Approximately 0.06 g of $La(dpm)_3$ were weighed in a nmr tube and 0.3 ml of the pyridine solution added. A series of pmr spectra were obtained at decreasing lanthanum complex concentration by adding measured aliquots of the pyridine solution to the nmr tube.

Analogous procedures were carried out for [Pyridine] = 0.274 M and [Pyridine] = 0.137 M solutions, which were prepared by dilution of the original stock solution. The concentration of $La(dpm)_3$ was determined by integration of the pmr spectra.

The calculation of the lanthanum complex concentrations was also based on the weighed amounts, but because the mixtures were frequently non-homogeneous, they in many cases did not match.

Measurements of CFS in Aliphatic Systems

The procedure described for pyridine-$La(dpm)_3$ in $CDCl_3$ was followed, with solutions of the substrates at the following concentrations:

[ethanol] = 1.44 M

[dimethylsulfoxide] = 0.574 M

[2-pentanone] = 0.941 M

[camphor] = 0.510 M

[diethylamine] = 0.937 M

The solvents in each case were reported in Table 10.

exo,exo-2,3-Camphanediol was synthesized by David Baillargeon by the method of Takeshita and Kitajima[105]. It was resublimed prior to use (mp 230-4°) because of its high hygroscopic characteristics. The CFS were determined using the same procedure as for pyridine-$La(dpm)_3$ in CCl_4, with a 0.755 M solution of the diol. The concentration of $La(dpm)_3$ was calculated by weight.

Direct Determination of Equilibrium Constants and Δ's.

$Eu(dpm)_3$ was purchased from Ventron Co. and purified prior to use by drying at 0.8 mm and 100° for one hour, followed by sublimation at 150° at the same reduced pressure: mp 185-6° (lit.[6] 187-9°).

$Eu(fod)_3$ was purchased from Alfa Inorganics and purified prior to use as described above: mp 209-213° (lit.[106] 205-212°).

Dimethoxyethane (DME) was distilled at atmospheric pressure; the fraction boiling at 76.5° was collected and kept over 4A molecular sieves which had been previously dried at 140° for 24 hours.

Dimethoxybenzene (DMB) was purchased from Aldrich and recrystallized from light petroleum ether. It was dried at < 2 mm for one hour at room temperature.

Borneol was sublimed prior to use at 50° (1 mm): mp 205-6°. $CDCl_3$ and CCl_4 were dried over 4A molecular sieves.

Borneol and $Eu(dpm)_3$

Two solutions of borneol in CCl_4 were prepared at concentrations 0.5120 and 0.2458 M. In six separated nmr tubes, an amount of $Eu(dpm)_3$ was weighted so that after the addition of 0.3 ml of each borneol solution, the final $\rho (= [Eu(dpm)_3]/[Borneol])$ would be approximately 0.65, 0.35 and 0.1.

Correction for the change in volume was performed by measuring the height on the nmr tube previously calibrated.

Different concentrations of $Eu(dpm)_3$ were further obtained by the addition of aliquots of the borneol solution of the same concentration, recording the pmr spectrum each time.

All volumetric measures were performed by the use of Hamilton syringes.

DME and $Eu(dpm)_3$

A 0.1720 M stock solution of DME in $CDCl_3$ was prepared and three portions of it were diluted to obtain three working solutions of DME = 0.0860 M, 0.0430 M, and 0.0215 M.

Into three separate volumetric flasks, each containing approximately 0.015 g of $Eu(dpm)_3$, 0.5 ml, 0.25 ml and 0.125 ml of the 0.1720 M DME solution were added. Each flask was diluted to one ml with $CDCl_3$, thereby the concentration of DME in each of these solutions is equal to one of the three working solutions previously prepared.

From each flask, 0.3 ml were measured into an nmr tube by a Hamilton syringe and aliquots of the DME solution of the same concentration were added, recording the pmr spectrum after each addition. To obtain lower values of ρ, 0.12 ml of each flask and 0.18 ml of the corresponding DME solution (of the same concentration) were mixed and further measurements were taken by adding additional aliquots of the DME solution of the same concentration.

The concentration of DME is kept constant in this way within any given run, and no calibration of the nmr tube is necessary.

The resulting concentrations and chemical shifts are reported in Tables 24-25.

DMB and $Eu(dpm)_3$

A similar procedure is used in this system. Experimental values are reported in Tables 27-29.

DME and $Eu(fod)_3$

Due to the higher solubility of $Eu(fod)_3$ (compared to $Eu(dpm)_3$) a different procedure was followed to prepare the original solutions. A stock solution was obtained by dissolving 0.2471 g of $Eu(fod)_3$ in 1 ml volumetric flask using $CDCl_3$ as the solvent.

A 0.2153 M stock solution of DME was also prepared in $CDCl_3$ (saturated with D_2O) and preparation of the nmr samples was obtained by mixing the two above solutions in the following proportions:

1) 0.15 ml of DME + 0.15 ml $Eu(fod)_3$ ([DME] = 0.1076 M);
2) 0.15 ml of DME + 0.06 ml of $Eu(fod)_3$ + 0.09 ml $CDCl_3$ ([DME] = 0.1076 M);
3) 0.075 ml of DME + 0.15 ml of $Eu(fod)_3$ + 0.075 ml $CDCl_3$ ([DME] = 0.0538 M);
4) 0.075 ml of DME + 0.06 ml of $Eu(fod)_3$ + 0.165 ml $CDCl_3$ ([DME] = 0.538 M);
5) 0.0375 ml of DME + 0.15 ml of $Eu(fod)_3$ + 0.1125 ml $CDCl_3$ ([DME] = 0.0269 M);
6) 0.0375 ml of DME + 0.06 ml of $Eu(fod)_3$ + 0.2025 ml $CDCl_3$ ([DME] = 0.0269 M);
7) 0.035 ml of DME + 0.03 ml of $Eu(fod)_3$ + 0.215 ml $CDCl_3$ ([DME] = 0.0269 M).

Different concentrations of $Eu(fod)_3$ were also obtained by addition of aliquots of the DME solution of the same concentration, which is prepared by dilution of the original DME solution.

Experimental concentrations and chemical shifts are reported in Tables 32-33.

Competitive Experiments

$Eu(dpm)_3$ and $Eu(fod)_3$ were used without further purification. The substrates were purified as follows:

1) 2-Butanone was distilled at atmospheric pressure, bp 74-5° and kept over 4A molecular sieves;
2) Neopentanol was distilled at atmospheric pressure, the fraction at 109-110° was collected; mp 53-5° (lit.[86] 52-3°);
3) n-Propylamine was distilled at atmospheric pressure over KOH pellets, the fraction at 47.5° was collected and kept over 4A molecular sieves;
4) Purification procedures for borneol and DMB were described previously.

With neopentanol and borneol (substrate B), ≃ 0.2 and 0.5 M solutions in $CDCl_3$ were prepared, along with solutions of approximately the same concentration in DME (substrate A). $Eu(dpm)_3$ [or $Eu(fod)_3$] was weighted in a nmr tube in approximately the amounts described below:

1) 0.017 g of $Eu(dpm)_3$ [or 0.025 g of $Eu(fod)_3$] to which 0.3 ml of 0.2 M solution of substrate B were added ($\rho \simeq 0.4$);
2) 0.017 g of $Eu(dpm)_3$ [or 0.025 g of $Eu(fod)_3$] to which 0.3 ml of 0.2 M solutions of substrate A were added ($\rho \simeq 0.4$);
3) 0.084 g of $Eu(dpm)_3$ [or 0.124 g of $Eu(fod)_3$] to which 0.3 ml of 0.5 M solution of substrate B were added ($\rho \simeq 0.8$);
4) 0.084 g of $Eu(dpm)_3$ [or 0.124 g of $Eu(fod)_3$] to which 0.3 ml of 0.5 M solution of substrate A were added ($\rho \simeq 0.8$).

The final volume is determined by the height of the solution in the nmr tube. Aliquots of the competing substrate are added up to a total of 0.3 ml, recording the pmr spectrum after each addition. Experimental values for neopentanol-DME are reported in Tables 36 and 41.

With DMB and DME, 0.2 M solutions of DMB and DME were prepared; the shift reagent was weighted in a nmr tube and mixed with the substrate solutions in the following proportions:

1) 0.035 g of $Eu(dpm)_3$ [or 0.050 g of $Eu(fod)_3$] + 0.28 ml of DME ($\rho \simeq 0.8$);
2) 0.035 g of $Eu(dpm)_3$ [or 0.050 g of $Eu(fod)_3$] + 0.28 ml of DMB ($\rho \simeq 0.8$);
3) 0.015 g of $Eu(dpm)_3$ [or 0.020 g of $Eu(fod)_3$] + 0.28 ml of DME ($\rho \simeq 0.35$);
4) 0.015 g of $Eu(dpm)_3$ [or 0.020 g of $Eu(fod)_3$] + 0.28 ml of DMB ($\rho \simeq 0.35$).

Aliquots of the competing substrate were added and the pmr spectrum of each mixture was recorded. Experimental values of chemical shifts are reported in Tables 30 and 34.

A procedure similar to neopentanol and borneol was used for the competition experiments between 2-butanone and DME in the presence of $Eu(dpm)_3$ and $Eu(fod)_3$. Due to the relatively weak binding constant for the 2-butanone, the following solutions were prepared:

1) With $Eu(dpm)_3$: 0.4 M solutions of 2-butanone and 0.1 M solutions of DME:
2) With $Eu(fod)_3$: 0.8 M solutions of 2-butanone and 0.1 M solutions of DME.

Experimental values are reported in Tables 43 and 45.

With n-propylamine, a different procedure was followed to increase the accuracy in the concentration of the two competing substrates. Stock solutions of DME and n-propylamine ($\simeq$ 0.3 M each) were prepared, and diluted in half. In volumetric flasks, the following approximated amounts of shift reagent and the 0.3 M solutions were mixed:

1) 0.085 g of $Eu(dpm)_3$ + 0.5 ml of DME (diluted to 1 ml with $CDCl_3$, [DME] = 0.15 M);
2) 0.085 g of $Eu(dpm)_3$ + 0.5 ml of n-propylamine (diluted to 1 ml with $CDCl_3$, [n-propylamine] = 0.15 M);
3) 0.25 g of $Eu(fod)_3$ were diluted to 1 ml with $CDCl_3$.

For the solutions involving $Eu(dpm)_3$ as the shift reagent, 0.3 ml of each solution were introduced in a nmr tube and aliquots of the 0.15 M competing substrate were added. Experimental chemical shifts are reported in Table 46.

For the solutions involving $Eu(fod)_3$ as the shift reagent, 0.15 ml of solution #3 were mixed with 0.15 ml of one of the competing substrates and aliquots of the 0.15 M solution of the other were added. Concentrations and chemical shifts are reported in Table 48.

BIBLIOGRAPHY

1. C. C. Hinckley, J. Amer. Chem. Soc., 91, 5160 (1969).

2. R. E. Sievers, Ed., "Nuclear Magnetic Resonance Shift Reagents," Academic Press, Inc., New York, N. Y., 1972.

3. A. F. Cockerill, G. L. O. Davies, R. C. Harden, and D. M. Rackham, Chem. Rev., 73, 553 (1973).

4. B. C. Mayo, Chem. Soc. Rev., 2, 49 (1973).

5. J. Reuben, Progr. Nucl. Magn. Resonance Spectrosc., 9, 1 (1973).

6. K. J. Eisentraut and R. E. Sievers, Inorg. Syntheses, Vol. XI, 94 (1968).

7. (a) H. L. Goering, J. N. Eikenberry, G. S. Koemer, and C. J. Lattimer, J. Amer. Chem. Soc., 96, 1493 (1974); (b) M. D. McCreary, D. W. Lewis, D. L. Wernick, and G. M. Whitesides, ibid., 96, 1471 (1974).

8. W. Kauzmann, "Quantum Chemistry," Academic Press, Inc., New York, N. Y., 1957.

9. F. A. Bovey, "Nuclear Magnetic Resonance Spectroscopy," Academic Press, Inc., New York, N. Y., 1969.

10. H. M. McConnell and R. E. Robertson, J. Chem. Phys., 29, 1361 (1958).

11. P. Lazlo, Progr. Inorg. Chem., 3, 231 (1967).

12. N. Bloemberg, E. M. Purcell, and R. V. Pound, Phys. Rev., 73, 679 (1948).

13. D. R. Eaton and W. D. Phillips, Advan. Magn. Resonance, 1, 103 (1965).

14. J. Reuben and D. Fiat, Inorg. Chem., 8, 1821 (1969).

15. F. W. Pijpers, H. E. Smeets, and L. B. Beentjes, Rec. Trav. Chim. Pays-Bas, 90, 1292 (1971).

16. I. Morishima, K. Okada, M. Ohashi, and T. Yonezawa, J. Chem. Soc., Chem. Commun., 33 (1971).

17. J. Reuben and D. Fiat, J. Chem. Phys., 51, 4909 (1969).

18. D. R. Eaton, A. D. Josey, W. D. Phillips, and R. E. Benson, Discussions Faraday Soc., 34, 77 (1962).

19. F. A. Cotton and G. Wilkinson, "Advanced Inorganic Chemistry," 3rd ed, Interscience Publishers, New York, N. Y., 1972.

20. E. R. Birnbaum and T. Moeller, J. Amer. Chem. Soc., 91, 7274 (1969).

21. C. C. Hinckley, M. R. Klotz, and F. Patil, ibid., 93, 2417 (1971).

22. H. Huber and C. Pascaul, Helv. Chim. Acta, 54, 913 (1971).

23. K. Tori, Y. Yoshimura, M. Kainosho, and K. Ajisaka, Tetrahedron Lett., 3127 (1973).

24. B. Bleaney, J. Magn. Resonance, 8, 91 (1972).

25. A. M. Grotens, J. J. Backus, F. W. Pijpers, and E. de Boer, Tetrahedron Lett., 1467 (1973).

26. A. Mookherji and S. P. Chachra, Ind. J. Pure Appl. Phys., 7, 560 (1969).

27. W. DeW. Horrocks, Jr. and J. P. Sipe III, Science, 177, 994 (1972).

28. W. DeW. Horrocks, Jr., J. P. Sipe III, and D. Sudnick, in ref. 2.

29. R. E. Cramer and K. Seff, J. Chem. Soc., Chem. Commun., 450 (1972).

30. W. DeW. Horrocks, Jr., J. P. Sipe III, and J. R. Luber, J. Amer. Chem. Soc., 93, 5258 (1971).

31. J. J. Uebel and R. M. Wing, ibid., 95 6046 (1973).

32. G. N. LaMar, W. DeW. Horrocks, Jr., and L. C. Allen, J. Chem. Phys., 41, 2126 (1964).

33. H. Huber, Tetrahedron Lett., 3559 (1972).

34. J. M. Briggs, G. P. Moss, E. W. Randall, and K. D. Sales, J. Chem. Soc., Chem. Commun., 1180 (1972).

35. D. S. Dyer, J. A. Cunningham, J. J. Brooks, R. E. Sievers, and R. E. Rondeau, in ref. 2.

36. B. Bleaney, C. M. Dobson, B. A. Levine, R. B. Martin, R. J. P. Williams, and A. V. Xavier, J. Chem. Soc., Chem. Commun., 791 (1972).

37. H. Sternlicht, J. Chem. Phys., 42, 2250 (1965).

38. K. J. Eisentraut, Inorg. Chem., 6, 1933 (1967).

39. N. Ahmad, N. C. Bhacca, J. Selbin, and J. D. Wander, J. Amer. Chem. Soc., 93, 2564 (1971).

40. I. Armitage and L. D. Hall, Can. J. Chem., 49, 2770 (1971).

41. W. DeW. Horrocks, Jr. and J. P. Sipe III, J. Amer. Chem. Soc., 93, 6800 (1971).

42. G. Montaudo, V. Librando, S. Caccamese, and P. Maravigna, ibid., 95, 6365 (1973).

43. K. L. Williamson, D. R. Clutter, R. Emch, M. Alexander, A. E. Burroughs, C. Chua, and M. E. Bogel, ibid., 96, 1471 (1974).

44. J. A. Glasel, Progr. Inorg. Chem., 18, 383 (1973).

45. P. E. Young, V. Madison, and E. R. Blout, J. Amer. Chem. Soc., 95, 6142 (1973).

46. M. Yirayama and Y. Hanyu, Bull. Chem. Soc. Jap., 46, 2687 (1973).

47. I. Armitage, G. Dunsmore, L. D. Hall, and A. G. Marshall, Can. J. Chem., 50, 2119 (1972).

48. J. K. M. Sanders, S. W. Hanson, and D. H. Williams, J. Amer. Chem. Soc., 94, 5325 (1972).

49. I. Armitage, G. Dunsmore, L. D. Hall, and A. G. Marshall, J. Chem. Soc., Chem. Commun., 1281 (1971).

50. (a) D. R. Kelsey, J. Amer. Chem. Soc., 94, 1764 (1972); (b) R. K. Mackie and T. M. Shepherd, Org. Magn. Resonance, 4, 557 (1972).

51. B. L. Shapiro and M. D. Johnston, Jr., J. Amer. Chem. Soc., 94, 8185 (1972).

52. J. Reuben, ibid., 95, 3535 (1973).

53. D. F. Evans and M. Wyatt, J. Chem. Soc., Chem. Commun., 312 (1972).

54. R. E. Cramer and R. Dubois, J. Amer. Chem. Soc., 95, 3801 (1973).

55. A. M. Grotens, J. J. M. Backus, F. W. Pijers, and E. de Boer, Tetrahedron Lett., 1467 (1973).

56. R. Porter, T. J. Marks, and D. F. Shriver, J. Amer. Chem. Soc., 95, 3548 (1973).

57. N. S. Angerman, S. S. Danyluk, and T. A. Victor, ibid., 94, 7137

58. B. Feibush, M. F. Richardson, R. E. Sievers, and C. S. Springer, Jr., ibid., 94, 6717 (1972).

59. F. A. Cotton and P. Legzdins, Inorg. Chem., 7, 1777 (1968).

60. IUPAC Bulletin, Inorg. Chem., 9, 1 (1970).

61. J. K. M. Sanders and D. H. Williams, J. Amer. Chem. Soc., 93, 641 (1971).

62. A. W. Johnson, E. Markham, and R. Price, Org. Syntheses, Vol. 42, 75 (1962).

63. L. E. Marchi, Inorg. Syntheses, Vol. II, 10 (1946).

64. G. T. Morgan and R. B. Tunstall, J. Chem. Soc., 125, 1963 (1924).

65. J. T. Adams, R. Levine, and C. R. Hauser, Org. Syntheses, Coll. Vol. III, 405 (1955).

66. T. F. Crimmins and C. R. Hauser, J. Org. Chem., 32, 2615 (1967).

67. (a) J. P. Collman, R. L. Marshall, W. L. Young III, and S. D. Goldby, Inorg. Chem., 1, 704 (1962); (b) R. C. Hester, Chem. Ind., 1397 (1963).

68. (a) R. H. Holm and F. A. Cotton, J. Amer. Chem. Soc., 80,5658 (1958); (b) J. A. S. Smith and E. J. Wilkins, J. Chem. Soc. A, 1749 (1966).

69. A. Brändström, P. Berntsson, S. Carlsson, A. Djurhuus, K. Gustavii, U. Junggren, B. Lamm, and B. Samulsson, Acta Chem. Scand., 23, 2202 (1969).

70. G. Schill, Sv. Kem. Tidskr., 80, 323 (1968); C. A., 70, 84114w (1969).

71. A. Brändström and U. Junggren, Acta Chem. Scand., 23, 2204 (1969).

72. A. Brändström and U. Junggren, ibid., 23, 2203 (1969).

73. A. Brändström and U. Junggren, ibid., 23, 3585 (1969).

74. A. Brändström and U. Junggren, ibid., 23, 2536 (1969).

75. A. Brändström and U. Junggren, Tetrahedron Lett., 473 (1972).

76. G. Beech and R. J. Morgan, ibid., 973 (1974).

77. N. H. Andersen, B. J. Bottino, and S. E. Smith, J. Chem. Soc., Chem. Commun., 1193 (1972).

78. K. K. Andersen and J. J. Uebel, Tetrahedron Lett., 5253 (1970).

79. C. Lussan, J. Chim. Phys., 60, 1100 (1963).

80. B. L. Shapiro, M. D. Johnston, and R. L. Towns, J. Amer. Chem. Soc., 94, 4381 (1972).

81. J. F. Caputo and A. R. Martin, Tetrahedron Lett., 4547 (1971).

82. J. Reuben and J. S. Leigh, J. Amer. Chem. Soc., 94, 2789 (1972).

83. T. B. Patrick and P. H. Patrick, ibid., 95, 5192 (1973).

84. G. E. Hawkes, D. Libfritz, D. W. Roberts, and J. D. Roberts, ibid., 95, 1659 (1973).

85. G. Ferguson, C. J. Fritchie, J. M. Robertson and G. A. Sim, J. Chem. Soc., 1976 (1961).

86. R. C. Weast, Ed., "Handbook of Chemistry and Physics," The Chemical Rubber Co., Cleveland, Ohio, 1969.

87. G. Dallinga and M. L. H. Toneman, Rec. Trav. Chim. Pays-Bas, 87, 795 (1968).

88. F. H. Allen and D. Rogers, J. Chem. Soc. B, 632 (1971).

89. J. F. Chiang, C. F. Wilcox, Jr., and S. H. Bauer, J. Amer. Chem. Soc., 90, 3149 (1968).

90. W. C. Hamilton, Acta Crystallogr., 18, 502 (1965).

91. I. M. Armitage, L. D. Hall, A. G. Marshall, and L. G. Werbelow, J. Amer. Chem. Soc., 95, 1437 (1973).

92. J. Briggs, F. A. Hart, G. P. Moss, and E. W. Randall, J. Chem. Soc., Chem. Commun., 364 (1971).

93. R. M. Wing, T. A. Early, and J. J. Uebel, Tetrahedron Lett., 4153 (1972).

94. D. E. Williams, ibid., 1345 (1972).

95. B. L. Shapiro, M. D. Johnston, Jr., and M. J. Shapiro, Org. Magn. Resonance, 5, 21 (1973).

96. J. Bouquant and J. Chuche, Tetrahedron Lett., 493 (1973).

97. A. Seidell, "Solubilities of Organic Compounds," Vol. II, 3rd ed, D. van Nostrand Company, Inc., New York, N. Y., 1941, p 12.

98. I. B. Rabinovich, "Influence of Isotopy on the Physicochemical Properties of Liquids," Consultants Bureau, New York, N. Y., 1970, pp 263-264.

99. C. S. Marvel and V. C. Sekera, Org. Syntheses, Coll. Vol. III, 366 (1955).

100. J. S. Birtwistle, K. Lee, J. D. Morrison, W. A. Sanderson, and H. S. Mosher, J. Org. Chem., 29, 37 (1964).

101. M. J. Brienne, C. Ouannes, and J. Jacques, Bull. Chim. Soc. Fr., 613 (1967).

102. H. N. Rydon, Org. Syntheses, Coll. Vol. III, 44 (1955).

103. A. W. Johnson, E. Markam, and R. Price, ibid., Vol. 42, 75 (1962).

104. J. W. Wilt, L. L. Maravetz, and J. F. Zawadzki, J. Org. Chem., 31, 3018 (1966).

105. T. Takeshita and M. Kitajima, Bull. Chem. Soc. Jap., 32 985 (1959).

106. C. S. Springer, Jr., D. W. Meek and R. E. Sievers, Inorg. Chem., 6 1105 (1967).

107. P. R. Bevington, "Data Reduction and Error Analysis for the Physical Sciences," McGraw-Hill Book Company, New York, N. Y., 1969.

108. D. W. Marquardt, J. Soc. Indus. Appl. Math., 11, 431 (1963); see also ref. 107.

109. I. S. Sokolnikoff and E. S. Sokolnikoff, "Higher Mathematics for Engineers and Physicists," 2nd ed, McGraw-Hill Book Company, Inc., New York, N. Y., 1941, p 141.

APPENDIX 1

Optimization of Parameters in Structure-Chemical Shifts Correlations

The fractional changes in the chemical shifts due to a dipolar mechanism and produced by a C_{2v} point dipole are given in equation 40:

$$SC_i = \frac{\Delta H_i}{H_o} = C_1\left(\frac{3\cos^2\Theta_i - 1}{r_i^3} - \frac{3}{2} C_2 \frac{\sin^2 \Theta_i \cos 2\Omega_i}{r_i^3}\right) \qquad (40)$$

where spherical coordinates for nucleus i in the symmetry coordinates of the C_{2v} point dipole are defined in Figure 25.

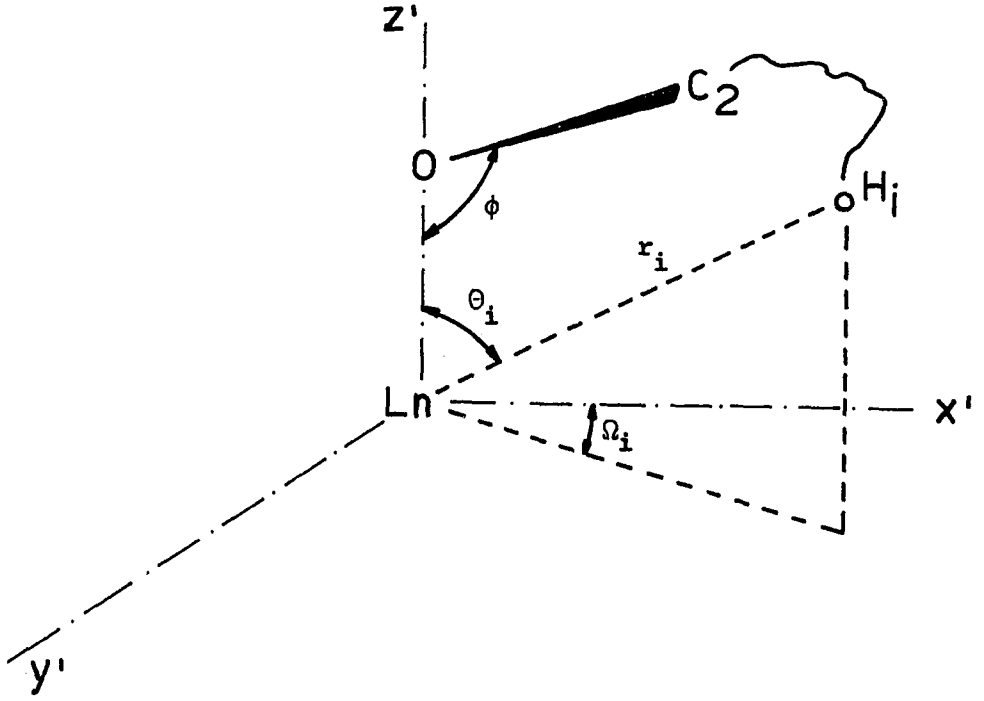

Figure 25 - Lanthanide Symmetry Coordinate System - H_i is a proton in the borneol molecule with a rigid geometry with respect to C_2 and O.

A version of a computer program PSEUDO[31], which analyzes chemical shifts of dipolar origin, was modified for use in the present study. Its algorithms are described below.

For n observations, a set of SO_i (i = 1,...,n) represents the observed chemical shifts with respect to the original position in the absence of the point dipole. A set of n coordinates must be available from a chosen model and are expressed in Cartesian coordinates with the coordination site located at (0, 0, 0). For the borneol case, analyzed in this work, the convention for the orientation of the molecule with respect to the Cartesian coordinates was described in Figure 6.

The idea is to locate the Ln ion such that in the symmetry coordinates of the Ln (Figure 25), equation 41 represents a minimum.

$$\frac{\sum_{i=1}^{n} (SO_i - SC_i)^2}{\sum_{i=1}^{n} SO_i^2} = R^2 \qquad (41)$$

The minimization process is performed by:

1) An initial guess for the lanthanide position is taken;

2) The proper rotation and translation is applied, such that in a new system of coordinates (x', y', z') the Ln ion will be located at (0, 0, 0) and the Ln-O bond will be colinear with the z' direction;

3) The SC_i are expanded in a Taylor series where only the first derivatives are considered (equation 42):

$$SC_{i,h} = SC_{i,h-1} + \sum_{j=1}^{m} \frac{\partial SC_i}{\partial t_j} \Delta t_j \qquad (42)$$

where the i subscript refers to the nucleus i, h refers to the iteration number, t is the representation of the parameter to be optimized and j refers to parameter number (j = 1,...,m);

4) In order to minimize equation 41, its derivative with respect to each parameter j must be 0., so:

$$\sum_{i=1}^{n} (SC_i - SO_i) \frac{\partial SC_i}{\partial t_j} = 0. \quad \text{for } j = 1,\ldots,m \tag{43}$$

Substituting equation 42 into 43:

$$\sum_{i=1}^{n} (SC_{i,h-1} - SO_i + \sum_{j=1}^{m} \frac{\partial SC_i}{\partial t_j} \Delta t_j) \frac{\partial SC_i}{\partial t_j} = 0. \tag{44}$$

Equation 44 can be rearranged, and in matrix form:

$$\underset{\sim}{A}\ \underset{\sim}{T} = \underset{\sim}{C} \tag{45}$$

where $\underset{\sim}{A}$ is a mxm matrix, $\underset{\sim}{T}$ is a vertical matrix, mx1, and $\underset{\sim}{C}$ is also a mx1 matrix. Their elements are defined by:

$$A_{j,k} = \sum_{i} \frac{\partial SC_i}{\partial t_j} \frac{\partial SC_i}{\partial t_k}$$

$$T_{j,1} = \Delta t_j \tag{46}$$

$$C_{j,1} = \sum_{i} (SO_i - SC_{i,h-1}) \frac{\partial SC_i}{\partial t_j}$$

5) Inversion of matrix $\underset{\sim}{A}$ is performed by standard procedures[107], so that:

$$\underset{\sim}{T} = \underset{\sim}{A}^{-1}\ \underset{\sim}{C} \tag{47}$$

and a new location of the lanthanide position is found by letting:

$$t_j = t_j + \Delta t_j \tag{48}$$

6) t_j resulting from the previous step is considered as the new initial guess and the procedure is repeated from step 2;

7) When the condition $\sum_j \Delta t_j^2 < 10^{-4}$ is met, the iteration process is stopped.

The seven steps above are the basis for the minimization process. A few details concerning the calculation of derivatives and chemical shifts by equation 40 are helpful.

Transformation from Substrate to Lanthanide Coordinates

The rotation and translation of the x, y, z system to x', y', z' involve:

1) Rotation by ψ around the x axis; this will locate the Ln on the xz plane.

2) Rotation by ϕ around the y axis; this will locate the Ln-O bond on the x axis.

3) Translation on the x axis from the coordination site (oxygen) at (0, 0, 0) to Ln at (0, 0, 0).

In other words and renaming the axes:

$$\begin{pmatrix} z' \\ y' \\ x' \end{pmatrix} = \begin{pmatrix} |Ln\text{-}O| \\ 0 \\ 0 \end{pmatrix} - \begin{pmatrix} \cos\phi & 0 & \sin\phi \\ 0 & 1 & 0 \\ -\sin\phi & 0 & \cos\phi \end{pmatrix} \begin{pmatrix} 1 & 0 & 0 \\ 0 & \cos\psi & -\sin\psi \\ 0 & \sin\psi & \cos\psi \end{pmatrix} \begin{pmatrix} x \\ y \\ z \end{pmatrix} \tag{49}$$

The operation will afford a situation similar to Figure 25. If the McConnell equation for axial symmetry is applied ($C_2 = 0.$ in equation 40) and the Ln-O bond is supposed colinar with the z' axis, classical analysis of LIS involves optimization of three parameters, Ln-O bond

distance and the angles ψ and ϕ.

If non-axial symmetry is assumed, that is $C_2 \neq 0.$ in equation 40, optimization of two more parameters is required. They are C_2 and the rotation around z' (which modifies Ω_i angles). Furthermore, if non-colinearity of z' and Ln-O bond is assumed, rotation around x' and y' will be necessary.

By convention, a positive angle of rotation is set when looking from the positive axis toward the origin in Figure 25, the movement is performed in the clockwise direction. The matrix expression of equation 50 results:

$$\begin{pmatrix} \cos\gamma & 0 & -\sin\gamma \\ 0 & 1 & 0 \\ \sin\gamma & 0 & \cos\gamma \end{pmatrix} \begin{pmatrix} 1 & 0 & 0 \\ 0 & \cos\beta & \sin\beta \\ 0 & -\sin\beta & \cos\beta \end{pmatrix}$$

$$\begin{pmatrix} \cos\alpha & \sin\alpha & 0 \\ -\sin\alpha & \cos\alpha & 0 \\ 0 & 0 & 1 \end{pmatrix} \begin{pmatrix} x' \\ y' \\ z' \end{pmatrix} = \begin{pmatrix} x'' \\ y'' \\ z'' \end{pmatrix} \qquad (50)$$

where α, β, γ are the angle of rotation around z', x', y', respectively. The new system of coordinates are named x", y", z".

ξ used in the section Colinearity of Magnetic Axis and Ln-O Vector represents the angle between z' and z" after rotation of x' and y' axes, its magnitude is calculated by simple vector product: If k' and k" are unitary vectors, along the z direction in the prime and second prime coordinates systems respectively, then:

$$k' \cdot k'' = \cos\xi \qquad (51)$$

Analogously, the angles between the other axes are found.

Calculation of Derivatives

The derivatives of SC_i with respect to a given parameter j is approximated to the difference of the value of the function theoretically calculated at $t_j = t_j$ and $t_j = t_j + 0.001$ for each i = 1,...,n. Equation 40 is applied in each case.

Rotamer Population Analysis

Three rotamers are the maximum number considered in the program. For all rotamers the Ln-O bond distances and the Ln-O-C_2 (ϕ) angles are assumed constant. This, of course, does not have to be true, but four more independent parameters would be introduced in order to alter the equality. The number of parameters is limited by the seven observations in borneol (only six parameters at a time are allowed to vary independently), so the above approximation cannot be avoided.

Input data regarding the rotamer population analysis are as follows (see Figure 26):

1) GROUPX = Ln-O bond distance, common for all rotamers;
2) RHO = Ln-O-C_2 (ϕ) angle, common for all rotamers;
3) TA1 = ψ angle defined in Figure 6 for the first rotamer;
4) TA2 = ψ angle defined in Figure 6 for the second rotamer;
5) FR2 = molar fraction of the second rotamer;
6) FR3 = molar fraction of the third rotamer;
7) NAVE = selection field that allows the options in Table 50.

Error Analysis

After convergence is reached, errors are calculated by:

TABLE 50

Relation Between NAVE and Rotamer Characteristics.

NAVE	Number of Rotamers	ψ angles	Mole fraction
1 (or 0)	1	TA1, - , -	1, 0, 0
2	2	TA1, TA1 + 180°	1 - FR2, FR2, 0
3	3	TA1, TA1 + 120°, TA1 + 240°	1 - 2 FR2, FR2, FR2
4	3	same as NAVE = 3	1 - (FR2 + FR3), FR2, FR3
5	3	0, TA1, -TA1	same as NAVE = 3
6	3	0, TA1, TA2	same as NAVE = 4
7	2	TA1, TA2, -	same as NAVE = 2
8	2	TA1, -TA1, -	same as NAVE = 2

$$\sqrt{\frac{\sum_{i=1}^{n} (SO_i - SC_i)^2}{(n-m)}} = SIG$$

$$\sqrt{\frac{\sum_{i=1}^{n} (SO_i - SC_i)^2}{\sum_{i=1}^{n} SO_i^2}} = R \qquad (52)$$

$$SIG.\sqrt{A^{-1}_{j,j}} = \text{standard deviation for parameter } j$$

where $A^{-1}_{j,j}$ is the diagonal element of the inverted matrix $\underset{\sim}{A}$ that corresponds to the parameter j.

Figure 26 is an output example for the optimization of three parameters in the application of equation 40 with axial symmetry approximation (C_2 = 0.). For description of symbols, see legend.

Legend to Figure 26

Some terms of Figure 26 were defined in the section Rotamer Population Analysis. Other notations include:

C2 = C_2 constant in equation 40.

The orientation of the two coordinate systems is represented by the α, β, γ angles for each rotamer.

COORDINATES AND SHIFTS AFTER CONVERGENCE

XX, YY, ZZ are Cartesian coordinates for atoms in the lanthanide coordinate system.

RI, CT are spherical coordinates (r and Θ) for atoms in the lanthanide coordinate system.

AXIAL = numerical value for McConnell equation.

PERP = numerical value for non-axial symmetric portion in equation 40.

SA = calculated chemical shift for each atom in each rotamer.

SC = calculated chemical shift.

SO = observed chemical shift.

D = SO - SC

K = scalar factor (C_1 in equation 40) = $\sum_i SO_i / \sum_i SC_i$.

RFACTOR = R (in equation 52) x 100.

```
GROUPX       RHO        TA1        TA2        FR2        FR3        C2         NAVE

 3.00000 110.00000  90.00000   0.0        0.0        0.0        0.0        1

     INITIAL RELATIVE ORIENTATION OF THE TWO COORDINATES SYSTEMS IN DEGREES
    AS THE ANGLE OF ROTATION AROUND EACH AXIS

     FOR FIRST ROTAMER              FOR SECOND ROTAMER             FOR THIRD ROTAMER

MAGNETIC     X          Y          MAGNETIC     X          Y          MAGNETIC     X          Y

 AXIS       AXIS       AXIS       AXIS       AXIS       AXIS       AXIS       AXIS       AXIS

 0.0        0.0        0.0        0.0        0.0        0.0        0.0        0.0        0.0

             PARAMETERS AT CONVERGENCE

GROUPX       RHO        TA1        TA2        FR2        FR3        C2         K/1000
          ORIENTATION OF THE TWO COORDINATES SYSTEMS                                     SIGMA

 2.98252 127.34671 109.30916   0.0        0.0        0.0        0.0
 0.0        0.0        0.0        0.0        0.0        0.0        0.0        0.0        0.0        0.21424

THEIR STANDARD DEVIATIONS

  0.04438    1.09279    3.55533**********************************************
**************************************************************************************************

AND THEIR DERIVATIVES

 -0.00067   -0.00556    0.00065**********************************************
**************************************************************************************************
```

Figure 26 - Typical Output for Correlation Between LIS and Geometrical Factors (continued on next page). See legend, page 167.

ROTAMER ANGLES, POPULATIONS AND ORIENTATION OF ORIGINAL SYSTEM WITH LANTHANIDE COORDINATES AS THE ANGLE BETWEEN EACH PAIR OF AXES

		MAG - Z	X.LN - X	Y.LN - Y
109.30916	1.00000	0.0	0.0	0.0

COORDINATES AND SHIFTS AFTER CONVERGENCE

	XX	YY	ZZ	RI	CT	AXIAL	PERP	SA	SC	SD	D
H-2	1.910	-0.564	3.389	3.933	30.512	24.317	0.0	24.317	24.317	24.300	-0.017
H3-X	2.701	1.390	3.833	4.891	38.398	8.685	0.0	8.685	8.685	8.650	-0.035
H3-N	1.111	2.143	3.369	4.144	35.622	16.650	0.0	16.650	16.650	16.630	-0.020
H-4	1.806	2.605	5.912	6.708	28.201	5.314	0.0	5.314	5.314	5.570	0.256
H6-N	-1.323	0.064	4.809	4.998	15.397	17.385	0.0	17.385	17.385	17.360	-0.025
1-ME	0.817	-2.326	5.508	6.034	24.111	8.232	0.0	8.232	8.232	8.470	0.238
ME7S	3.542	-0.077	6.067	7.026	30.286	4.303	0.0	4.303	4.303	4.220	-0.083
ME7A	1.564	0.283	8.028	8.183	11.198	4.153	0.0	4.153	4.153	3.840	-0.313
H-5N	-0.745	2.337	5.021	5.588	26.038	9.828	0.0	9.828	9.828		
H-5X	-0.509	1.964	6.787	7.084	16.648	5.951	0.0	5.951	5.951		
H-6X	-1.015	-0.034	6.600	6.677	8.750	7.821	0.0	7.821	7.821		
1H10	1.831	-2.307	5.245	6.015	29.316	7.098	0.0	7.098	7.098		
2H10	0.532	-2.207	6.510	6.894	19.225	6.165	0.0	6.165	6.165		
3H10	0.086	-2.463	4.768	5.368	27.336	10.664	0.0	10.664	10.664		
1H7S	3.326	-0.996	6.517	7.384	28.051	4.004	0.0	4.004	4.004		
2H7S	3.787	0.752	6.660	7.698	30.098	3.293	0.0	3.293	3.293		
3H7S	3.515	0.016	5.023	6.130	34.981	5.309	0.0	5.309	5.309		
1H7A	1.840	-0.727	7.973	8.215	13.933	3.973	0.0	3.973	3.973		
2H7A	2.300	1.024	8.117	8.498	17.234	3.413	0.0	3.413	3.413		
3H7A	0.551	0.552	7.992	8.030	5.577	4.592	0.0	4.592	4.592		
C.C.	0.0	0.0	2.983	2.983	0.0	90.929	0.0	90.929	90.929		

K/1000	SIG	RFACTOR
1.206	0.214	1.290

Figure 26 (continued).

APPENDIX 2

Theoretical Treatment for Competitive Experiments in the Formation of 1:1 Adducts

Consider the following system:

$$\begin{aligned} A + R &\overset{K_A}{\rightleftharpoons} A{\cdot}R \\ B + R &\overset{K_B}{\rightleftharpoons} B{\cdot}R \end{aligned} \tag{53}$$

where A and B are two independent substrates and R the shift reagent.

Expressions for K's in equation 53 are:

$$K_A = \frac{[A{\cdot}R]}{[A]\ [R]}$$

$$K_B = \frac{[B{\cdot}R]}{[B]\ [R]} \tag{54}$$

where all terms are concentrations at equilibrium of the species involved.

Their ratio, K_r is:

$$K_r = \frac{K_A}{K_B} = \frac{[A{\cdot}R]\ [B]}{[B{\cdot}R]\ [A]} \tag{55}$$

and, by mass balance:

$$\begin{aligned} [A] &= A_o - [A{\cdot}R] \\ [B] &= B_o - [B{\cdot}R] \end{aligned} \tag{56}$$

where A_o and B_o represent initial concentrations of the respective substrates.

If $x = [A{\cdot}R]$ and $y = [B{\cdot}R]$, then the chemical shift of A (δ_A) will be shift from the original position ($\delta_{A\ free}$, in the absence of the shift reagent) by an amount proportional to the molar fraction of A bound to the shift reagent. Analogous considerations for B affords:

$$\delta_A = \delta_{A\ free} + \frac{x}{A_o}\ \Delta_A$$

$$\delta_B = \delta_{B\ free} + \frac{y}{B_o}\ \Delta_B \qquad (57)$$

where Δ_A and Δ_B represent the chemical shifts of the 1:1 adducts with respect to the original values ($\delta_{A\ free}$ and $\delta_{B\ free}$, respectively). From equation 57:

$$x = \frac{(\delta_A - \delta_{A\ free})\ A_o}{\Delta_A}$$

$$y = \frac{(\delta_B - \delta_{B\ free})\ B_o}{\Delta_B} \qquad (58)$$

Substituting equations 56 and 58 into 55:

$$K_r = \frac{K_A}{K_B} = \frac{\dfrac{\Delta_B}{\delta_B - \delta_{B\ free}} - 1}{\dfrac{\Delta_A}{\delta_A - \delta_{A\ free}} - 1} \qquad (59)$$

and rearranging equation 59:

$$\frac{1}{\delta_A - \delta_{A\ free}} = \frac{K_B}{K_A}\ \frac{\Delta_B}{\Delta_A}\ \frac{1}{\delta_B - \delta_{B\ free}} + \frac{1}{\Delta_A}\left(1 - \frac{K_B}{K_A}\right) \qquad (60)$$

Least square fit to the straight line of equation 60 is performed following standard procedures[107].

Instrumental Error Analysis

The instrumental errors in $1/(\delta_A - \delta_{A\ free})$ is given by the derivative of the expression:

$$d\ \frac{1}{\delta_A - \delta_{A\ free}} \simeq \frac{d(\delta_A - \delta_{A\ free})}{(\delta_A - \delta_{A\ free})^2} \qquad (61)$$

If δ's are measured in the ppm scale, the precision in their magnitude is ± 0.02 ppm. So, the precision for $1/\delta$ (where $\delta = \delta_A - \delta_{A\ free}$) increases with the square of the magnitude of the observed shifts. Table 51 gives values for few representative δ, from which it is clear that high values of δ are desirable. Furthermore, if high shifts are measured, even the uncertainties in the δ_{free} values introduce only a small error in the $1/\delta$ expression.

TABLE 51

Magnitude and Associated Errors for $1/\delta$ Expressions.

δ (in ppm)	$1/\delta$	$d(1/\delta)$ [a]	% Error
0.1	10.	4	40%
1.	1.	0.04	4%
5.	0.2	1.6×10^{-3}	0.8%
10.	0.1	4×10^{-4}	0.4%

a) $d(\delta_A - \delta_{A\ free}) = d\delta = 0.04$ ppm.

The determination of K and Δ by plotting L_o *vs.* $1/\delta$ at constant [R], reviewed in the Introduction, requires low values of [R]. As a consequence, high values for $1/\delta$ result which are shown to be associated with a high uncertainty. Even if spectra were recorded with an expanded scale, in order for $1/\delta = 10\ ppm^{-1}$ be associated with an error $\pm 0.5\ ppm^{-1}$, a precision of 0.005 ppm is required for $\delta_A - \delta_{A\ free}$. This is especially difficult in these types of spectra because of broadening of signals produced by the shift reagent.

Standard Deviations for K and Δ

The errors associated with K and Δ from each straight line analysis are calculated by simple derivation. If m and b are the slope and the intercept respectively for $1/\delta$ vs. $1/\delta$ plots, then:

$$\frac{1}{K_r} = \frac{K_B}{K_A} = 1 - b\,\Delta_A \tag{62}$$

$$d\,\frac{K_B}{K_A} = b\,d\Delta_A + \Delta_A\,db \tag{63}$$

and

$$dK_B = \frac{K_B}{K_A}\,dK_A + K_A\,d\,\frac{K_B}{K_A} \tag{64}$$

Furthermore:

$$m = \frac{K_B}{K_A}\,\frac{\Delta_B}{\Delta_A} \tag{65}$$

so

$$\Delta_B = \frac{m\,\Delta_A}{\frac{K_B}{K_A}}$$

and

$$d\Delta_B = \frac{\frac{K_B}{K_A}\,(\Delta_A\,dm + m\,d\Delta_A) - m\,\Delta_A\,d\frac{K_B}{K_A}}{\left(\frac{K_B}{K_A}\right)^2} \tag{66}$$

By statistical analysis[107], for n observations of a quantity A, each one associated with a standard deviation σ_i ($i = 1,\ldots,n$), the standard deviation of the average of the A_i values (σ) is given by:

$$\sigma^2 = \sum_{i=1}^{n} \left(1/\sigma_i^2\right)^{-1} \tag{67}$$

Equation 67 was used to estimate σ values for equilibrium constants and Δ from all competitive experiments.

APPENDIX 3

General Iteration Procedure for Equilibria Programs

The general procedure for the resolution of equilibrium systems is described in this appendix and is based on the iterative process of Marquardt[108].

Let $f_1,\ldots,f_n$ be functions of m parameters, with the condition $m < n$:

$$\begin{aligned} f_1 &= f_1\ (t_1,\ldots,t_m) \\ &\ldots\ldots\ldots\ldots\ldots \\ f_n &= f_n\ (t_1,\ldots,t_m) \end{aligned} \tag{68}$$

where $t_1,\ldots,t_m$ are the independent variables.

Let $F_1,\ldots,F_n$ be the observed values of each function which leads to the problem of determining $t_1,\ldots,t_m$ so that:

$$\sigma^2 = \sum_{i=1}^{n} (f_i - F_i)^2 = \text{minimum} \tag{69}$$

So:

$$\frac{\partial \sigma^2}{\partial t_j} = 0. = \sum_{i=1}^{n} (f_i - F_i)\ \frac{\partial f_i}{\partial t_j} \qquad \text{for } j = 1,\ldots,m \tag{70}$$

Let $a_1,\ldots,a_m$ be initial guesses of the t_j parameters, so by developing f_i in a Taylor series:

$$\begin{aligned} f_i\ (a_1 + \Delta a_1,\ldots,\ a_m + \Delta a_m) &= \\ &= f_i\ (a_1,\ldots,\ a_m) + \sum_{j=1}^{m} \frac{\partial f_i\,(a_1,\ldots,\ a_m)}{\partial t_j}\ \Delta t_j \end{aligned} \tag{71}$$

where only the first derivatives are considered.

The process is analogous to the one described in Appendix 1, since by substituting equation 71 into 70, the following matrix expression results:

$$\underset{\sim}{A}\ \underset{\sim}{T} = \underset{\sim}{C} \tag{72}$$

where $\underset{\sim}{A}$ is a mxm matrix, $\underset{\sim}{T}$ and $\underset{\sim}{C}$ are vertical matrices mx1. Their elements are defined as:

$$A_{j,k} = \sum_{i=1}^{n} \frac{\partial f_i}{\partial t_j} \frac{\partial f_i}{\partial t_k}$$

$$T_j = \Delta t_j \tag{73}$$

$$C_j = \sum_{i=1}^{n} (F_i - f_i) \frac{\partial f_i}{\partial t_j}$$

Matrix $\underset{\sim}{A}$ is normalized, that is a new matrix $\underset{\sim}{B}$ is constructed, which will have 1 as diagonal elements:

$$B_{j,k} = \frac{A_{j,k}}{\sqrt{A_{j,j}\ A_{k,k}}} \tag{74}$$

A λ factor is added to the diagonal elements of $\underset{\sim}{B}$, which is set equal to 0.001 at the beginning of the program. The purpose of λ will be explained at the end of this appendix.

Matrix $\underset{\sim}{B}$, modified by the λ factors, is inverted, and the parameter increments, Δt_j, are calculated by:

$$\Delta t_j = \sum_{k=1}^{m} \frac{B^{-1}_{j,k}\ C_k}{\sqrt{A_{j,j}\ A_{k,k}}} \tag{75}$$

where $B^{-1}_{j,k}$ represents the j,k element of the inverted matrix $\underset{\sim}{B}$. σ^2 is calculated with the t_j and with the $t_j + \Delta t_j$ parameters, so two cases may result:

1) $\sigma^2(t_j) > \sigma^2(t_j + \Delta t_j)$, in which case λ is decreased by a factor of 10, the new parameters are set to $t_j + \Delta t_j$, new derivatives at $t_j + \Delta t_j$ are calculated and the interation is repeated starting from the construction of new $\underset{\sim}{A}$, $\underset{\sim}{B}$, and $\underset{\sim}{C}$ matrices;

2) $\sigma^2(t_j) < \sigma^2(t_j + \Delta t_j)$, in which case λ is increased by a factor of 10, the matrix B is modified with the new λ and the iteration process is repeated starting from the inversion of the modified $\underset{\sim}{B}$ matrix.

When the difference between the two σ^2 is less than 0.1% and $\lambda < 10^{-4}$, the iteration procedure is stopped.

Function of λ

The gradient-expansion algorithm combines the advantages of the gradient search minimization with the method of linearizing the fitting function by expansion in a Taylor series.

The gradient search process, as its name suggests, involves the approach of the minimum by the direction of steepest descent. It is very effective when approaching the minimum from far away, but does not converge rapidly in its neighborhood, since it is difficult to asyntotically approach the bottom of the minimum.

On the other hand, the linearization of the function by expansion to a Taylor series will converge very rapidly in the vicinity of the minimum, but less effectively when the starting point (that is, the t_j parameters) is far away from the solution.

By altering the diagonal elements of the matrix $\underset{\sim}{B}$, the λ factor

will control which of the two methods to be of a major contribution to the minimization process:

1) If λ is very small, the linearization of the function will predominate, and the minimum will be located in few iterations if in its neighborhood.

2) If λ is very large, the diagonal terms in the B matrix will predominate and the matrix equation 72 will degenerate into m separate equations, that are identified with the gradient search procedure.

In addition to decreasing the number of iterations necessary to obtain convergence, computational time is also decreased, since calculation of derivatives in each iteration is not necessary if λ is going to be increased in that particular step.

APPENDIX 4

Theoretical Calculation of Competing Substrates

(1:1 and 2:1 Adducts)

Let us consider the theoretical problem of calculating the equilibrium concentrations of the species involved in equation 76:

$$\begin{aligned} A + R &\overset{K_A}{\rightleftharpoons} A{\cdot}R \\ B + R &\overset{K_{B1}}{\rightleftharpoons} B{\cdot}R \\ B{\cdot}R + B &\overset{K_{B2}}{\rightleftharpoons} B_2{\cdot}R \end{aligned} \tag{76}$$

The input parameters are K_A, K_{B1}, K_{B2}, A_o, B_o, and R_o (where the o subscript refers to the initial concentrations of the substrates A and B, and the shift reagent, R). The following relations must be satisfied:

$$\begin{aligned} K_A &= \frac{[A{\cdot}R]}{[A]\ [R]} \\ K_{B1} &= \frac{[B{\cdot}R]}{[B]\ [R]} \\ K_{B2} &= \frac{[B_2{\cdot}R]}{[B{\cdot}R]\ [B]} \end{aligned} \tag{77}$$

where expressions in brackets represent equilibrium concentrations of the several species. Let:

$$\begin{aligned} [A{\cdot}R] &= x \\ [B{\cdot}R] &= y \\ [B_2{\cdot}R] &= z \end{aligned} \tag{78}$$

then, by mass balance, at equilibrium:

$$[R] = R_o - x - y - z$$

$$[A] = A_o - x \qquad (79)$$

$$[B] = B_o - y - 2z$$

Substituting equations 79 into 77:

$$K_A = \frac{x}{(A_o - x)\ (R_o - x - y - z)}$$

$$K_{B1} = \frac{y}{(B_o - y - 2z)\ (R_o - x - y - z)} \qquad (80)$$

$$K_{B2} = \frac{z}{y\ (B_o - y - 2\ z)}$$

Since an analytical solution of this problem could be quite complicated, an iterative process is preferred. The following equalities relate the present problem (calculation of x, y, and z) with the nomenclature used in Appendix 3:

$$f_1 = K_A$$

$$f_2 = K_{B1}$$

$$f_3 = K_{B2} \qquad (81)$$

$$t_1 = x$$

$$t_2 = y$$

$$t_3 = z$$

In order to apply the procedure described in Appendix 3, the derivatives of f_i must be calculated. From equation 80:

$$\frac{\partial K_A}{\partial x} = K_A \left(\frac{1}{x} + \frac{1}{A_o - x} + \frac{1}{R_o - x - y - z} \right)$$

$$\frac{\partial K_A}{\partial y} = \frac{\partial K_A}{\partial z} = \frac{K_A}{R_o - x - y - z}$$

$$\frac{\partial K_{B1}}{\partial x} = \frac{K_{B1}}{R_o - x - y - z}$$

$$\frac{\partial K_{B1}}{\partial y} = K_{B1} \left(\frac{1}{x} + \frac{1}{B_o - y - 2z} + \frac{1}{R_o - x - y - z} \right)$$

$$\frac{\partial K_{B1}}{\partial z} = K_{B1} \left(\frac{2}{B_o - y - 2z} + \frac{1}{R_o - x - y - z} \right) \qquad (82)$$

$$\frac{\partial K_{B2}}{\partial x} = 0.$$

$$\frac{\partial K_{B2}}{\partial y} = K_{B2} \left(\frac{1}{B_o - y - 2z} - \frac{1}{y} \right)$$

$$\frac{\partial K_{B2}}{\partial z} = K_{B2} \left(\frac{1}{z} + \frac{1}{B_o - y - 2z} \right)$$

When the minimum is reached (σ^2 will be zero, since there are three observations with three restrictions), the chemical shifts (SC) and their reciprocals (1/SC) are calculated:

$$SC_A = \frac{x}{A_o} \quad \Delta_A$$

$$SC_B = \frac{y}{B_o} \quad \Delta_{B1} + \frac{2z}{B_o} \quad \Delta_{B2} \qquad (83)$$

Output includes values of x, y, z, SC_A, SC_B, $1/SC_A$, and $1/SC_B$, along with the initial concentrations of A, B, and R.

Figure 27 is an example for the data represented in Figure 12.

SUBSTRATE A FORMS ONLY 1:1 COMPLEXES, PRINTED RESULTS CORRESPOND TO VALUES OF:

K = 100.0000 SHIFT OF 1:1 = 20.0000

SUBSTRATE B FORMS 1:1 AND 2:1 COMPLEXES, PRINTED RESULTS CORRESPOND TO VALUES OF:

K1 = 100.0000 SHIFT OF 1:1 = 30.0000

K2 = 1.0000 SHIFT OF 2:1 = 30.0000

INITIAL CONCENTRATION OF			EQUILIBRIUM CONCENTRATION OF			OBSERVED SHIFT OF		1/OBSERVED SHIFT OF	
LANTHANIDE	SUBSTRATE A	SUBSTRATE B	A-LN	B-LN	B(2)-LN	A	B	A	B
0.0727	0.1818	0.0182	0.0614	0.0061	0.0001	6.7574	10.2952	0.1480	0.0971
0.0632	0.1579	0.0421	0.0465	0.0122	0.0004	5.8881	9.1900	0.1698	0.1088
0.0558	0.1395	0.0605	0.0362	0.0154	0.0007	5.1966	8.2890	0.1924	0.1206
0.0500	0.1250	0.0750	0.0290	0.0170	0.0010	4.6464	7.5542	0.2152	0.1324
0.0453	0.1132	0.0868	0.0237	0.0177	0.0012	4.1959	6.9395	0.2383	0.1441
0.0413	0.1034	0.0966	0.0197	0.0179	0.0014	3.8105	6.3993	0.2624	0.1563
0.0727	0.0182	0.1818	0.0060	0.0555	0.0063	6.5641	11.2499	0.1523	0.0889
0.0632	0.0421	0.1579	0.0121	0.0426	0.0045	5.7249	9.8187	0.1747	0.1018
0.0558	0.0605	0.1395	0.0154	0.0337	0.0034	5.0746	8.6902	0.1971	0.1151
0.0500	0.0750	0.1250	0.0171	0.0274	0.0025	4.5665	7.7878	0.2190	0.1284
0.0413	0.0966	0.1034	0.0184	0.0191	0.0016	3.7992	6.4288	0.2632	0.1555
0.3636	0.4545	0.0455	0.3110	0.0305	0.0004	13.6838	20.7052	0.0731	0.0483
0.3158	0.3947	0.1053	0.2377	0.0605	0.0024	12.0460	18.6177	0.0830	0.0537
0.2500	0.3125	0.1875	0.1503	0.0830	0.0074	9.6181	15.6628	0.1040	0.0638
0.2264	0.2830	0.2170	0.1231	0.0860	0.0096	8.6982	14.5455	0.1150	0.0687
0.3636	0.0455	0.4545	0.0321	0.2758	0.0318	14.1085	22.3993	0.0709	0.0446
0.3158	0.1053	0.3947	0.0645	0.2081	0.0274	12.2467	19.9869	0.0817	0.0500
0.2791	0.1512	0.3488	0.0814	0.1632	0.0229	10.7677	17.9678	0.0929	0.0557
0.2500	0.1875	0.3125	0.0900	0.1321	0.0187	9.6008	16.2690	0.1042	0.0615
0.2264	0.2170	0.2830	0.0940	0.1091	0.0156	8.6670	14.8724	0.1154	0.0672
0.2069	0.2414	0.2586	0.0954	0.0920	0.0129	7.9061	13.6751	0.1265	0.0731

Figure 27 - Theoretical Analysis of 1:1 and 2:1 Adducts Formation for B.

APPENDIX 5

Direct Determination of Equilibrium Constant and Δ

This appendix considers the calculation of equilibrium constant and Δ for equation 84, where A is a substrate with n groups each producing a different signal in the nmr spectrum.

$$A + R \underset{}{\overset{K}{\rightleftharpoons}} A \cdot R \tag{84}$$

Using a nomenclature similar to the one already introduced in Appendix 2:

$$K = \frac{x}{(A_o - x)\ (R_o - x)} \tag{85}$$

$$SC_{j,i} = \delta_{j\ free} + \frac{x}{A_o}\ \Delta_j \tag{86}$$

where x is the concentration of the adduct, A_o and R_o represent the initial concentrations of the substrate and the shift reagent respectively in the i observation, $SC_{j,i}$ refers to the chemical shift of group j in A for the i observation, Δ_j refers to the chemical shift of the group j in the adduct taking $\delta_{j\ free}$ as reference.

Solving equation 85 for x:

$$x = \frac{1}{2}\left[A_o + R_o + \frac{1}{K} - \sqrt{(A_o - R_o)^2 + \frac{1}{K^2} + 2\,\frac{A_o + R_o}{K}}\right] \tag{87}$$

where the negative signed solution to the quadratic equation is selected in order to fulfill the requirement $0 < x < A_o$ and $0 < x < R_o$.

The analogy with the procedure used in Appendix 3 is evident if:

$$\begin{aligned} f_{j,i} &= SC_{j,i} \\ t_1 &= K \\ t_{2j} &= \delta_{j\ free} \\ t_{2j+1} &= \Delta_j \end{aligned} \tag{88}$$

From equations 86 and 87:

$$\frac{\partial SC_j}{\partial K} = \frac{\Delta_j}{A_o}\,\frac{\partial x}{\partial K} = \frac{\Delta_j}{2A_o K^2}\,\frac{A_o + R_o + K^{-1}}{\sqrt{(A_o-R_o)^2 + K^{-2} + 2(A_o+R_o)\,K^{-1}}}$$

$$\frac{\partial SC_j}{\partial \delta_{h\ \text{free}}} = \begin{cases} 0 & \text{for } j \neq h \\ 1 & \text{for } j = h \end{cases} \qquad (89)$$

$$\frac{\partial SC_j}{\partial \Delta_h} = \begin{cases} 0 & \text{for } j \neq h \\ \dfrac{x}{A_o} & \text{for } j = h \end{cases}$$

The minimization criteria involve an expression slightly different from the one in Appendix 3, and it is:

$$\sum_{j=1}^{n}\ \sum_{i=1}^{m} (SC_{j,i} - SO_{j,i})^2 = \text{minimum} \qquad (90)$$

where m refers to the number of observations corresponding to each group j. The minimization procedure is also the gradient-expansion method with the corresponding $\underset{\sim}{A}$ and $\underset{\sim}{C}$ matrices as follows:

1) $\underset{\sim}{A}$ will be a n+1 x n+1 matrix whose elements are defined by:

$$A_{1,1} = \sum_{j=1}^{n}\ \sum_{i=1}^{m} \left(\frac{\partial SC_{i,j}}{\partial K}\right)^2$$

$$A_{1,h} = A_{h,1} = \sum_{i=1}^{m} \frac{\partial SC_{h-1,i}}{\partial K}\,\frac{\partial SC_{h-1,i}}{\partial \Delta_{h-1}} \quad \text{for } h=2,\ldots,n+1 \qquad (91)$$

$$A_{h,h} = \sum_{i=1}^{m} \left(\frac{\partial SC_{h-1,i}}{\partial \Delta_{h-1}}\right)^2 \quad \text{for } h = 2,\ldots,n+1$$

$$A_{k,h} = 0. \quad \text{for} \quad \begin{cases} h \neq k \\ h \text{ and } k = 2,\ldots,n+1 \end{cases}$$

2) $\underset{\sim}{C}$ will be a n+1 x 1 matrix, whose elements are defined by:

$$C_1 = \sum_{j=1}^{n} \sum_{i=1}^{m} (SO_{j,i} - SC_{j,i}) \frac{\partial SC_{j,i}}{\partial K} \tag{92}$$

$$C_h = \sum_{i=1}^{m} (SO_{h-1,i} - SC_{h-1,i}) \frac{\partial SC_{h-1,i}}{\partial \Delta_{h-1}} \qquad \text{for } h = 2,\ldots,n+1$$

APPENDIX 6

Calculation of K's and Δ's for the Competing Substrate B (1:1 and 2:1 Adducts)

Let us reanalyze the system described in Appendix 4 (that is, equation 93), from the opposite point of view. A series of chemical shifts for A and B are available in the presence of a shift reagent and the problem consists in evaluating K_{B1}, K_{B2}, Δ_{B1}, and Δ_{B2}, assuming that equilibrium constant and Δ values for A are known.

$$\begin{aligned} A + R &\overset{K_A}{\rightleftharpoons} A\cdot R \\ B + R &\overset{K_{B1}}{\rightleftharpoons} B\cdot R \\ B\cdot R + B &\overset{K_{B2}}{\rightleftharpoons} B_2\cdot R \end{aligned} \qquad (93)$$

From the expressions of the equilibrium constants of Appendix 4 (equation 77), the following equations are derived (in which the concentration of the shift reagent R is eliminated):

$$\begin{aligned} K_r &= \frac{K_A}{K_{B1}} = \frac{[A\cdot R]\ [B]}{[A]\ [B\cdot R]} \\ K_{B2} &= \frac{[B_2\cdot R]}{[B\cdot R]\ [B]} \end{aligned} \qquad (94)$$

The following equalities relate this problem to the general procedure described in Appendix 3:

$$\begin{aligned} f_i &= SC_i & t_3 &= \delta_{B\ free} \\ t_1 &= K_r & t_4 &= \Delta_{B1} \\ t_2 &= K_{B2} & t_5 &= \Delta_{B2} \end{aligned} \qquad (95)$$

where SC_i are the calculated chemical shifts for substrate B.

For substrate A:

$$\delta_A = \delta_{A\ free} + \frac{[A \cdot R]}{A_o} \Delta_A$$

and rearranging:

$$[A \cdot R] = \frac{\delta_A - \delta_{A\ free}}{\Delta_A} A_o \qquad (96)$$

so, $[A \cdot R]$ can be calculated directly from the chemical shifts of A if only Δ_A is known.

Using the previous nomenclature of Appendix 4:

$$[A \cdot R] = x$$

$$[B \cdot R] = y \qquad (97)$$

$$[B_2 \cdot R] = z$$

the chemical shifts for B are calculated from:

$$SC_i = \delta_{B\ free} + \frac{1}{B_o} (y \Delta_{B1} + 2z \Delta_{B2}) \qquad (98)$$

where $\delta_{B\ free}$, Δ_{B1}, and Δ_{B2} are three initial guesses (or the parameters obtained after a successful iteration). Values of y and z are calculated with the K_r and K_{B2} guesses (or the resulting from a successful iteration). Rewriting equation 94, using the above nomenclature for $[A \cdot R]$, $[B \cdot R]$, and $[B_2 \cdot R]$:

$$K_r = \frac{x\ (B_o - y - 2z)}{y\ (A_o - x)}$$

$$K_{B2} = \frac{z}{y\ (B_o - y - 2z)} \qquad (99)$$

from which, values of y and z are calculated by:

$$y = \frac{-(D + x) + \sqrt{D(D + 2x + 8x\ B_o\ K_{B2}) + x^2}}{4\ D\ K_{B2}} \tag{100}$$

$$z = \frac{K_{B2}\ y\ (B_o - y)}{1 + 2\ y\ K_{B2}}$$

where $D = K_{B1}\ (A_o - x)$.

It is also necessary to calculate the derivatives of SC_i with respect to each t_i listed in equation 95. For t_i $(i = 3,4,5)$, by derivation of equation 98:

$$\frac{\partial SC_i}{\partial \delta_{B\ free}} = 1.$$

$$\frac{\partial SC_i}{\partial \Delta_{B1}} = \frac{y}{B_o} \tag{101}$$

$$\frac{\partial SC_i}{\partial \Delta_{B2}} = 2\ \frac{z}{B_o}$$

Also from equation 98:

$$\frac{\partial SC}{\partial K_r} = \frac{\Delta_{B1}}{B_o}\ \frac{\partial y}{\partial K_r} + 2\ \frac{\Delta_{B2}}{B_o}\ \frac{\partial z}{\partial K_r}$$

$$\frac{\partial SC}{\partial K_{B2}} = \frac{\Delta_{B1}}{B_o}\ \frac{\partial y}{\partial K_{B2}} + 2\ \frac{\Delta_{B2}}{B_o}\ \frac{\partial z}{\partial K_{B2}} \tag{102}$$

where the i subscript has been eliminated for simplification purposes, but it is tacitly implicit.

Equation 102 is treated as an implicit function[109], so:

$$\frac{\partial K_r}{\partial K_r} = 1. = \frac{\partial K_r}{\partial y}\frac{\partial y}{\partial K_r} + \frac{\partial K_r}{\partial z}\frac{\partial z}{\partial K_r}$$

$$\frac{\partial K_{B2}}{\partial K_r} = 0. = \frac{\partial K_{B2}}{\partial y}\frac{\partial y}{\partial K_r} + \frac{\partial K_{B2}}{\partial z}\frac{\partial z}{\partial K_r} \qquad (103)$$

and:

$$\frac{\partial K_r}{\partial K_{B2}} = 0. = \frac{\partial K_r}{\partial y}\frac{\partial y}{\partial K_{B2}} + \frac{\partial K_r}{\partial z}\frac{\partial z}{\partial K_{B2}}$$

$$\frac{\partial K_{B2}}{\partial K_{B2}} = 1. = \frac{\partial K_{B2}}{\partial y}\frac{\partial y}{\partial K_{B2}} + \frac{\partial K_{B2}}{\partial z}\frac{\partial z}{\partial K_{B2}} \qquad (104)$$

From equation 103, $\partial y/\partial K_r$ and $\partial z/\partial K_r$ can be calculated; the respective derivatives with respect to K_{B2} can be obtained from equation 104.

From equation 99:

$$\frac{\partial K_r}{\partial y} = -K_r \left(\frac{1}{B_o - y - 2z} + \frac{1}{y}\right)$$

$$\frac{\partial K_r}{\partial z} = -2\frac{K_r}{B_o - y - 2z}$$

$$\frac{\partial K_{B2}}{\partial y} = K_{B2}\left(\frac{1}{B_o - y - 2z} - \frac{1}{y}\right) \qquad (105)$$

$$\frac{\partial K_{B2}}{\partial z} = K_{B2}\left(\frac{2}{B_o - y - 2z} + \frac{1}{z}\right)$$

The common determinant for the system of equations 103 and 104 is:

$$D = \begin{bmatrix} \frac{\partial K_r}{\partial y} & \frac{\partial K_r}{\partial z} \\ \frac{\partial K_{B2}}{\partial y} & \frac{\partial K_{B2}}{\partial z} \end{bmatrix} = -K_r K_{B2} \frac{B_o - 2z}{y z (B_o - y - 2z)} \qquad (106)$$

So, from equation 103:

$$\frac{\partial y}{\partial K_r} = - \frac{y\ (B_o - y)}{K_r\ (B_o + 2z)}$$

$$\frac{\partial z}{\partial K_r} = - \frac{z\ (B_o - 2y - 2z)}{K_r\ (B_o + 2z)} \qquad (107)$$

and from equation 104:

$$\frac{\partial y}{\partial K_{B2}} = - \frac{2y\ z}{K_{B2}\ (B_o + 2z)}$$

$$\frac{\partial z}{\partial K_{B2}} = \frac{z\ (B_o - 2z)}{K_{B2}\ (B_o + 2z)} \qquad (108)$$

Equations 101, 107 and 108 are used in the gradient-expansion iterative minimization procedure described in Appendix 3.

After the convergence is reached, standard deviations, theoretical chemical shifts and R factors are calculated.

Figure 28 is an example of the output obtained from this procedure and corresponds to the competition experiments between n-propylamine and DME, shift reagent $Eu(fod)_3$.

INITIAL CONCENTRATION		EQUILIBRIUM CONCENTRATION			OBSERVED CHEMICAL SHIFT OF		CALCULATED CHEMICAL SHIFT OF	SO-SC
A	B	A-LN	B-LN	B(2)-LN	A	B(SO)	B(SC)	
0.0341	0.1074	0.0003	0.0012	0.0205	3.4600	2.7900	2.6869	0.1031
0.0417	0.1007	0.0007	0.0019	0.0247	3.5300	3.2500	3.2037	0.0463
0.0536	0.0903	0.0029	0.0038	0.0289	3.8500	3.9600	3.9533	0.0067
0.0625	0.0824	0.0073	0.0059	0.0289	4.3900	4.3200	4.3069	0.0131
0.0590	0.0726	0.0216	0.0116	0.0262	6.5000	4.6400	4.6227	0.0173
0.0652	0.0658	0.0306	0.0134	0.0230	7.3700	4.6700	4.6204	0.0496
0.0728	0.0575	0.0421	0.0152	0.0188	8.3000	4.6000	4.5728	0.0272
0.0823	0.0470	0.0574	0.0167	0.0136	9.3100	4.4800	4.4564	0.0236
0.0948	0.0333	0.0760	0.0165	0.0076	10.1900	4.1500	4.2302	-0.0802
0.1118	0.0147	0.1093	0.0137	0.0005	11.6900	3.5500	3.5311	0.0189
0.1223	0.0290	0.0110	0.0026	0.0076	4.1600	3.5200	3.5499	-0.0299
0.1147	0.0354	0.0125	0.0033	0.0102	4.3200	3.7300	3.7985	-0.0685
0.1028	0.0455	0.0145	0.0046	0.0145	4.5900	4.0000	4.0848	-0.0848
0.0939	0.0531	0.0157	0.0056	0.0178	4.8100	4.1500	4.2440	-0.0940
0.0757	0.0687	0.0174	0.0081	0.0246	5.3400	4.4600	4.4821	-0.0221
0.0679	0.0752	0.0181	0.0094	0.0274	5.6500	4.5500	4.5626	-0.0126
0.0587	0.0830	0.0222	0.0129	0.0306	6.6100	4.6400	4.6763	-0.0363
0.0473	0.0926	0.0192	0.0145	0.0346	6.8300	4.7500	4.7228	0.0272
0.0329	0.1048	0.0189	0.0214	0.0383	8.2600	4.8900	4.7740	0.1160

REFERENCE A HAS A FREE CHEMICAL SHIFT OF 3.3950, AND A CHEMICAL SHIFT FOR THE 1:1 COMPLEX OF 8.4800

	EQUILIBRIUM CONSTANT		CHEMICAL SHIFTS FOR		
	KA/KB1	KB2	FREE B	B-LN	B(2)-LN
	0.4243	264.7271	0.9100	2.5115	4.5827
STANDARD DEVIATIONS	0.0568	46.1651**********		0.0855	0.0764
DERIVATIVES	-0.0000	0.0000**********		0.0000	0.0000

STANDARD DEVIATION OF AN OBSERVATION OF UNIT WEIGHT 0.0641

R FACTOR (IN PERCENTAGE) 1.3558

EXECUTION TERMINATED. EXECUTION TIME 10.282 SECONDS.

Figure 28 - Computer Output from Competition Experiments

APPENDIX 7

Theoretical Analysis of 1:1 and 2:1 Adducts Formation

The problem consists in calculating equilibrium concentrations of each species involved in the following system:

$$L + R \underset{}{\overset{K_1}{\rightleftharpoons}} L{\cdot}R$$
$$L{\cdot}R + L \overset{K_2}{\rightleftharpoons} L_2{\cdot}R \qquad (109)$$

from values of K_1 and K_2 (the equilibrium constants in each step) and L_o and R_o (the initial concentrations of the substrate and the shift reagent respectively).

Let $x = [L{\cdot}R]$ and $y = [L_2{\cdot}R]$; the expression for the K's will be:

$$K_1 = \frac{x}{(R_o - x - y)\ (L_o - x - 2y)} \qquad (110)$$

$$K_2 = \frac{y}{x\ (L_o - x - 2y)} \qquad (111)$$

From equation 111:

$$y = \frac{K_2\ x\ (L_o - x)}{1 + 2\ K_2\ x} \qquad (112)$$

The problem is relatively simple since it involves resolution of a cubic equation, that results from substituting equation 112 into 110 and rearrangement:

$$x^3 + P\ x^2 + Q\ x + T = 0. \qquad (113)$$

where:

$$P = \frac{1}{K_2} - \frac{2 K_1 R_o}{K_1 - 4 K_2}$$

$$Q = \frac{K_1 [K_2 L_o (2 R_o - L_o) - (R_o + L_o)] - 1}{K_2 (K_1 - 4 K_2)} \qquad (114)$$

$$T = \frac{K_1 R_o L_o}{K_2 (K_1 - 4 K_2)}$$

Analytical solution of a cubic equation affords three roots of x, only one[86] is real and has physical meaning ($0 < x < L_o$ and $0 < x < R_o$). Let:

$$q = \frac{3Q - P^2}{9}$$

$$r = \frac{P Q - 3T}{6} - \frac{P^3}{27}$$

$$b = (q^3 + r^2)^{\frac{1}{2}} \qquad (115)$$

$$s_1 = (r + b)^{1/3}$$

$$s_2 = (r - b)^{1/3}$$

Then:

1) For $K_1 < 4K_2$

$$x = s_1 + s_2 - \frac{P}{3} \qquad (116)$$

2) For $K_1 > 4K_2$

$$x = -\frac{s_1 + s_2}{2} - \frac{s_1 - s_2}{2} \, i\sqrt{3} - \frac{P}{3} \qquad (117)$$

Values of y are calculated by using equation 112. Chemical shifts of L (SC) are then calculated by:

$$SC = \delta_{L\ free} + \frac{1}{L_o} (x\ \Delta_1 + 2y\ \Delta_2) \qquad (118)$$

where $\delta_{L\ free}$, Δ_1, and Δ_2 are also known parameters and correspond to the chemical shift of L in the absence of the shift reagent and the chemical shifts of the 1:1 and 2:1 adducts, respectively.

APPENDIX 8

Calculation of K's and Δ's for 1:1 and 2:1 Adducts Formation (Direct Determination)

Let us reconsider the system of Appendix 7 (equation 119) from the opposite point of view:

$$L + R \underset{}{\overset{K_1}{\rightleftharpoons}} L{\cdot}R$$
$$L{\cdot}R + L \overset{K_2}{\rightleftharpoons} L_2{\cdot}R \qquad (119)$$

The problem in this case will be to determine values of K_1, K_2, Δ_1, Δ_2 and $\delta_{L\ free}$ (terms defined in the previous appendix) from a set of experimental chemical shifts for L (δ_L) and initial concentrations of L and R (L_o and R_o, respectively). The following expressions are recalled:

$$K_1 = \frac{x}{(L_o - x - 2y)\ (R_o - x - y)} \qquad (120)$$
$$K_2 = \frac{y}{x\ (L_o - x - 2y)}$$

$$\delta_L = \delta_{L\ free} + \frac{1}{L_o}\ (x\ \Delta_1 + 2y\ \Delta_2) \qquad (121)$$

The following equalities relate this problem to the general procedure of Appendix 3:

$$f_i = SC_i \qquad t_3 = \Delta_2$$
$$t_1 = \delta_{L\ free} \qquad t_4 = K_1 \qquad (122)$$
$$t_2 = \Delta_1 \qquad t_5 = K_2$$

With the initial guess of the five unknowns (or their values after a successful iteration), chemical shifts of L (SC_i) are calculated by the procedure of Appendix 7.

The necessary derivatives are:

$$\frac{\partial SC_i}{\partial \delta_{L\ free}} = 1.$$

$$\frac{\partial SC_i}{\partial \Delta_1} = \frac{x}{L_o} \qquad (123)$$

$$\frac{\partial SC_i}{\partial \Delta_2} = 2\,\frac{y}{L_o}$$

From equation 120:

$$\frac{\partial K_1}{\partial K_1} = 1. = \frac{\partial K_1}{\partial x}\,\frac{\partial x}{\partial K_1} + \frac{\partial K_1}{\partial y}\,\frac{\partial y}{\partial K_1}$$

$$\frac{\partial K_2}{\partial K_1} = 0. = \frac{\partial K_2}{\partial x}\,\frac{\partial x}{\partial K_1} + \frac{\partial K_2}{\partial y}\,\frac{\partial y}{\partial K_1} \qquad (124)$$

and:

$$\frac{\partial K_1}{\partial K_2} = 0. = \frac{\partial K_1}{\partial x}\,\frac{\partial x}{\partial K_2} + \frac{\partial K_1}{\partial y}\,\frac{\partial y}{\partial K_2}$$

$$\frac{\partial K_2}{\partial K_2} = 1. = \frac{\partial K_2}{\partial x}\,\frac{\partial x}{\partial K_2} + \frac{\partial K_2}{\partial y}\,\frac{\partial y}{\partial K_2} \qquad (125)$$

Also from equation 120:

$$\frac{\partial K_1}{\partial x} = \frac{K_1}{x}\,[1 + K_1\,(R_o - x - y) + K_1\,(L_o - x - 2y)]$$

$$\frac{\partial K_1}{\partial y} = \frac{K_1^2}{x}\,[2\,(R_o - x - y) + L_o - x - 2y]$$

$$\frac{\partial K_2}{\partial x} = \frac{K_2^2}{y}\,[x - (L_o - x - 2y)] \qquad (126)$$

$$\frac{\partial K_2}{\partial y} = \frac{K_2}{y}\,(1 + 2\,K_2\,x)$$

So the systems 124 and 125 can be solved for $\partial x/\partial K_1$, $\partial x/\partial K_2$, $\partial y/\partial K_1$ and $\partial y/\partial K_2$:

$$\frac{\partial x}{\partial K_1} = \frac{\frac{\partial K_2}{\partial y}}{D}$$

$$\frac{\partial y}{\partial K_1} = \frac{-\frac{\partial K_2}{\partial x}}{D} \qquad (127)$$

$$\frac{\partial x}{\partial K_2} = \frac{-\frac{\partial K_1}{\partial y}}{D}$$

$$\frac{\partial y}{\partial K_2} = \frac{\frac{\partial K_1}{\partial x}}{D}$$

where D is the common determinant of the systems 124 and 125.